Evaluation of performance of magnetized activated carbon in removal of antibiotics from contaminated waters

A Thesis Submitted to the College of

Graduate and Postdoctoral Studies

In Partial Fulfillment of the Requirements

For the Degree of Master of Science

In the Department of Chemical and Biological Engineering

University of Saskatchewan

Saskatoon, Saskatchewan

By

Kharazm Khaledi

PERMISSION TO USE

In presenting this thesis in partial fulfillment of the requirements for a Postgraduate degree from the University of Saskatchewan, I agree that the Libraries of this University may make it freely available for inspection. I further agree that permission for copying of this thesis in any manner, in whole or in part, for scholarly purposes may be granted by the professor or professors who supervised my thesis work or, in their absence, by the Head of the Department or the Dean of the College in which my thesis work was done. It is understood that any copying or publication or use of this thesis or parts thereof for financial gain shall not be allowed without my written permission. It is also understood that due recognition shall be given to me and to the University of Saskatchewan in any scholarly use which may be made of any material in my thesis.

Requests for permission to copy or to make other uses of materials in this thesis in whole or part should be addressed to:

Head of the Department of Chemical and Biological Engineering
57 Campus Drive
University of Saskatchewan
Saskatoon, Saskatchewan S7N 5A9
Canada

OR

Dean of the College of Graduate and Postdoctoral Studies
University of Saskatchewan
116 Thorvaldson Building, 110 Science Place
Saskatoon, Saskatchewan, S7N 5C9, Canada

ABSTRACT

The widespread use of antibiotics contributes to the discharge of a large amount of these pharmaceuticals into the environment worldwide. To address ever-increasing concerns about negative impacts of antibiotics in the environment, especially antimicrobial resistance, various treatments have been used to control the release of antibiotics. Among the applied treatments, adsorption with powder activated carbon has attracted great attention due to several advantages. Although activated carbon is a promising adsorbent, it suffers from difficulties in subsequent separation from the treated water, which can be considered the inherent disadvantage of the adsorption process. It can also cause turbidity in the treated effluent. To overcome these disadvantages, one possibility is the development of magnetized activated carbon. In contrast to traditional adsorbents, which are mostly removed by screening, magnetized activated can be effectively separated from waste streams by applying an external magnetic field.

In this research, a commercial activated carbon was magnetized using a co-precipitation method. The physicochemical properties of the developed adsorbent were investigated using different characterization techniques. The performance of the prepared adsorbent in removing tetracycline and lincomycin as two different model antibiotics from water was studied. The obtained adsorption data were modelled by Langmuir and Freundlich isotherms. Additionally, some preliminary adsorption experiments were performed for direct removal of tetracycline from liquid manure supernatant. It is expected that the outcomes of this research will contribute to addressing the existing problems of adsorption process and make it a step closer to sustainable treatment of wastewater.

The results of characterization techniques show that iron oxide nanoparticles (γ-Fe_2O_3) with an average particle size of 10.2 nm were deposited into commercial activated carbon. It was also found that the developed adsorbent was sufficiently magnetized to be separated from water using a simple magnet. Notably the prepared adsorbent possesses superparamagnetic properties. This confirms that the developed magnetic adsorbent can be easily re-dispersed in water after removing the magnetic field.

The results of adsorption studies indicate that the initial concentration of the antibiotics in the single- or binary-solute adsorption process affected the adsorption uptake. Also, the adsorption capacity of activated carbon decreased after magnetization process, but it

still has a relatively high adsorption capacity. Interestingly, the obtained results indicated that the adsorption capacity of magnetic activated carbon toward tetracycline (mg g^{-1}) was up to 4 times higher than that of lincomycin at room temperature depending on the equilibrium concentration of antibiotic in the liquid phase. Moreover, the results indicated that tetracycline was preferably adsorbed when both antibiotics were present in water. In addition, the overall adsorption capacity in binary-solution adsorption was higher than that of the individual antibiotics. On the other hand, the presence of each of these two antibiotics in mixture decreased the adsorption capacity of the adsorbents toward the other one.

The adsorption of tetracycline from liquid manure supernatant was studied at 60 mg L^{-1} manure solution using three dosages of adsorbents (1500, 2500 and 4000 mg L^{-1}). The obtained adsorption data indicated that the effective removal of tetracycline from liquid manure supernatant requires around 15 times more adsorbent compared to adsorption in water.

ACKNOWLEDGEMENTS

First, I would like to express my sincerest gratitude to my supervisors, Prof. Mehdi Nemati, Prof. Jafar Soltan and Prof. Bernardo Predicala for supporting me during this research work. They shared their knowledge and experience with me, correcting my mistakes patiently and offering me much advice. To be honest, this thesis would not have been completed without them. I would also like to gratefully acknowledge my Graduate Advisory Committee members, Prof. Venkatesh Meda and Prof. Catherine Niu for their valuable advice. Additionally, I would like to thank Mr. Richard Blondin and Ms. Montserrat Valdes Labrada for technical assistance and development of analytical methods.

I would like to express my gratitude and thanks to my group members, Hamid, Nazanin, Shahab, Khaled, Mehraneh, Mojtaba, and Shafi. This journey would not have been possible without their continued support. No act of gratitude can relay what their support and encouragement have meant to me. Also, I would like to especially thank Younes, who made so many unforgettable memories during this period of my life.

I gratefully acknowledge the Saskatchewan Ministry of Agriculture and the University of Saskatchewan for the financial support of this research work. I feel very privileged to have been given the opportunity to study at the University of Saskatchewan. This experience had afforded me the opportunity to work with many valuable people in a very safe and comfortable environment.

In the pursuit of this project, nobody has been more important to me than my family members. I must express my very profound gratitude to my parents, whose guidance and love are with me in whatever I pursue. I also wish to thank my lovely brother who provides unending inspiration. Thank you for continuing to encourage me to follow my dreams.

Finally, I would like to thank everyone who helped me along the way and contributed to complete my thesis work successfully.

Dedication

To my parents and my brother for their unconditional love and support.

TABLE OF CONTENTS

LIST OF TABLES

LIST OF FIGURES

NOMENCLATURE

C_0	Initial concentrations of the solute (mg L^{-1})
C_e	Equilibrium concentrations of the solute (mg L^{-1})
d10	Particle diameter corresponding to 10% cumulative undersize particle size distribution
d50	Particle diameter corresponding to 50% cumulative undersize particle size distribution
d90	Particle diameter corresponding to 90% cumulative undersize particle size distribution
E	Magnetic separation efficiency
H	Magnetic field (oersted)
K_c	Thermodynamic equilibrium constant
K_F	Freundlich isotherm model constant (mg g^{-1}) (L $mg^{-1})^{1/n}$
K_L	Langmuir isotherm model constant (L mg^{-1})
m	Mass of adsorbent (g)
M_R	Magnetic remanence (emu g^{-1})
M_S	Saturation magnetization (emu g^{-1})
n	Freundlich adsorption affinity parameter
Oe	Oersted
pKa	Acid dissociation constant
q_e	Adsorption capacity (mg adsorbate mg adsorbent $^{-1}$)
q_{max}	Monolayer maximum adsorption capacity in Langmuir and Sip isotherm model (mg adsorbate mg adsorbent $^{-1}$)
R	Universal gas constant (8.314 J K^{-1} mol^{-1})
rpm	Revolutions per minute
T	Absolute temperature (K)
UV	Ultraviolet
V	Volume of the solution (L)
$\Delta G°$	Gibbs free energy change of adsorption (J mol^{-1})
$\Delta H°$	Standard enthalpy change of adsorption (J mol^{-1})
$\Delta S°$	Standard entropy change of adsorption (J $mol^{-1}K^{-1}$)

ABBREVIATIONS

AC	Activated carbon
BET	Brunauer-Emmett-Teller
BJH	Barrett-Joyner-Halenda
CGS	Centimeter–Gram–Second System of Units
FE-SEM	Field Emission Scanning Electron Microscopy
GRC	Generalized Reduced Gradient
HGMS	High gradient magnetic separators
HPLC	High-performance liquid chromatography
IUPAC	International Union of Pure and Applied Chemistry
JCPDS	Joint Committee on Powder Diffraction Standards
LM	Lincomycin
MAC	Magnetized Activated Carbon
MAPE	Mean Absolute Percentage Error
MOFs	Metal-Organic Frameworks
PPMS	Physical Property Measurement System
PZC	Point of zero charge
SI	International System of Units
TC	Tetracycline
TEM	Transmission Electron Microscopy
TG	Thermal Gravimetric
XPS	X-ray Photoelectron Spectroscopy
XRD	X-ray powder diffractio

1 INTRODUCTION

Use of antibiotics in animal production is one of the major sources of antibiotics in the environment. According to the Public Health Agency of Canada, tetracyclines and lincosamides are among the most commonly used antibiotics for animals [1]. The widespread use of these antibiotics contributes to the high amount of their discharge into the environment. In fact, residual concentration of the antibiotics can be found in animal urine and faeces because of their incomplete metabolism. As a result, there is a considerable level of tetracyclines and lincosamides in the waste stream of animal production facilities, which could eventually reach surface-water bodies [2].

There are increasing concerns about negative impacts of antibiotics presence in the environment, especially the development of antimicrobial resistance. To address these concerns, various methods have been used so far to remove antibiotics from aqueous matrices. Among the applied methods, the adsorption process has attracted great attention because this process can remove a wide range of antibiotics with different physiochemical properties, either at a high or low level of concentrations [3].

Among various adsorbents used for antibiotic removal, activated carbon is one of the commonly used adsorbents in the industry since it has high adsorption capacity and can remove a wide range of antibiotics. The high adsorption capacity of both powdered and granular activated carbons is related to their large surface area and high microporosity.

Adsorption by granular activated carbon is one of the most commonly used processes in water treatment processes. On the other hand, powder activated carbon is considered a more efficient adsorbent than granular activated carbon as far as the removal of contaminants is concerned. Although powder activated carbon is a more effective adsorbent in removing contaminants from a continuous flow system, its large-scale application has been limited because it causes turbidity in effluent and requires further separation processes such as filtration [4, 5]. To take advantage of relatively high adsorption capacity of powder activated carbon, one needs to address the mentioned problem associated with its small particle size. In this regard, one possibility is the development of magnetic activated carbon, so that a magnetic field can prevent the fine particles from being carried over by effluent.

In this research work, a commercial activated carbon was magnetized using co-precipitation method. Also, the physiochemical properties of magnetic activated carbon were studied through different characterization techniques. The developed magnetic adsorbent was used to study the adsorptive removal of individual tetracycline and lincomycin from water for a wide range of concentrations and temperatures. This was followed by investigating the adsorption in a mixture of these two antibiotics. Conducting the tetracycline adsorption experiments at different temperatures allowed the thermodynamic characterization of the adsorption process. Additionally, the adsorptive removal of tetracycline from liquid swine manure supernatant was studied. To allow the establishment of a benchmark, in all cases similar experiments were also carried out using non-magnetized activated carbon. Finally, the acquired adsorption data were fitted into a suitable isotherm model.

This thesis consists of five chapters including introduction, literature review and research objectives, materials and methods, results and discussion, and conclusions and recommendations for future work.

2 LITERATURE REVIEW AND RESEARCH OBJECTIVES

2.1 Use of Antibiotic

Human and animal antimicrobial uses are two major sources of antibiotics in the environment. According to the most recent annual report issued by the Public Health Agency of Canada, around 78% of antimicrobials sold or distributed in 2016 were used for animal production, 20% for humans, and 2% for crops and companion animals [1]. The report indicates that although antimicrobials used for humans and animals are similar, some classes of antibiotics were predominantly used for humans and others for animals. According to this report, cephalosporins and fluoroquinolones, for example, are mostly used in humans, but tetracyclines and lincosamides are commonly used for animals. The annual report pointed out that in 2016, 22% of grower-finisher pig farms used lincosamides and tetracyclines for growth promotion. Similar to antimicrobials used for humans, antimicrobials use for production and companion animals result in the development of antimicrobial-resistant bacteria. These bacteria can be easily transferred to humans mainly through food processes, direct contact, and waterborne routes [1]. In this regard, use of antibiotics as a growth promoter is restricted in Canada through recently passed regulations. For example, it has not been allowed that medically important antimicrobials be labelled as growth promotor since 2018 [6]

2.2 Physiochemical properties of selected antibiotics

2.2.1 Tetracycline

The structure of tetracycline is depicted in Figure 2.1. As can be seen, tetracycline has a C6-hydroxyl group. This antibiotic is produced from bacteria categorized as the *Streptomyces* family [7], and it is active against various gram-positive and gram-negative organisms [8]. Three pKa values, 3.3, 7.68 and 9.69, are reported for tetracycline, indicative of the tricarbonyl system, phenolic diketone system, and the dimethylammonium group, respectively [9]. Henry's constant for tetracycline is relatively low, indicating this molecule is hardly lost through volatilization (3.45×10^{-24} - 3.91×10^{-26} atm m^3 mol^{-1}). In addition, the water solubility of tetracycline is high (0.008 – 0.062 mol L^{-1}) and its n-octanol/water partition coefficient is low, indicating its hydrophilic nature (log K_{ow} is in the range of -1.25 to -1.12) [10].

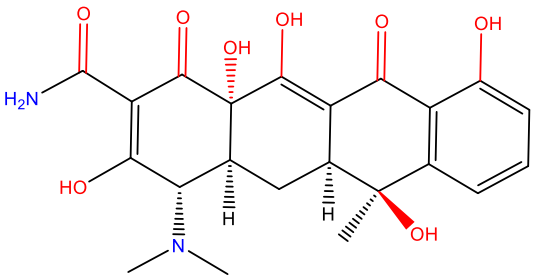

Figure 2.1 Structure of the tetracycline molecule

2.2.2 Lincomycin

Although the Public Health Agency of Canada has classified both lincosamides and tetracyclines as medically important antimicrobials, lincosamides are classified as highly important drugs in human medicine [1]. Lincomycin is categorized as a lincosamide antibiotic, and it is produced from the bacteria *Streptomyces lincolnensis*. Lincomycin is active against both gram-positive and anaerobic bacteria [11]. The lincomycin structure is shown in Figure 2.2. Lincomycin is a basic compound consisting of a single amino acid, which is linked to an amino sugar. This free base is soluble in water and most organic solvents, and its pKa value is 7.6 [12].

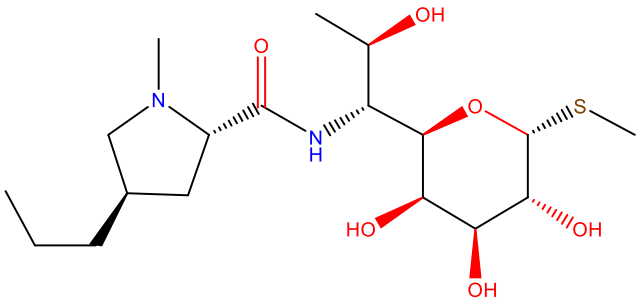

Figure 2.2 Structure of the lincomycin molecule

2.3 Treatments for removal of antibiotics from water

2.3.1 Conventional treatments

To address ever-increasing concerns about antimicrobial resistance, various treatments have been used to control the concentration of antibiotics in aqueous matrices. Over the last two decades, conventional treatments such as biological processes, coagulation/flocculation and filtration have been used to remove antibiotics from water. However, these treatments cannot completely remove antibiotics from water. For example, in

2011 Deblonde et al. [13] reported that the removal rate of tetracycline in sewage treatment plants were around 95%. In fact, they reported that the concentrations of tetracycline in the influent and effluents of sewage treatment plants were around 48.0 and 2.4 μg L^{-1}, respectively. Similarly, in 2004, Miao et al. [14] reported that residual concentrations of tetracycline were in the range of 0.15 to 0.97 μg L^{-1} in the final effluents of eight water treatment plants in Canada. The problem of incomplete removal is that the residual antibiotic can enter surface waters and eventually reach groundwater. Thus, to protect human health, it is essential to find efficient techniques to completely remove antibiotics from wastewater [3].

2.3.2 Recent treatment approaches

New alternative treatments such as membrane separation, adsorption, and advanced oxidation processes have been shown to remove antibiotics effectively [3, 17]. Despite their superiority over traditional methods, these treatment methods have some drawbacks. In advanced oxidation processes, antibiotics are degraded by highly reactive hydroxyl radicals. However, advanced oxidation processes require high energy and specific reactor designs, and are not flexible for treating wide range of contaminated water [3]. These drawbacks limit the application of advanced oxidation processes in industrial wastewater treatment. The membrane process is a separation method that transfers antibiotics into a more concentrated phase. Although membrane processes have shown high efficiency in antibiotic removal, structural damage and fouling have limited their long-term application, especially in the treatment of more-concentrated water [3].

The adsorption process transfers antibiotics from the liquid phase to the solid phase (the adsorbent surface). This process can be used to remove a wide range of antibiotics with different physicochemical properties from water. Additionally, the adsorption process can be used to treat water containing high antibiotics concentrations. Many studies suggest that adsorption process is one of the most efficient methods for antibiotics removal from water [3].

2.4 Adsorption process

Although adsorption is a well-known process, its application in removal of antibiotics has not been extensively studied. Adsorptive removal of antibiotics refers to the adhesion of antibiotic molecules from contaminated water to an adsorbent surface, involving chemical and/or physical adsorption. Depending on the composition of the waste stream, different

types of adsorbents can be used for antibiotic removal. The most studied adsorbents include activated carbon, carbon nanotube, bentonite, biochar and ion exchange resins [7, 18].

Among various adsorbents used for antibiotic removal, activated carbon has received great attention. Activated carbons usually have high adsorption capacity and can remove a wide range of antibiotics. The high adsorption capacity of both powdered and granular activated carbons is related to their well-developed surface area and high microporosity. The effectiveness of activated carbon in removing antibiotics through adsorption largely depends on the properties of the chosen activated carbon, such as the specific surface area, pore structures, surface polarity and functionality, as well as characteristics of the adsorbate compound, such as shape, hydrophobicity and charge [7, 18].

So far, several mechanisms have been proposed to explain the adsorption of antibiotics onto the carbon-based adsorbents such as activated carbon. Using the proposed mechanisms, antibiotics are adsorbed into carbon-based adsorbents mainly through electrostatic interaction, hydrophobic interaction, π–π interactions, hydrogen bonds, partition to uncarbonized fractions, surface precipitation and pore filling [17].

The adsorption process is an effective technique for removing tetracycline from contaminated water. So far, various types of adsorbents have been developed and their efficiency in tetracycline removal have been studied, including alkali bio-char [18], HCl-modified zeolite [19], graphene oxide [20], anaerobic granular sludge [21] and activated carbon [22]. Among developed adsorbents, activated carbon is one of the most promising adsorbents when its preparation cost and adsorption capacity toward tetracycline are considered [22].

In 1968, Ezra and Coughlin [25, 26] reported that the adsorption of aromatics on activated carbon is largely governed by π–π interactions. This finding suggests that tetracycline is adsorbed on activated carbon mostly due to π–π interactions between π electrons of the activated carbon and π electrons of the tetracycline aromatic ring. In addition to π–π interactions, the formation of hydrogen bonds between the oxygenated groups of activated carbon and the phenolic groups of tetracycline favour this adsorption [23].

Although lincomycin is often detected in water resources, few studies have focused on its adsorptive removal from water. One of these few studies was published in 2014 by Hyunook Kim et al. [25]. They studied the adsorption of lincomycin onto carbon-based adsorbents including activated carbon, single-wall carbon nanotubes and multi-walled carbon nanotubes in water. Based on their findings, the kinetics of lincomycin adsorption onto activated carbon can be divided into two different processes; first, the initial adsorption of

lincomycin to outer surfaces; second, slow diffusion of lincomycin into interlayers of activated carbon. Although they have not investigated the mechanism of lincomycin adsorption, they suggest that since pharmaceuticals like lincomycin are highly hydrophilic, hydrogen bonds and electrostatic interactions may contribute to this adsorption process [25].

2.4.1 Factors affecting the adsorption process

2.4.1.1 Nature of the adsorbent

Different types of adsorbent materials, such as zeolites, carbon-based materials, metal-organic frameworks (MOFs) and clays, can be used to remove antibiotics from aquatic media. Although adsorbents categorized in the same family of materials have some similarities in their adsorption performance, each one has unique characteristics. In the case of activated carbon, for example, the source of raw materials (e.g. coconut shells, different type of wood or bituminous coal), the method of carbonization (reactor temperature and holding time) and the method of activation (base, acid or steam) determine the important physiochemical characteristics [26]. The surface chemistry, the chemical composition and the pore shapes and porosity are among these characteristics [26]. The surface chemistry of activated carbon controls the intermolecular interaction between the adsorbent and adsorbate. Naturally, the surface of activated carbon is hydrophobic but this can vary depending on the applied activation method [27]. The particle size can affect the adsorption kinetics by controlling the diffusion pathways; the smaller particle size, the shorter diffusion pathways. Moreover, the pore size distribution determines the accessibility of adsorption sites inside the porous structure. Molecules cannot diffuse into the pores that are smaller than the molecular diameter [26].

2.4.1.2 Nature of the adsorbate

The adsorbate properties such as polarity, hydrophobicity, aromaticity and molecular weight determine its interaction with the adsorbent [30, 31]. In the case of adsorption by activated carbon, the affinity of adsorbate to activated carbon can vary largely depending on the adsorbate properties. According to the literature, activated carbon can most effectively remove more hydrophobic, non-polar, uncharged compounds with a lower solubility in water, which is indicative of their higher affinity to carbon surface than that of water [28].

2.4.1.3 Operating conditions

The findings of many studies indicate that adsorption of antibiotics more or less depends on the initial concentration of antibiotics, the pH of the solution, the environment temperature, contact time, and the dosage of adsorbent [30].

The initial concentration of antibiotics is an important parameter in adsorption process as a given mass of adsorbent can only adsorb a specific amount of antibiotics. In general, the percentage of antibiotic removal is higher at lower initial concentrations. In this condition, the adsorbent surface still has unoccupied active sites, while by increasing the initial concentration of antibiotics, the active sites required for the adsorption of the antibiotics will be lacking. On the other hand, the actual amount of antibiotic adsorbed per unit mass of an adsorbent will increase by increasing the concentration of the antibiotics. From mass transfer point of view, this can be explained by the relatively high driving force at higher initial concentrations [30].

The pH value of the solution is another important parameter affecting the interaction between the adsorbent and adsorbate by determining the surface charge of the adsorbent. The pH of system can affect the surface properties of the adsorbent as well as ionization or dissociation of the adsorbate molecule [30]. Therefore, the pH value has a profound effect on the adsorptive uptake.

Depending on the nature of the adsorption process, temperature as an important operational parameter can control the adsorption process. Higher temperatures are in favour of adsorption processes with endothermic nature. This means that, in higher temperatures, the favorable intermolecular forces between adsorbate and adsorbent are much stronger than those between adsorbate and solvent. In contrast, exothermic adsorption process occurs more readily at lower temperatures (Le-Chatelier's Principle) [31].

Generally, the amount of adsorbed materials on adsorbent increases with increasing the contact time until reaching the equilibrium state, and since then a further increase in contact time will not increase the adsorption uptake. The time needed to reach the state of equilibrium is referred to as the equilibrium time. At this point, the rate of the antibiotics being adsorbed onto the adsorbent is in a dynamic equilibrium with the rate of the antibiotics desorbing from the adsorbent [30].

Moreover, the percentage of antibiotic removal increases by increasing the adsorbent dosage - not necessarily linearly. Afshin et al. [32], for example, investigated the effect of dosage of $ZnCl_2$-impregnated activated carbon in the range of 0.25 to 3.5 g L^{-1} on the rate of

tetracycline removal. They found that the removal percentage of tetracycline from 50 mg L^{-1} solution when 1, 1.5 and 3 g L^{-1} adsorbent were added was around 65, 95 and 99%, respectively. According to their results, the rate of increase in adsorption capacity at lower adsorbent dosages was high and by increasing the dosage of the adsorbent it gradually decreased.

Although all the above-mentioned operational factors affect the adsorption process, the magnitude of their impacts can be different for each adsorption process. For instance, Pouretedal and Sadegh [33] studied the adsorption of amoxicillin, tetracycline and penicillin G onto activated carbon prepared from vine wood and activated by NaOH. Their finding suggests that the impact of adsorption variables on the uptake of the antibiotics is followed by the order of initial concentration > the dosage of activated carbon > the pH of solution > the ambient temperature.

2.4.1.4 Adsorption media

The properties of the water matrix such as pH, ionic force, and its mineral and organic content have influence on the surface chemistry of both activated carbon and the adsorbate. For example, the presence of natural organic matters in water generally reduces the removal efficiency of activated carbon toward target molecules. This happens because of the direct competition between the targeted molecules and natural organic matters for occupying the adsorption sites and/or unavoidable blockage of accessible pores by the organic matters [26].

As the number of components within a matrix increases, the adsorption media become more complex. Manure can be considered as an example of adsorption media with a high level of complexity. Karine et al. [34] provided a list of components within the real liquid swine manure. Based on their results, liquid swine manure mainly consists of sodium propionate, sodium acetate, lactic acid, ethanol, ammonium bicarbonate, potassium phosphate and potassium sulphate [34].

2.4.2 Magnetic adsorbents

Adsorption by granular activated carbon is one of the most commonly used processes used in large-scale water treatment. However, powder activated carbon is considered to be a more efficient adsorbent than granular activated carbon for the removal of contaminants. Although powder activated carbon is a more effective adsorbent for removing contaminants

from a continuous flow system, its large-scale application has been limited because it causes turbidity in effluent and requires extra separation processes such as filtration [4, 5]. These processes can also lead to the loss of the solid particles or the blockage of filters. One creative approach to address this disadvantage is the development of magnetic powder activated carbon which can be magnetically separated from water after treatment.

Generally, the application of magnetism for water treatment is an established concept, reported back in the mid-19th century [35], and since then it has been used for different water treatment methods such as coagulation [36], and biological processes [37,38]. However, the application of magnetism for the adsorption process is a relatively new concept receiving increasing attention in the field of water treatment. For example, the rate of publications on magnetic activated carbon has been increased since 2002. In 2017, the number of publications on magnetic activated carbon was ten times higher that of 2006 [39].

Magnetic adsorbents show magnetic behavior due to the presence of magnetic particles in their structures. Although magnetic metals such as Fe, Ni, and Co can introduce magnetic properties to adsorbents, oxides of these metals are mostly preferred as they are more stable [40]. So far, different types of absorbents such as zeolites, ion exchange resins, activated carbon, polymeric adsorbents, and even nanoparticles have been magnetized [35].

In contrast to traditional adsorbents, which are mostly removed by screening, magnetic adsorbents can be effectively separated from waste streams just by applying an external magnetic field [41]. Magnetic filtration, which can be used as one step in water treatment plant, rapidly and effectively removes used magnetic adsorbents from aqueous waste streams [41]. This way of separation, is also space-saving and no chemical is involved in it [39]. These advantages of magnetic adsorbents over traditional adsorbent have led scientists to develop different low-cost, magnetic adsorbents with relatively high adsorption capacity and wide selectivity to various environmental contaminants.

In this work, the word "magnetization" refers to a process in which iron oxide particles are deposited into a material to prepare a magnetically separable adsorbent. Even though the main purpose of magnetization is developing an adsorbent that can be easily separated, it also provides the possibility of reusing the spent adsorbent after magnetic recovery. The regeneration of adsorbent is more applicable for expensive adsorbents. Based on the literature, one of the most common approaches for desorption of adsorbate from adsorbent is extraction using an appropriate organic solvent [42]. Beside extraction, thermal, chemical and electrochemical methods have also been used for this aim [43].

2.4.2.1 Magnetic separation in water treatment

Magnetic separators can generate magnetic field using permanent magnets based on iron, nickel, cobalt or rare earth compounds, and they can be categorized as low, medium or high intensity separators. When it comes to magnetic powder activated carbon, high intensity/high gradient separators are needed to provide enough magnetic force to allow the separation from the liquid flow. The magnetic field is measured in amperes per metre (A/m) and oersteds (Oe) in SI and CGS units, respectively [44]. High gradient magnetic separators (HGMS) can provide a magnetic fields of 1600 kA/m, which is around 10 times higher than those of low intensity separators, as well as gradients in the range of 16000 to 160000 MA/m ^{2}, which is around 104 times higher than those that are mostly generated by electromagnets [45]. In the case of wet separation, there are various types of HGMS such as the Jones separator and matrix-loaded separators that can provide high gradients with completely inhomogeneous fields[46]. The matrix-loaded HGMS is made of filter filled with fine particles. To separate the particles, the magnetic field is switched on and then the fluid is passed through the matrix. After one cycle of separation, the magnetic field is removed and then backwash takes place to flush out the magnetic adsorbent [47]. HGMS have high separation efficiency, even at relatively high flow rates, and they show low pressure drops across the filter [48]. Therefore, a matrix-loaded HGMS is a promising separator for removing magnetic powdered activated carbon from drinking water treatment plants.

2.4.2.2 Magnetic states

The magnetic states of materials can be classified into different classes including ferromagnetism, ferrimagnetism, superparamagnetism and diamagnetism. Herein, a short overview of different magnetic states is offered to clarify the interactions between magnetic materials and magnetic fields in particle.

The saturation magnetisation (M_S) is defined as the maximum amount of field that can be generated by a magnetic material. In the case of ferro- and ferrimagnetic materials, magnetic separation is relatively simple as they can be strongly attracted by a magnetic field due to their relatively high M_S. Iron, iron oxides (maghemite and magnetite), nickel and cobalt are classified into these magnetic states. These materials form small regions of uniform alignment that tend to minimize the overall magnetic energy. In exposure to the magnetic field (H), the orientation of these domains would become aligned parallel to the applied magnetic field, (Figure 3). As a consequence, ferro- and ferrimagnetic materials are attracted

by the North- and South Pole of the magnet. Another important characteristic of ferro- and ferrimagnetic materials can be explained by a phenomenon referred to as remanence. In fact, the magnetization of these materials increases by escalating magnetic field strength until the saturation level, but it does not disappear completely after removing the magnetic field (Figure 4, panel a). The remanent magnetization (M_R) causes so-called typical hysteresis loop. The opposite magnetic field can be applied to remove the remaining magnetization. The magnitude of the opposite magnetic field is referred to as coercively (H_C).

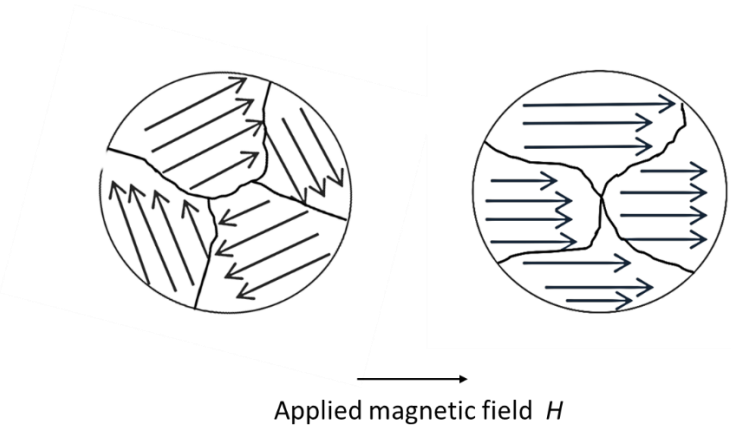

Figure 2.3 The orientation of the domains within ferromagnetic materials in a magnetic field

When the particle size of ferro- or ferrimagnetic materials is sufficiently small (usually smaller than 20 nm), superparamagnetic behaviours dominate below the critical temperature. At this magnetic regime, when no field is applied, thermal fluctuations of the magnetization for each particle cancel out the average magnetization. Consequently, the magnetization curve of superparamagnetic materials does not show hysteresis (Figure 4, panel b). In this case, no remnant magnetization remains after removing the magnetic field [44]. This phenomenon makes this class of materials highly attractive for water treatment applications because they can easily be re-dispersed in water without forming agglomerates after removing the magnetic field.

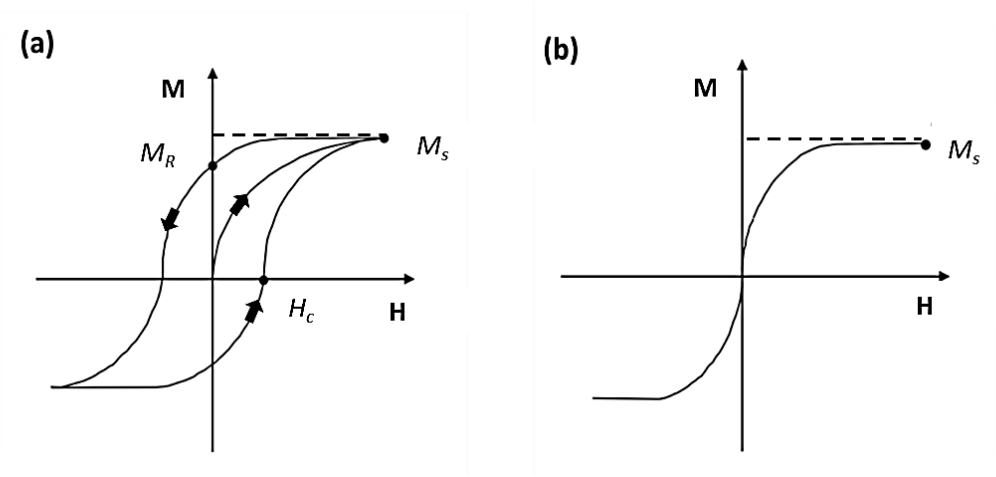

Figure 2.4 Typical hysteresis curve of ferro- and ferrimagnetic materials (a), typical magnetization curve of superparamagnetic materials (b)

On the other hand, diamagnetic materials show an extremely weak magnetization, which is antiparallel to the applied magnetic field. For example, activated carbon is a diamagnetic material as it is not attracted by a magnet. Therefore, the magnetic separation of activated carbon particle is possible only if they are seeded with magnetic particles.

2.4.2.3 Deposition of magnetic nanoparticles

In order to magnetize adsorbents, magnetic particles, mostly iron oxides, are deposited into the structures of the adsorbents. Different iron oxides can be formed during the oxidation reactions such as Fe_3O_4 (magnetite), γ-Fe_2O_3 (maghemite) and α-Fe_2O_3 (hematite), but only Fe_3O_4, and γ-Fe_2O_3 iron oxides show strong magnetic behaviours [49]. Fe_3O_4 particles have higher saturation magnetization compared to the γ-Fe_2O_3 particles [50]. On the other hand, γ-Fe_2O_3 particles are more stable than Fe_3O_4 when it comes to oxidation. Fe_3O_4 particles can be oxidized to different phases of Fe_2O_3 depending on applied oxidation condition. In other words, the stability of Fe_3O_4 particles with respect to oxidation is considered a practical problem affecting its long-term applications while γ-Fe_2O_3 particles are more stable to further oxidation [51].

There are different methods for synthesis of magnetic particles. Among these synthesis methods, precipitation and impregnation are more commonly studied in the literature [52]. Regardless of the preparation methods, three approaches have been applied so far to develop magnetic activated carbon using iron oxide particles. The first approach is a one-pot synthesis of magnetic adsorbent (concurrent activation and magnetization processes).

For example, André L et al. [53] used carbonized coconut shell and $FeCl_3$ to synthesize magnetically activated carbons with simultaneous activation and magnetization processes. Their findings suggest that the prepared sample was sufficiently magnetized to be separated by a magnet. They also found that the magnetite phase as a major crystal phase is formed into the carbon matrix [53]. The second approach is the in-situ formation of iron oxide particles into the prepared or commercial activated carbon. The last approach is the synthesis of magnetic iron oxide particles separately, and then depositing them into activated carbon. Among the procedures that have been used for developing magnetic activated carbons, in-situ co-precipitation of iron precursors into activated (approach 2) and impregnation of magnetic nanoparticles into activated carbon (approach 3) can be considered as the main routes [52].

In addition to the synthesis procedure, the iron oxide content is an important factor affecting both adsorption capacity and magnetic property of the prepared adsorbent. Manh Huy Do et al. [54] magnetized activated carbon with different contents of Fe_3O_4 (5 to 30 wt%). They found that although using the high content of iron oxide boosted the saturation magnetization of the prepared adsorbent, it decreased the adsorption capacity due to the loss of surface area [54].

2.4.2.4 Long-term stability

Long-term stability of magnetic properties is a decisive factor in choosing an appropriate magnetic adsorbent for industrial applications. According to the literature, the magnetic properties of magnetic activated carbon can significantly change over time. Lee et al. [55], for example, investigated the stability of magnetic activated carbon in exposure to air for 5 months. Based on their observation, the saturation magnetization of the adsorbent decreased by around 50% after 5 months at 2 K [55]. In another study, the performance of Fe_3O_4-activated carbon composite that was stirred in water almost remained constant for two months [5]. Naturally, there are two main parameters affecting the magnetic properties of adsorbent during the adsorption process: first, oxidation of iron oxide particles, and second, dissolution of iron oxide particles.

Magnetite iron oxide particles are not very stable and can be easily oxidized to maghemite under ambient conditions [41]. For example, the oxidation to maghemite in the presence of bacteria in water was investigated by Auffan et al.[56]. According to their investigation, this phenomenon can be attributed to the high electrons mobility within the Fe(II)/Fe(III) structure of magnetite [56]. Interestingly, the oxidation of magnetite to

maghemite is not a constraint for magnetic adsorbent applications since maghemite is a ferrimagnet that possesses similar magnetic behaviours as magnetite [57].

Dissolution of iron oxide particles, besides oxidation, can affect the stability of magnetic adsorbent. Zahoor and Mahramonlioglu [58] studied the effect of this parameter in the pH range of 1 to 8. They found that, for magnetic activated carbon, dissolution occurred below pH 4.8, and it led to the loss of iron content [58]. They also reported that abrasion, which may occur because of shear forces during pumping and mixing, can be considered as another influencing parameter that has not been studied yet. Also, the effect of colonization of iron oxide particles in long-term applications is another important issue that has not been investigated so far [39].

Based on the literature review, many efforts have been done to understand the adsorptive removal of tetracycline and lincomycin from water, but still, there are some important questions that require answers to improve our knowledge. As mentioned, the only study that investigated the adsorption of lincomycin onto activated carbon was reported by Hyunook Kim et al., in 2014 [25]. This study investigated the adsorptive removal of lincomycin from water at 20 ± 1 °C. It would be interesting to also know the effect of temperature on the adsorption to determine whether this adsorption is an endothermic or exothermic process. Regarding tetracycline, Martins et al. [59] studied the adsorptive removal of tetracycline from water in the concentration range of 250-800 mg L^{-1} using activated carbon. Zhu et al. [60] also did the same investigation but in the concentration range of 5-80 mg L^{-1}. Similarly, many other studies have been done in this area, but they also focused either on low or high concentrations of tetracycline. Moreover, despite the fact that tetracycline and lincomycin commonly co-exist in livestock operations, the behaviour of binary adsorption system is still unknown. Also, the possibility of direct removal of lincomycin or tetracycline from animal manure has not been investigated yet.

2.4.3 Adsorption models

The performance of adsorbent in removal of pollutant is usually investigated through batch experiments at the equilibrium time. Generally, equilibrium is referred to the state that the concentration of the adsorbate in the liquid phase reaches a constant value. The adsorption capacity of a specific adsorbent in equilibrium is related to the temperature and the adsorbate concentration. This relation can be explained by an adsorption isotherm recorded at a constant temperature [61].

$$q_{eq} = f(c_{eq}) \qquad T = constant \qquad \text{Eq. 2.1}$$

Where q_{eq} is the adsorption capacity of adsorbent in equilibrium time. The value of q_{eq} can be obtained from the initial and final concentrations of the solute (C_0 and C_{eq}), solute volume (V_L) and the mass of adsorbent (m), according to the following formula:

$$q_{eq} = \frac{V_l}{m}(c_0 - c_{eq}) \qquad \text{Eq. 2.2}$$

In general, Langmuir and Freundlich models are among the two-parameter models that are most frequently used to model adsorption data in the literature.

In Langmuir isotherm, it is assumed that the adsorbent surface is covered by a monolayer of adsorbate balancing the relative rates of adsorption and desorption with dynamic equilibrium. It is assumed that the adsorption rate is proportional to the fraction of the adsorbent surface that is uncovered, while the desorption rate is proportional to the fraction of adsorbent surface that is covered. Additionally, this model accounts for the homogenous surface with equivalent sites [61]. The Langmuir equation is presented as follow:

$$q_{eq} = \frac{(q_{max}\, k_l c_{eq})}{(1+k_l c_{eq})} \qquad \text{Eq. 2.3}$$

Where q_{max} and k_l are maximum adsorption capacity and Langmuir constant, respectively.

The linear form of Langmuir equation can be written as follow:

$$\frac{c_{eq}}{q_{eq}} = \frac{1}{q_{eq} k_l} + \frac{c_{eq}}{q_{eq}} \qquad \text{Eq. 2.4}$$

The parameters q_{max} and k_l at Langmuir isotherm (Eq. 2.3) are temperature dependent and are mostly obtained through linear or non-linear regression methods [62].

The temperature dependence forms of q_{max} and k_l Langmuir isotherm parameters can be written as below:

$$q_{max} = q^o_{max} \exp(\delta(T - T_0)) \qquad \text{Eq. 2.5}$$

$$k_l = k^o_L \, exp\left(\frac{-\Delta H}{RT_0}\right) \qquad \text{Eq. 2.6}$$

Where q^o_{max} and δ are the maximum adsorption capacity of adsorbent at T_0 and the expansion coefficient of adsorbate, respectively. The k^o_L parameter is the adsorption affinity of the Langmuir isotherm at reference temperature (T_0). ΔH represents the enthalpy change during the adsorption process. 275 K is mostly considered as the reference temperature [63].

Moreover, Langmuir isotherm is not limited to single-solute adsorption. Based on various assumptions, Langmuir isotherm has been extended in different forms for multi-solute adsorption. Jain and Snoeyink proposed an extension of the Langmuir equation for binary mixtures [62]. They assume that both components are adsorbed on the same fraction of adsorption sites. Based on this assumption, they derived the following equations:

$$q_{e,1} = \frac{(q_{max,1} - q_{max,2}) k_{L,1} C_{e,1}}{1 + k_{L,1} C_{e,1}} + \frac{q_{max,2} k_{L,2} C_{e,2}}{1 + k_{L,2} C_{e,2} + k_{L,1} C_{e,1}} \quad \text{Eq. 2.7}$$

$$q_{e,2} = \frac{q_{max,2} k_{L,2} C_{e,2}}{1 + k_{L,2} C_{e,2} + k_{L,1} C_{e,1}} \quad \text{Eq. 2.8}$$

Where all parameters are specified with the index corresponding to the component number.

Freundlich isotherm is an empirical model, which is applicable to adsorption processes that take place on heterogonous surfaces. Freundlich isotherm accounts for surface heterogeneity as well as the exponential distribution of active sites and their energies [61]. The Freundlich equation is presented as follow:

$$q_{eq} = k_f \, c_{eq}^{1/n} \quad \text{Eq. 2.9}$$

Where k_f characterizes the strength of adsorption and n determines the curvature of the isotherm. The Freundlich equation can be also written with the following linear form:

$$log q_{eq} = log k_f + \frac{1}{n} \, log c_{eq} \quad \text{Eq. 2.10}$$

2.4.4 Adsorption thermodynamic characterization

In addition to fitting adsorption data with established isotherm models, the thermodynamic characteristics of the system can be studied in the equilibrium state. From a thermodynamic point of view, parameters like enthalpy, entropy and Gibbs free energy change can provide useful information about the strength of bonding, spontaneity, mechanism and the endothermic or exothermic nature of the adsorption process [64]. To determine thermodynamic parameters, the equilibrium constant value should be calculated first [64]. The following sections present a brief review of the thermodynamic parameters, with special focus on the methods that can be used to determine the thermodynamic equilibrium constant.

2.4.4.1 Fundamentals of the adsorption thermodynamics

Gibbs free energy change as well as adsorption enthalpy, and entropy changes are the most important thermodynamic parameters that describe an adsorption process. The thermodynamic equations that can be used to determine these parameters are presented as follow:

$$\Delta G^0 = -RTlnK_c \quad \text{Eq. 2.11}$$

$$ln\,K_c = -\frac{\Delta H^0}{RT} + \frac{\Delta S^0}{R} \quad \text{Eq. 2.12}$$

$$\Delta G^0 = \Delta H^0 - T\Delta S^0 \quad \text{Eq. 2.13}$$

Where R is the universal gas constant (8.314 J mol^{-1} K^{-1}), K_c is the thermodynamic equilibrium constant (dimensionless), and T is the temperature (K). The variation of the enthalpy and entropy are linked by the van't Hoff equation (Eq. 2.12). This equation can be used to determine variations of the enthalpy and entropy based on the slope and the intercept of the linearized variation of ln K_c with T^{-1}.

The value of Gibbs free energy change explains the spontaneity of the process. A negative value of this energy change is indicative of a spontaneous adsorption process. The greater negative absolute value of Gibbs free energy change, the more favourable is the adsorption process. In contrast, the positive value of this energy change indicates that the adsorption process will not occur spontaneously [65].

Enthalpy change, which is also referred to as the heat of adsorption, can be used to determine the exothermic or endothermic nature of the adsorption process. A negative value of enthalpy change for an adsorption process is indicative of its exothermic nature. This thermodynamic parameter can also differentiate between chemical and physical adsorption and provide information about the type of bonding. Generally, it is known that the enthalpy change with values higher than 80 kJ mol^{-1} indicates chemisorption and lower values of enthalpy change corresponds to physisorption [66].

In general, in chemical adsorption, the main type of binding force is chemical bonds, while physical adsorption is mostly governed by Van der Waals force. Also, physical adsorption is fully reversible as a result of its weak bonding force, while chemical adsorption is an irreversible process. Additionally, although chemical adsorption induces monolayer coverage, in the case of physical adsorption, multilayer coverage can also occur [66]. Entropy is indicative of randomness in a system. The positive change of this thermodynamic parameter represents the increase of randomness in the solid-liquid system [67].

2.4.4.2 Determination of thermodynamic parameters

According to the Eq. 2.11 and 2.12, the principal thermodynamic parameters can be calculated based on the equilibrium constant. The important point is that the value of this thermodynamic constant can vary depending on the mathematical method used for its determination. So far, different methods have been proposed to determine the equilibrium constant. One simple method is to assume that the value of the equilibrium constant is equal to the Langmuir constant. Although this method is the easiest procedure, it is not very reliable because the Langmuir constant has a unit (L mg^{-1}), while the thermodynamic equilibrium constant is dimensionless [68].

The other method is finding the equilibrium constant using the distribution coefficient. This method was first proposed by Khan and Singh [69] and then modified by Milonjic' [70]. In this method, the distribution coefficient is identified by the following equation:

$$K_d = \frac{q_{eq}}{C_{eq}} \qquad \text{Eq. 2.14}$$

Where K_d (L g^{-1}) is the distribution coefficient, and C_{eq} (mg L^{-1}) and q_{eq} (mg g^{-1}) are the adsorbate concentration and adsorption capacity at equilibrium, respectively [68].

Based on Henry's law, the distribution coefficient value can be found from the plot of $\ln(q_{eq}/C_{eq})$ versus C_{eq}. In this method, the intercept is the distribution coefficient value. [68].

However, this method still has the same problem as the first method regarding the incompatibility of the units. The thermodynamic equilibrium constant proposed by this method still has a dimension (L g^{-1}). To solve this problem, Milonjic' suggested that if the value of the equilibrium constant is multiplied by the density of water at 25 °C (1000 g L^{-1}), it may be considered as a dimensionless constant [70]. Therefore, it was concluded that the equilibrium constant value can be calculated through the following equation:

$$\Delta G^0 = -RTlnK_L = -RTln(1000 * K_d) \qquad \text{Eq. 2.15}$$

2.5 Knowledge gaps and research objectives

2.5.1 Knowledge gaps

The negative consequences of the presence of tetracycline and lincomycin on the environment, especially development of antimicrobial resistance, have been extensively discussed in the literature. The advantages of the adsorption process in removal of antibiotics from the aquatic environment are also known. However, there are still knowledge gaps and

challenges regarding the adsorptive removal of tetracycline and lincomycin antibiotics from wastewater, which are listed below:

- Although lincomycin has been frequently detected in the environment, just a few studies have focused on the adsorptive removal of this antibiotic, and as a result, much of this process is still unknown.
- Despite the advantage of magnetic activated carbon in terms of the ease of separation after the treatment, its performance in the adsorptive removal of lincomycin has not been investigated and understanding of the process for tetracycline is not thorough because most of the previous studies were done at a limited range of concentrations.
- Although actual wastewaters are contaminated by different types of antibiotics, most of the previous research studies focused on the adsorptive removal of single antibiotic from water.
- Despite the considerable concentration of tetracycline and lincomycin in the waste stream of livestock production facilities, the direct adsorption of these antibiotics from manure slurry has not been studied.

2.5.2 Objectives

This study aimed to develop magnetic activated carbon to remove two commonly used antibiotics, tetracycline and lincomycin, first from water and then from liquid swine manure supernatant. Herein, the main objective is the synthesis of a magnetic activated carbon which not only shows high adsorption capacity toward the two targeted antibiotics but can also be easily separated after the adsorption process by applying an external magnetic force. By considering the above-mentioned knowledge gaps, the objectives of this study are as follows:

1. Preparation and characterization of magnetized activated carbon through the incorporation of iron oxide nanoparticles.
2. Evaluating the performance of the prepared magnetic adsorbent in treatment of waters contaminated by tetracycline and lincomycin either individually or as a mixture.
3. Investigating the possibility of direct adsorptive removal of the antibiotics from the waste stream of livestock production facilities.

3 MATERIALS AND METHODS

The following chapter first specified materials used during the magnetization procedure and in adsorption experiments. Second, adsorbent preparation, experimental procedures and analytical methods are described in detail.

3.1 Materials

Crystalline powder tetracycline (93%, $C_{22}H_{24}N_2O_8$) and lincomycin hydrochloride (95%, $C_{18}H_{34}N_2O_6S.HCl$) were purchased from Alfa Aesar (MA, USA). Commercial granular activated carbon (Norit GAC1240, M-2125) was purchased from Cabot Norit American Inc. (TX, USA). Iron (II) chloride tetrahydrate (98%, $FeCl_2.4H_2O$) was obtained from Alfa Aesar (MA, USA) and iron (III) chloride hexahydrate (98%, $Cl_3Fe.6H_2O$) was purchased from Alfa Aesar (LA, UK). Ammonium hydroxide (NH_4OH) and ethyl alcohol (100%, C_2H_5OH) were purchased from Fisherbrand (ON, Canada) and Greenfield Global (ON, Canada), respectively.

3.2 Procedures

The experimental phase includes preparation of adsorbent, characterization, and batch adsorption experiments, which are described in the following sections.

3.2.1 Adsorbent preparation

As shown in Figure 3.1, the preparation of magnetic adsorbent includes two main steps: preparation and magnetization. The granular activated carbon was pulverized first followed by magnetization as described below. The applied magnetization method followed the procedure offered by Puri et al. [71].

3.2.1.1 Preparation of activated carbon (AC)

The granular activated carbon was first crushed using a mortar and pestle. The resulting powder was separated by metal sieves, 60 and 120 mesh (250-125μm), then it was

washed and filtered four times with deionized water. Finally, the powder activated carbon (AC) was dried at 110°C for 24 h under air flow.

3.2.1.2 Magnetization of AC

Milli-Q water was used as the reaction medium for magnetization. To remove dissolved oxygen from Milli-Q water, it was degassed using N_2 gas and a sonication bath. To obtain around 4 g of magnetic activated carbon (MAC) composite with around 20% iron oxide, 1.84 g of $FeCl_3 \cdot 6H_2O$ and 0.72 g of $FeCl_2 \cdot 4H_2O$ were dissolved in 800 ml of degassed Milli-Q water. Then, 3.2 g of AC was dispersed in the solution using a sonicator probe for 10 min. The solution was put in the sonication bath at 50°C and ammonium hydroxide was introduced dropwise as a precipitant to the solution using a burette until the pH reached 10. After 50 min of aging, the resulting powder was filtered and washed with deionized water several times until the pH of supernatant reached 7. Thereafter, the sample was washed using ethanol, filtered and finally dried in an oven at 70 °C for 1 h.

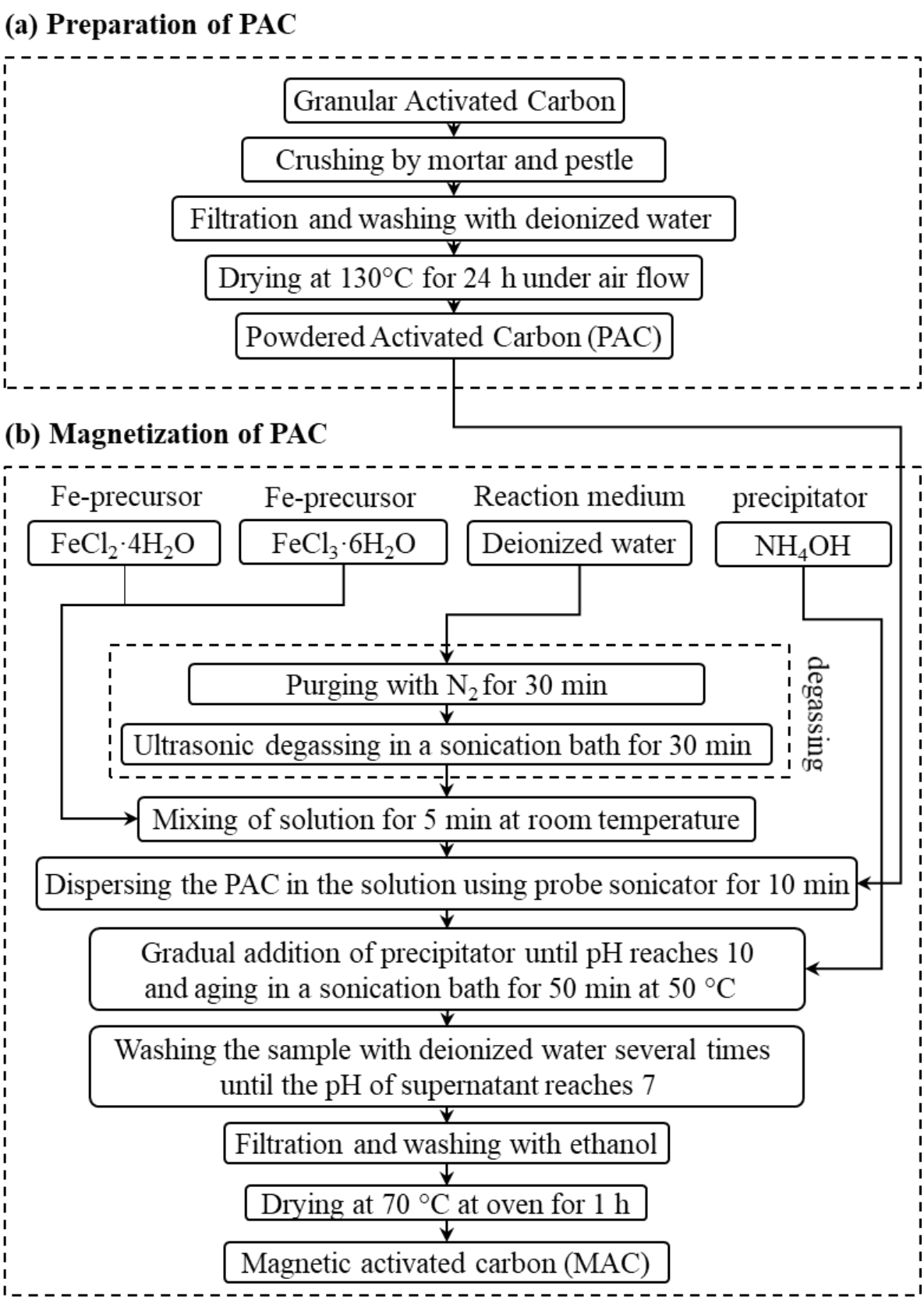

Figure 3.1 Schematic of MAC synthesis procedure

3.2.2 MAC Characterization techniques

To obtain a proper understanding of the physiochemical properties of the adsorbent, the developed MAC was characterized using various characterization techniques including X-ray powder diffraction (XRD), X-ray Photoelectron Spectroscopy (XPS), Brunauer-Emmett-Teller (BET)- Barrett-Joyner-Halenda (BJH), field emission scanning electron microscopy (FE-SEM), transmission electron microscopy (TEM), thermal gravimetric (TG), physical property measurement system (PPMS), particle size and zeta potential analyses. The powder AC was also characterized by a number of these techniques to provide useful information about the effects of magnetization. The used characterization techniques along with the information each of them provides are listed in Table 3.1.

Table3.1 List of used characterization techniques along with the information they provide

Characterization techniques	**Information**
XRD-XPS	Crystalline and electronic structures
BET-BJH	Surface area and pore volume distribution
FE-SEM, TEM	Morphology and iron oxide particle size
TG	Iron oxide content
XPS	Surface composition
PPMS	Magnetic properties
Particle Size Analyzer	Particle size distribution
Zeta Potential Measurement	Surface electrical charge

3.2.3 Determination of magnetic separation efficiency

Different approaches can be used to investigate the magnetic separation efficiency of MAC in either batch or continuous adsorption systems. Herein, a simple method was used to study the separation effectiveness for the prepared magnetic adsorbent from water in a batch system. For this purpose, 1g of MAC was added into a beaker containing 100 ml deionized water, and the beaker contents was then vigorously mixed. After agitation, a block magnet was vertically placed next to the beaker for 24 h. Afterwards, while the magnet was still kept in place, the beaker was tilted to remove water containing MAC particles that were not attracted to the external magnet. To dry remaining adsorbent out, the beaker was placed in the

oven at 70 °C for 12 h. The resulting sample was considered as a portion of the adsorbent that was magnetically separated, and its weight was measured and referred to as m_s.

Once again, this procedure was similarly repeated, except for the magnetic separation step. This time, the magnetic sample was separated from water using an appropriate filter paper that would not allow MAC particles to pass. The weight of the resulting sample was measured after a similar drying step. The measured weight was used for calculating the separation efficiency as a reference and referred to as $m_{ref.}$

The magnetic separation efficiency (% E) was calculated as follow:

$$E = \frac{m_s}{m_{ref}} \times 100 \qquad \text{Eq. 3.1}$$

3.2.4 Adsorption experiments

The performance of the prepared adsorbent in adsorptive removal of the antibiotics from both water and liquid manure supernatant were studied. Adsorption experiments were carried out at natural pH of the solutions, and no pH adjustment was applied.

3.2.4.1 Adsorption experiments in water

The batch adsorption experiments in water were carried out in four stages: first, the equilibrium time was determined ; second, the adsorptive removal of tetracycline from water was investigated at different temperatures using both AC and MAC; third, the same adsorption experiments were replicated for lincomycin at room temperature; last, the performances of AC and MAC in treatment of waters contaminated by the mixture of tetracycline and lincomycin were studied.

Equilibrium time

To determine the equilibrium time for individual antibiotics, two solutions of tetracycline (TC) and lincomycin (LM) with concentrations of 100 and 200 mg L^{-1} were prepared and then 100 ml of each solution was added to an amber flask each containing 10 mg of AC or MAC. Flasks were shaken at 130 rpm at room temperature (22 ±2 °C). The adsorption set-up used in this experiment is shown in Figure 3.2. During the experiment 1mL samples were taken from each flask on a bi-daily basis until the concentrations reached a constant value. The minimum time when no detectable change in residual concentration was observed was considered as the adsorption equilibrium time.

In the case of mixture of antibiotics, the experiments were repeated with the solutions containing a mixture tetracycline and lincomycin with the overall concentrations of 100 and 200 mg L^{-1}. The minimum time which the residual concentrations of both tetracycline and lincomycin reach a constant value was considered as the adsorption equilibrium time.

Figure 3.2 The set-up used for adsorption experiments

Adsorption of individual antibiotics

For the batch adsorption experiments, 300 mg L^{-1} stock solutions of tetracycline and lincomycin were prepared using Milli-Q water, and then the solutions were diluted to the concentrations of 20, 40, 60, 100 and 200 mg L^{-1}. In the next step, 100 ml of each of the prepared solutions with 10 mg (100 mg L^{-1}) of AC or MAC was added to 120 ml amber flasks and placed on an orbital shaker at 130 rpm and room temperature. The amount of adsorbent in case of 20 mg L^{-1} tetracycline solution was 5 mg (50 mg L^{-1}) as 10 mg activated carbon could completely remove the tetracycline before the equilibrium time. To evaluate the reproducibility, the experiments with the lowest and highest concentrations (20 and 300 mg L^{-1}) were repeated for MAC at each set of adsorption experiments. The amber colour of flasks prevents photodegradation of tetracycline. The concentration of antibiotic in flasks were determined by regular sampling until the equilibrium time. The first sample was taken right after the addition of the adsorbent and subsequent samples were taken every two or three days. For sampling, 1 mL of contaminated water was withdrawn from each flask and filtered using 0.45 and 0.2 µm nylon syringe filter. Samples were analyzed using high-performance liquid chromatography (HPLC). To investigate the effect of temperature on the adsorptive removal of tetracycline from water, the adsorption experiment was repeated at 5,

15 and 35 °C in the Chemviron temperature-controlled chambers. The resulting data were used to determine the equilibrium adsorption capacity of both AC and MAC under various experimental conditions.

Adsorption from mixture of antibiotics

To study the adsorption process for mixture of antibiotics, different mixtures of tetracycline and lincomycin were prepared with compositions listed in Table 3.2. The rest of the experimental procedures including sampling and analyses were the same as for a single antibiotic. For this set of experiments, the sum of tetracycline and lincomycin concentrations was assumed as the overall concentration. The resulting data were used to determine the equilibrium adsorption capacity of both AC and MAC under various experimental conditions.

Table 3.2 Mixtures of antibiotics used in adsorption experiments

Overall concentration ($mg\ L^{-1}$)	TC concentration ($mg\ L^{-1}$)	LM concentration ($mg\ L^{-1}$)
20	10	10
40	20	20
60	60	60
100	50	50
200	100	100
300	150	150

3.2.4.2 Adsorption experiments in liquid manure supernatant

The batch adsorption experiments in liquid manure supernatant were carried out in three stages: first, a method of preparation for collected manure was prepared; second, the stability of tetracycline in the prepared liquid manure supernatant was investigated; third, the performance of prepared adsorbent in the adsorptive removal of tetracycline from liquid manure supernatant was studied at one concentration.

Manure collection and preparation

Manure was collected from swine barn of the Prairie Swine Centre Inc., Saskatoon, SK. Within the swine barn, manure slurry was collected from the manure pit of a production room allocated to the grower pigs weighing between 25 to 28 kg, which were not treated with

antibiotics. Collected manure was screened using a commercial wire mesh with the pore size of 120 μm and kept in six 10 L containers. The containers were brought to the laboratory at the University of Saskatchewan, and then their contents were transferred into a 60 L container and kept in a refrigerator at 4 ℃.

Before each experiment, manure in the main container was vigorously shaken. Thereafter, 1 L of manure was collected from the container and poured into an Erlenmeyer flask. The Erlenmeyer flask was kept in the refrigerator at 4 ℃ for 24 hours to let suspended particulates settle down. In the next step, 500 mL of the manure supernatant was removed and centrifuged twice. The first and second centrifugations were carried out at 15,000 and 18,000 rpm, respectively, and each batch took 20 min. The resulting manure supernatant was used in the adsorption experiments.

Tetracycline stability in liquid manure supernatant

To study adsorption of tetracycline from liquid manure supernatant, it is necessary to first investigate whether tetracycline concentration remains stable in manure supernatant or it changes over time. For this purpose, manure solutions with tetracycline concentrations of 50 and 160 mg L^{-1} were prepared and antibiotic concentration was monitored over time. To run the experiment, the required amounts of tetracycline were weighted and then added to a flask which contained liquid manure prepared based on the developed procedure. Thereafter, the manure solution was stirred for 2 hours. Finally, 100 ml of the manure solution was poured into an amber-coloured flask. The flask was shaken at 130 rpm and sampled regularly. To prevent tetracycline degradation in samples, they were kept in the freezer at -80℃.

Tetracycline batch adsorption experiment

The adsorptive removal of tetracycline from the liquid manure supernatant was studied at the concentration of 60 mg L^{-1} with three different dosages of AC and MAC (1500, 2500 and 4000 mg L^{-1}). In each experiment, 100 ml of the solution containing 60 mg L^{-1} tetracycline was poured into 120 ml amber flasks and different amounts of adsorbents ware added to them. Flasks were placed on an orbital shaker at 130 rpm at room temperature. During the experiment, 1mL samples were taken from each flask on a daily basis until the concentration of tetracycline reached a constant value. The minimum time when no detectable change in residual concentration was observed was considered as the adsorption

equilibrium time. To prevent tetracycline degradation in samples, they were kept in the freezer at -80℃.

3.2.5 Analytical methods

3.2.5.1 Specifications of characterization methods

MAC was characterized by x-ray diffraction (XRD, Rigaku Ultima IV) operated at 40kV and 44mA. The Joint Committee on Powder Diffraction Standards (JCPDS) was used as a reference for identifying the crystalline structure. The electronic structure of MAC was identified by x-ray photoelectron spectroscopy (XPS, Kratos- AXIS Supra). An accelerating voltage of 15 keV and an emission current of 15 mA were used for the analysis. Brunauer-Emmett-Teller (BET) surface area analysis and Barrett-Joyner-Halenda (BJH) pore size and volume analysis were carried out using Micromeritics ASAP 2020. The morphology of prepared materials was investigated by the high-resolution field emission scanning electron microscope (FE-SEM, Hitachi SU8000), with a voltage of 3keV. Transmission electron microscopy (TEM, Hitachi HT7700) operated with a voltage of 100 keV was also used for morphology study. Additionally, TEM images were used to determine the particle size distribution of iron oxide nanoparticles using ImageJ® processing program. In this method, 100 randomly selected iron oxide particles were fitted into the best circle possible and the radius of the circles is considered as the size of particles. The iron oxide content of MAC was determined using Thermogravimetric analysis (TGA, Q500 V20.13 Build 39). Physical property measurement system (PPMS, DynaCool) was used to characterize the MAC within the magnetic field range from -2 to 2 tesla (kg s^{-2} A^{-1}) at 300 K. The magnetic field was set to sweep with the rate of 500 Oe s^{-1} within the range. Laser diffraction particle size analyzer (Mastersizer 3000, Malvern Panalytical) was also used with stir speed of 2560 rpm. The possibility of separating the MAC from contaminated water was investigated using a simple block magnet (NdFeB, Grade N52). In addition, the pH of adsorption media was determined using a pH benchtop meter (Accumet AE150, Fisher Scientific).

3.2.5.2 Determination of the antibiotics concentration in water

The concentration of tetracycline and lincomycin samples were determined using Agilent HPLC (1200 Series, G1316A Thermostatted Column Compartment (TCC) module) with a ZORBAX column (SB-C18, 4.6 x 150 mm, 5 µm). The mobile phase used for the analysis consisted of 80% KH_2PO_4 (50mM- Potassium phosphate monobasic) and 20%

CH_3CN (acetonitrile), with the rate of 1 mL min^{-1}. For the analysis, the injection volume was set at 20 µL. Tetracycline and lincomycin were detected by HPLC UV detector at the wavelengths of 360 and 200 nm and the retention time of 4.3 ± 0.5 and 3.12 ± 0.5 min, respectively.

During the adsorption experiment, each sample taken from adsorption flask was analyzed by two consequent injections and the average value was considered as the final value. The error bars are calculated based on the variation between two sequential injections of HPLC. Subsequently, these error bars are indicative of the analytical errors, mostly attributed to the quality of HPLC and the accuracy of the developed HPLC method. Concentration values were determined based on the calibration curves developed for each antibiotic. The calibration curves of both tetracycline and lincomycin were plotted and presented in Appendix A.

3.2.5.3 Determination of tetracycline concentration in manure supernatant

The concentration of tetracycline in liquid manure supernatant was determined using the same HPLC and the same column as water experiments. The mobile phase consisted of 85% CH_2O_2 (1 mmolar- Formic acid) and 15% CH_3CN (acetonitrile), flowing through the column at the rate of 1 mL min^{-1}. Tetracycline was detected by HPLC UV detector at the wavelengths of 360 nm, and the retention time of 7 ± 0.5 min. For the analysis, the injection volume was set at 20 µL.

During the study of tetracycline stability, the adsorption flasks was sampled twice and then each sample was analyzed by two consequent injections. As a result, each test had four HPLC results, which their average value was considered as the final value. Also, the error bars were calculated based on the standard deviation between two samples.

During the adsorption experiment, each adsorption flasks was sampled and then analyzed by two consequent injections. Since in this study each adsorption experiment had a duplicate, every single test had four HPLC results, which their average value was considered as the final value. Also, the error bars were calculated based on the standard deviation between two adsorption tests. Eventually, the concentration of tetracycline in liquid manure supernatant was determined based on the developed calibration curve presented in Appendix A.

3.2.6 Analysis of Adsorption Data

The following equation was used to determine the adsorption capacity.

$$q_e = \frac{(C_0 - C_e)V}{M} \quad \text{Eq. 3.2}$$

Where q_e (mg g^{-1}) represents the amount of adsorbate per gram of adsorbent at equilibrium. C_0 (mg L^{-1}) and C_e (mg L^{-1}) are the initial and equilibrium concentrations of adsorbate in solution, respectively. V (L) is the volume of solution and M (g) indicates the mass of adsorbent.

In this research study, Langmuir and Freundlich isotherms were used to model the experimental data. The obtained adsorption data were fitted to the Freundlich model using Eq. 2.9 as explained in section 2.4.3. To model the adsorption data, it was always assumed that the adsorption capacity of adsorbents is zero when no antibiotic is added to the solution.

TC adsorption experiments were carried out at four temperatures. The obtained adsorption data were fitted to Langmuir model in two different ways: first, each set of adsorption data was fitted separately to the Langmuir model using Eq. 2.3; second, all sets of adsorption data were non-isothermally fitted to the temperature-dependent form of Langmuir model using Eq. 2.5 and Eq. 2.6. The second approach also provided direct estimation from the enthalpy change of TC adsorption process. Since LM adsorption experiments were carried out only at room temperature, obtained data were simply fitted to Langmuir model using Eq. 2.3.

Binary adsorption data were fitted to non-extended form of Langmuir model using Eq.2.3 and also extended form using Eq. 2.7 and Eq. 2.8. In the non-extended form, the summation of tetracycline and lincomycin concentrations was assumed as the overall concentration in the solution. Also, the summation of tetracycline and lincomycin adsorption capacities was considered as the overall adsorption capacity.

The obtained adsorption data were fitted to the Freundlich and non-extended form of Langmuir model linearly. Also, Excel software was used for nonlinear fitting the experimental data to temperature-dependent and extended forms of Langmuir model. For this aim, the GRC nonlinear function was selected as the solving method. GRG stands for "Generalized Reduced Gradient". This method determines the value of variables in a way that minimizes the objective function (Eq. 3.3). Herein, the objective function was defined as the sum of squares of differences between the experimental and predicted adsorption capacities.

$$f = \sum_i \left(q_{e,i} - q_{p,i}\right)^2 \quad \text{Eq. 3.3}$$

Where q_e and q_p are the experimental and predicted adsorption capacities, respectively. Also, i is an indicator of data point at each initial concentration [68].

R^2 parameter were calculated using Eq.3.4 to discuss how close the adsorption data are to the fitted isotherm line.

$$R^2 = 1 - \frac{\sum_i (q_{e,i} - q_{p,i})^2}{\sum_i (q_{e,i} - q_{e,mean})^2} \quad \text{Eq. 3.4}$$

Where $q_{e,mean}$ refers to the average value of all the experimental adsorption capacities [68].

Additionally, mean absolute percentage error (MAPE) were calculated to measure prediction accuracy of the adsorption models using Eq.3.5. This parameter shows average percentage errors by which adsorption capacities forecasted by a model differ from experimental values.

$$MAPE = \frac{100\%}{n} \sum_{i=1}^{n} \frac{\sqrt{(q_{e,i} - q_{p,i})^2}}{q_{e,i}} \quad \text{Eq. 3.5}$$

4 RESULTS AND DISCUSSION

The following chapter first presents the results obtained from different characterization techniques conducted on the prepared AC and the developed magnetic AC including X-ray powder diffraction (XRD), X-ray Photoelectron Spectroscopy (XPS), Brunauer-Emmett-Teller (BET)- Barrett-Joyner-Halenda (BJH) measurement, field emission scanning electron microscopy (FE-SEM), transmission electron microscopy (TEM), thermal gravimetric (TG), physical property measurement system (PPMS), particle size and zeta potential analyses. The results were interpreted to explain the physiochemical properties of the prepared AC and MAC. In the next section, the adsorption results obtained in the batch adsorption experiments in water are presented. These adsorption experiments include the adsorption of tetracycline and lincomycin as an individual and in mixture presented in sections 4.2.1 and 4.2.2, respectively. The presented adsorption data were also fitted to an appropriate isotherm model and the results are discussed in detail. In the last section, the stability of tetracycline in liquid manure supernatant was evaluated and then the performances of prepared adsorbents in direct removal of tetracycline from liquid manure supernatant were investigated at single concentration.

4.1 Adsorbent characterization

The prepared AC and MAC were examined by various characterization techniques including XRD, XPS, BET-BJH, FE-SEM, TEM, TG, PPMS, particle size and zeta potential analyses. The interpretation of the results obtained from the characterizations and comparison with the literature provided a broad understanding of physicochemical properties of the adsorbents. Also, the comparison of AC and MAC showed how magnetization affects the characteristics of AC.

4.1.1 XRD and XPS analysis

In order to characterize the electronic and crystalline structures of adsorbents, both AC and MAC were analyzed by XRD and XPS techniques. The XRD pattern of AC and MAC are depicted in Figure 4.1 (panel a). The wide peak detected at around $2\theta = 24$ and 44° are related to the amorphous carbon structures. The presence of sharp peaks at the XRD pattern of MAC reveals high crystallinity of iron oxide phase. More detail information about

the crystalline structure of MAC can be found in Figure 4.1 (panel b). In the presented XRD pattern, there is no unexpected peak, implying there is no impurity in the crystalline phase. The phase purity of the prepared adsorbent confirmed that each step of the magnetization procedure was done appropriately. Additionally, the presence of sharp peaks at around 2θ = 35, 43, 57 and 63° indicate the formation of iron oxide phase with high crystallinity. The crystal size of iron oxide particles is estimated as 7.2 nm using the Scherer equation [72]. The XRD patterns are fairly compatible with both presented reference patterns of Fe_3O_4, and γ-Fe_2O_3 (JCPDS, 19-0629 and 39-1346, respectively). It should be mentioned that XRD is not an ideal method to determine crystalline state of iron oxide phase as magnetite (Fe_3O_4) and maghemite (γ-Fe_2O_3) have similar crystalline structures. In this regard, XPS spectroscopy was used to distinguish between Fe_3O_4 (magnetite) and γ-Fe_2O_3 (maghemite) since these two iron oxides have different valence states of iron ions.

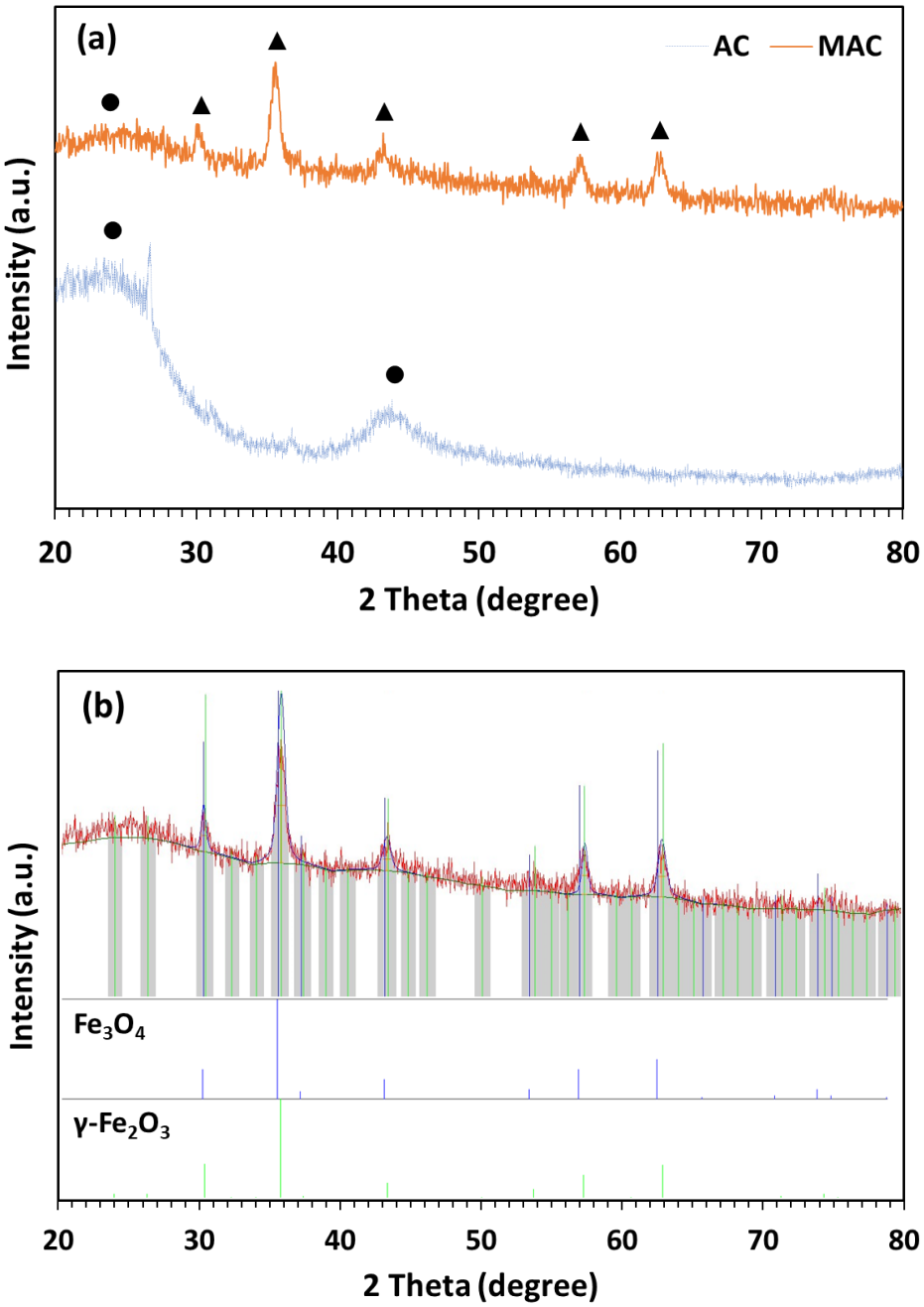

Figure 4.1 XRD patterns of AC and MAC (a), and XRD pattern of MAC compared to two iron oxide reference patterns (b). ▲ represent the peaks corresponding to the iron oxide and ● represent the peaks of carbon structure.

Figure 4.2 (panel a) displays the XPS survey spectra of AC and MAC as well as their surface elemental compositions. As can be seen from the spectra, MAC contains carbon, oxygen, and iron. Specifically, peaks with binding energy values of 285.08, and 531.08 eV are corresponding to C 1s and O 1s, respectively [75, 76]. The double peaks in the range between 712 and 724 eV are related to Fe2p [75]. The Fe2p XPS spectrum of MAC is shown

in Figure 4.2 (panel b). The XPS spectra of Fe $2p_{3/2}$ at ~712 eV and Fe $2p_{1/2}$ at ~724 eV correspond to the electron peak of Fe2p of Fe_2O_3 and Fe_3O_4, whereas, the shakeup satellite peak recorded at ~719 eV, is the fingerprint of the electronic structures of γ-Fe_2O_3 [76]. Finally, it can be confirmed from the results of this analysis the formation of γ-Fe_2O_3 species rather than Fe_3O_4.

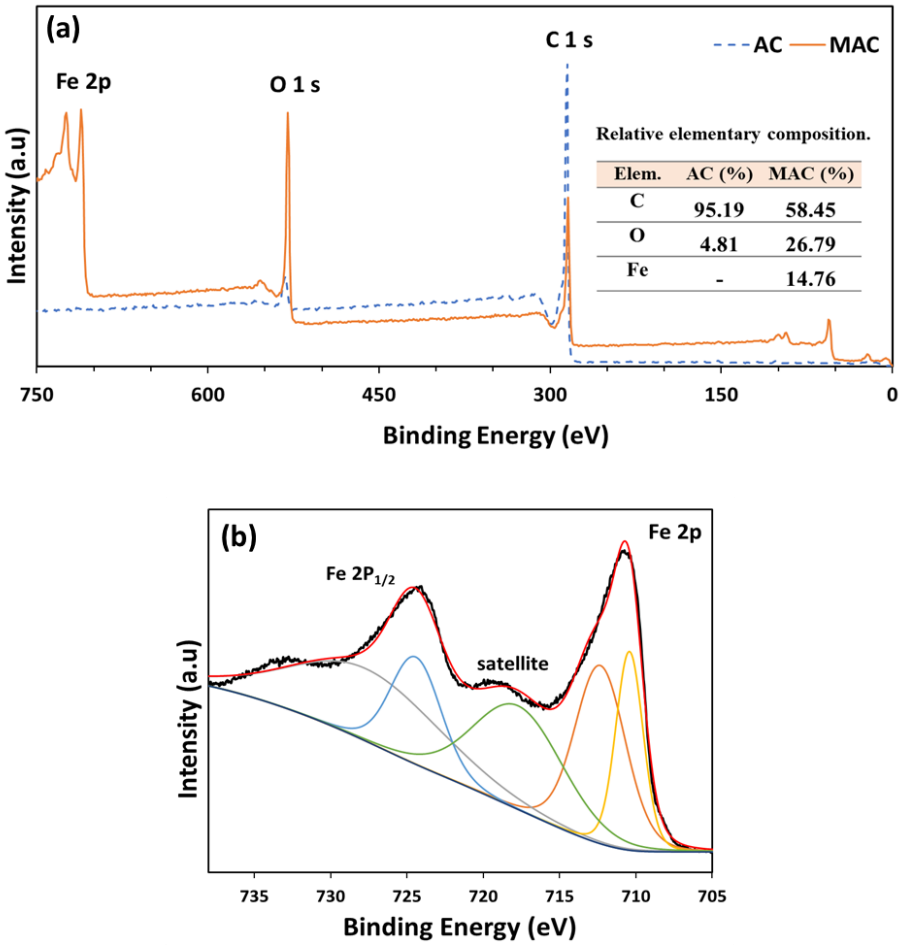

Figure 4.2 XPS spectra of AC and MAC and their surface elemental compositions (a), and Fe2p XPS spectrum of MAC (b)

4.1.2 BET-BJH analysis

Figure 4.3 (panel a) shows the N_2 adsorption-desorption isotherms of AC and MAC. Both samples exhibit a combination of Type I and Type II adsorption-desorption isotherms based on the IUPAC classification, indicating simultaneous presence of micro- and mesopores. The hysteresis loops in the isotherms of AC and MAC are assigned to type H4 (in agreement with IUPAC classifications), indicative of the presence of slit-shaped pores characteristic of activated carbons [77].

The BJH pore size distributions of AC and AMC are shown in Figure 4.3. (panel b). As can be seen, the pore size distributions of both samples are fairly close to each other. The average pore width (4V/A) calculated by BJH adsorption for AC and MAC are 5.1 and 6.6 nm, respectively. The slightly longer pore width of MAC can be attributed to the use of sonication during the magnetization procedure. As can be seen from the inset figure, the only difference in the depicted pore distributions is that the portion of mesopores at MAC structure is slightly higher than that of AC.

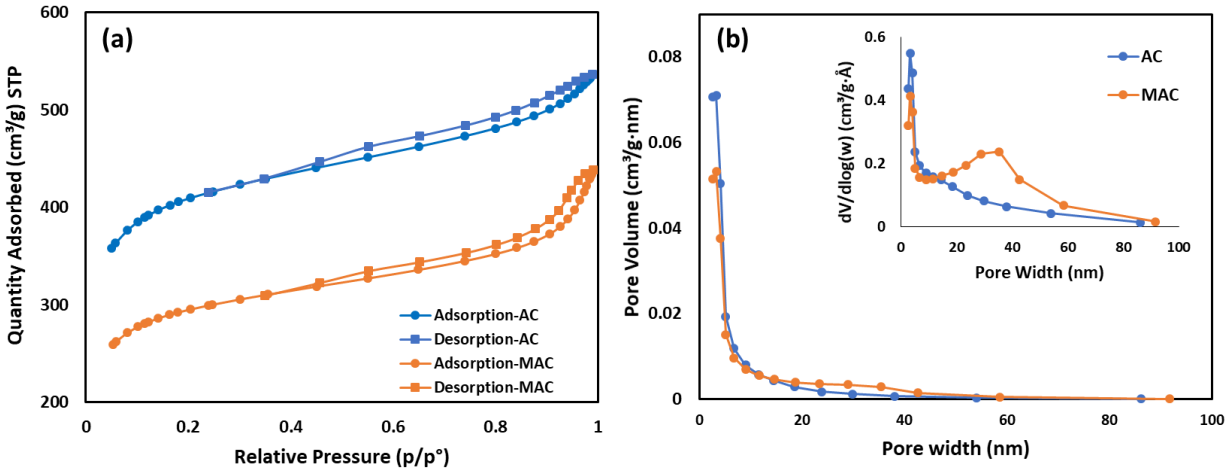

Figure 4.3 N_2 adsorption-desorption isotherms of AC and MAC (a), and BJH pore size distribution of AC and MAC (b)

The textural parameters of AC and MAC are presented in Table 4.1. The presented data indicate that the magnetization process decreased the BET surface area and pore volume of AC. This can be explained by two points: first, the formation of iron oxide nanoparticles unavoidably blocks some porous structure of the activated carbon; second, the magnetized sample contains a portion of γ-Fe_2O_3 nanoparticles, which has a relatively small surface area and pore volume [78].

Table 4.1 Textural characteristics of AC and MAC obtained from the N_2 adsorption isotherms

Sample	S_{BET} ($m^2\ g^{-1}$)	V_{micro} ($cm^3\ g^{-1}$)	V_{meso} ($cm^3\ g^{-1}$)	V_t ($cm^3\ g^{-1}$)
AC	1302	0.38	0.45	0.82
MAC	940	0.27	0.40	0.67

The important point is that although MAC lost part of the porosity due to the presence of γ-Fe_2O_3 nanoparticles, it still has a relatively large BET surface area and a high micro- and mesopore volume. Table 4.2 presents the BET surface area and pore volumes for different types of activated carbons and magnetic activated carbons reported in the literature. A review of the presented information reveals that the prepared magnetic activated carbon has a relatively high surface area and pore volume compared to those reported in the literature, either for activated carbon or magnetic activated carbon. This is because the used commercial activated carbon has a very high porosity. The applied magnetization procedure was also effective in preserving the porosity of activated carbon during the deposition of iron oxide particles.

Table 4.2 List of BET surface area and pore volumes for various types of activated carbon and magnetic activated carbon reported in the literature

Sample	S_{BET} ($m^2\ g^{-1}$)	V_t ($cm^3\ g^{-1}$)	Reference
Apricot nut shells derived PAC	308	0.19	[79]
Coconut derived PAC	799	0.61	[80]
Arya peels based activated carbon	1243	0.71	[81]
Macadamia nut shells derived PAC	1524	0.83	[59]
$MnFe_2O_4$/AC	383- 553	0.36- 0.48	[80]
Iron oxide /AC	527	0.97	[41]
AC	1302	0.82	Present work
γ-Fe_2O_3 /AC	940	0.67	Present work

4.1.3 FE-SEM analysis

The SEM images of AC and MAC are presented in Figure 4.4. The SEM images of AC (Figure 4.4, panels a, c, e and g) show its macro-structure with disorganized structural pattern and relatively rough external surface. The images also reveal that pores with various sizes and shapes are distributed on the adsorbent surface. Some large macropores were also observed in the structure of AC. The SEM images of MAC (Figure 4.4, panels b, d, f and h) obviously show that iron oxide nanoparticles (γ-Fe_2O_3) with spherical morphology are deposited on the surface of AC. Iron oxide particles largely covered the surface of AC but still the external carbon surface can be seen locally. Additionally, it can be observed that iron oxide particles are agglomerated in some parts of the sample.

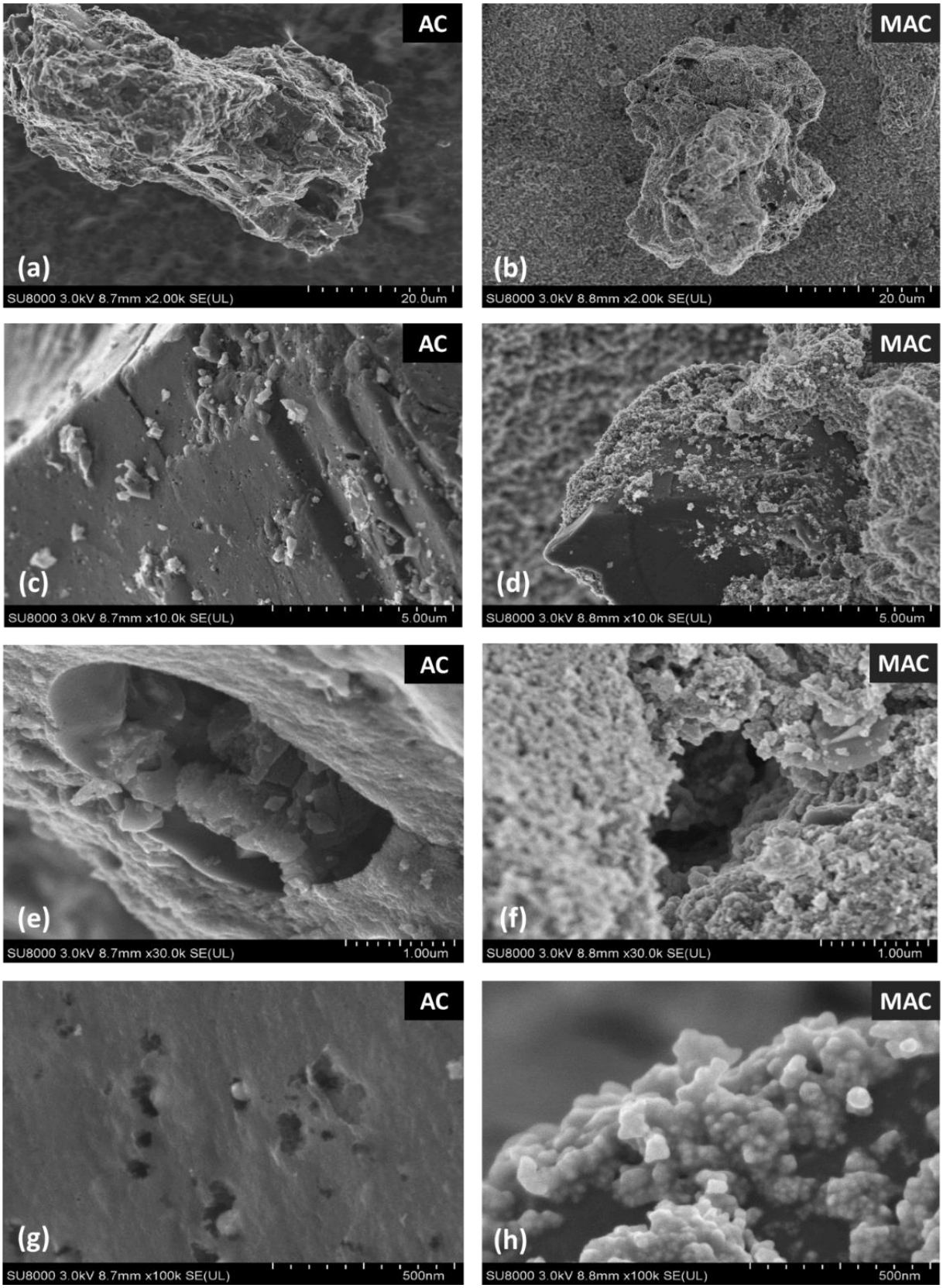

Figure 4.4 FE-SEM images of AC (a, c, e and g) and MAC (b, d, f and h)

4.1.4 TEM analysis

TEM images of MAC are shown in Figure 4.5. Light gray regions represent AC, while darker regions represent iron oxide particles (γ-Fe_2O_3). According to the presented images, iron oxide nanoparticles are dispersed onto macro-structure of AC, but they occasionally form separate phases as well.

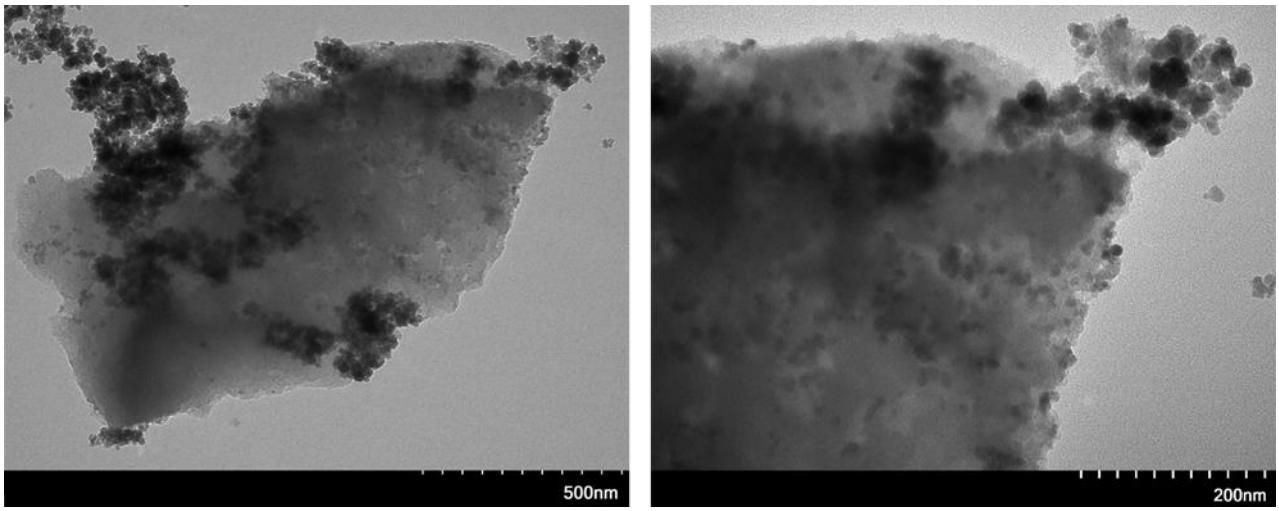

Figure 4.5 TEM images of MAC

The size distribution of iron oxide nanoparticles (γ-Fe_2O_3) is calculated using ImageJ® processing program and presented in Figure 4.6. Detailed information about the particle size is presented in Table 4.3. The particle size distribution of iron oxide nanoparticles was calculated based on the size of 100 random particles selected from the presented TEM images (Figure 4.6). According to the acquired results, the particle size of iron oxides is in the range of 5.1 to 14.4 nm with an average of 10.2 nm. Previously, the result of XRD analysis gave an estimation of 7.2 nm for the crystal size of iron oxides, which interestingly is in good agreement with the acquired results.

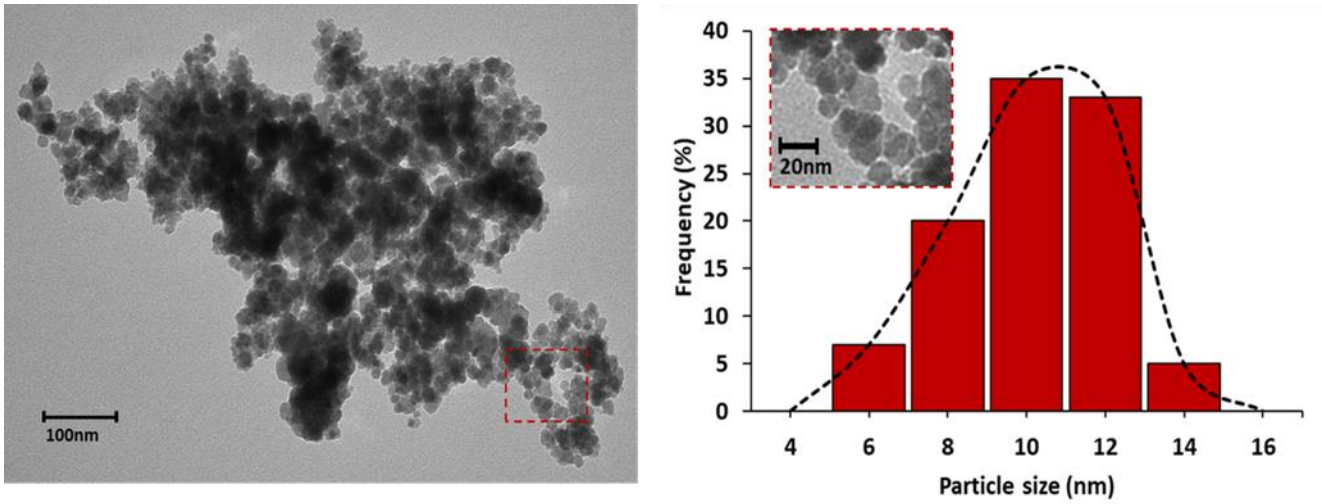

Figure 4.6 Particle size distribution of γ-Fe_2O_3 nanoparticles based on the TEM image

Table 4.3 γ-Fe_2O_3 particle size information

Statistical population (TEM)	100 Particles
Minimum particle size	5.1 nm
Mean particle size	10.2 nm
Maximum particle size	14.4 nm
Standard deviation	1.9 nm

4.1.5 TG analysis

The content of magnetic phase is an important parameter affecting both magnetic properties and adsorption capacity of magnetic adsorbents. Practically, low contents of magnetic phase cannot introduce enough saturation magnetization to the adsorbent to be separated from the liquid phase after treatment. On the other hand, excessive contents of magnetic phase leads to decrease of adsorbent's adsorption capacity because of decrease in specific surface area and pore volume [54,82].

In this study, it was aimed to develop a magnetic adsorbent with iron oxide content of 20%. This was chosen based on the findings of other similar studies. According to the literature, some studies tried to develop magnetic activate carbon with a reasonable iron oxide content to ensure the developed adsorbent had acceptable magnetic properties and good adsorption capacity [4,54,82]. Their findings suggest that regardless of importance of many

parameters such as synthesis procedure or crystalline structure of iron oxide phase, adsorbents with iron oxide content of 10 to 25% showed the best performances.

In this regard, TGA was used to determine the actual content of iron oxide in the prepared MAC. As can be seen in Figure 4.7, the TGA curve of MAC shows an obvious weight loss of 76.8 wt. % in the temperature range of 500–650 °C. According to the literature, the weight of iron oxides remains almost constant at this temperature range [83]. By assuming that AC is pure or only has a very low percentage of ash, the oxidization of AC mainly caused this weight loss. After the complete oxidation of AC, the weight of the residual sample became constant at about 23.2 wt% of the original sample, leading to the conclusion that iron oxides (γ-Fe_2O_3) content of MAC was approximately 23 wt%. The acquired data is fairly close to the iron oxide content aimed as part of the synthesis procedure (20 wt%.).

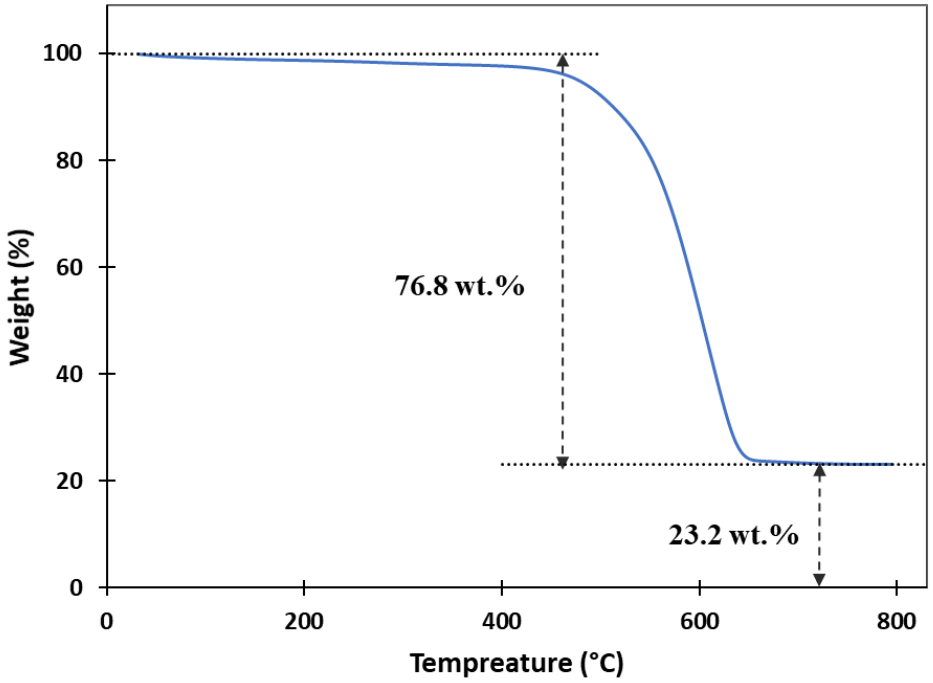

Figure 4.7 TGA curve of MAC

4.1.6 MPMS analysis

Magnetic Property Measurement System is used to investigate the magnetic property of MAC. The magnetic moment was measured within the magnetic field range of -2 to 2 tesla at room temperature (300 K). Figure 4.8 illustrates the magnetic curve of MAC with the M_s of 13 emu g^{-1}. As can be seen from Figure 4.9, the introduced saturation magnetization is

sufficient to separate it from aqueous solution using a block magnet. It is worth noting that the obtained value for saturation magnetization is relatively high compared with those of other MAC materials recently reported in the literature. For example, Saucier et al. [84] reported that the saturation magnetization of magnetic activated carbon (AC/$CoFe_2O_4$) is around 3.07 emu g^{-1} at room temperature. Huy Do et al. [54] synthesized three magnetic activated carbon (AC/Fe_3O_4) with iron contents of 5, 10 and 30 % and the saturation magnetization of 0.3, 4.7 and 7.0 emu g^{-1}, respectively. Liu et al. [85] developed a magnetic activated carbon prepared from rice straw-derived hydrochar with the saturation magnetization of 12.4 emu g^{-1}. Cazetta et al. [86] prepared a series of magnetically activated carbons via simultaneous activation and magnetization processes with different iron oxide contents; they reported that the saturation magnetizations of MAC was increased from16.56 to 28.69 emu g^{-1} by increasing the weight ratio of Fe to carbonized coconut shell from 1:1 to 1:3 in the magnetization process. For comparison, a list of magnetic activated carbon including their magnetic phase, magnetic content and obtained saturation magnetization is presented in Table 4.4.

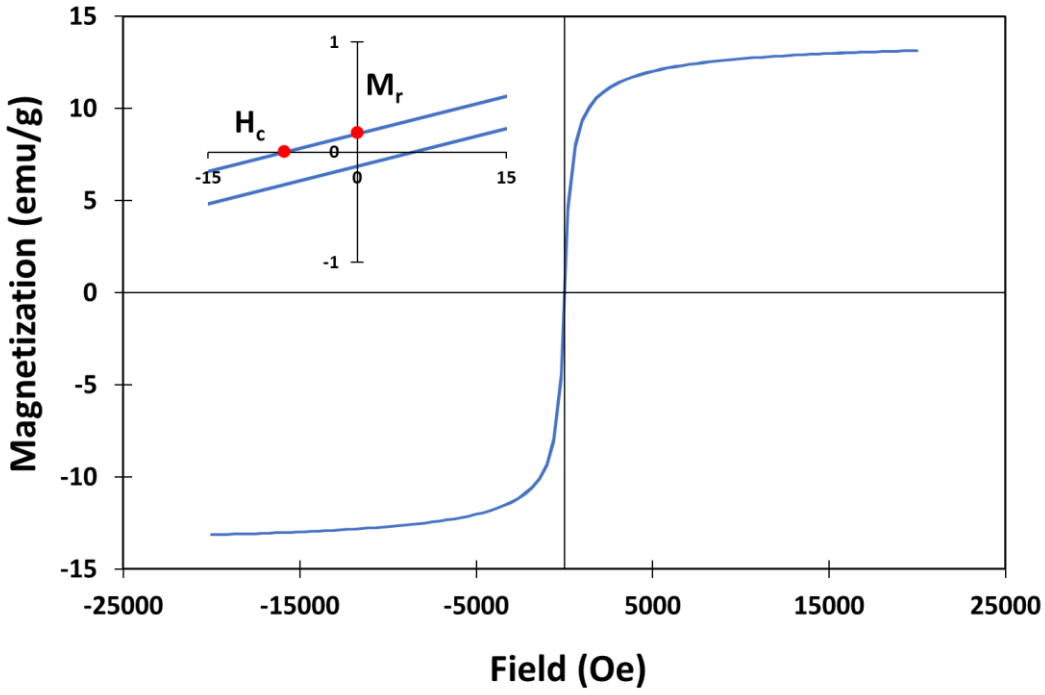

Figure 4.8 Magnetization curves of MAC obtained at room temperature (300 K)

Figure 4.9 Magnetic separation of prepared MAC using a block magnet

According to the magnetic curve, the values of H_c and M_r are 7.30 Oe and 0.17 emu g^{-1}, respectively. Furthermore, the magnetic nature of MAC is defined using the ratio of M_r to M_s. It was found that the prepared MAC has superparamagnetic properties at room temperature because the ratio of M_r to M_s for this material is lower than 0.25 (M_r/M_s is equal to 0.01). Interestingly, this can be also confirmed by the iron oxide particle size, previously determined by TEM. As a matter of fact, the magnetic nature of materials is attributed to their energy level at a microscopic scale, which is a function of their particle size. Generally, magnetic iron oxide particles with diameters smaller than 20 nm possess superparamagnetic behaviour at room temperature [87], which is consistent with the mean particle size of the iron oxide particles in the developed MAC which is around 10.2 nm.

Table 4.4 List of various types of magnetic activated carbon with different magnetic properties reported in the literature

Activated carbon	Magnetic phase	Magnetic content (%)	M_s (emu g^{-1})	Reference
Rice husk based	Fe_3O_4	23	2.8	[5]
Commercial	Ni	12	4.4	[88]
Coconut shell based	Fe_3O_4	5 - 30	0.3 – 7.0	[54]
Commercial	$CuFe_2O_4$	20	8.1	[89]
Commercial	γ-Fe_2O_3	-	29.2	[90]
Waste biomass	Fe_3O_4	39	47.7	[91]
Commercial	γ-Fe_2O_3	23	13	Present work

Moreover, the efficiency of magnetic separation for MAC was investigated based on the procedure explained in chapter 3 section 3.2.3. It was found that the prepared magnetic adsorbent can be separated from water with the efficiency of 95 ± 3%. Interestingly, as the prepared MAC has superparamagnetic behaviour, it was re-dispersed in water right after removing the magnetic force. The superparamagnetic behaviour as well as high magnetic separation efficiency makes the prepared magnetic adsorbent a potential candidate for wastewater treatment applications.

4.1.7 Particle size analysis

The particle size of adsorbent is an important parameter affecting its performance during the adsorption process. In this regard, a laser diffraction particle size analyzer was used to determine the particle size distribution of AC and MAC. This analysis was carried out four times for each adsorbent and the results are presented in Figure 4.10. The results indicate that the mean particle size of AC and MAC were 260 ± 4 and 172 ± 4 µm, and 50 volume percent of their particles are smaller than 252 ± 4 and 163 ± 4 µm, respectively. The results also indicate that MAC has a wider particle size distribution and a smaller mean particle size than AC. This particle size shift can be attributed to the use of sonication at different steps of the magnetization procedure.

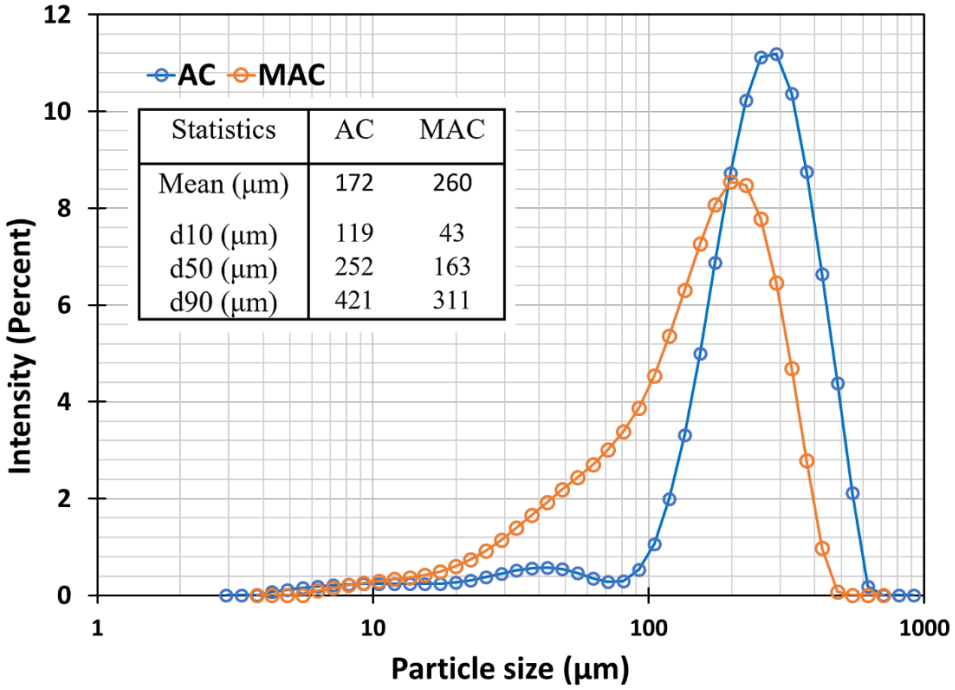

Figure 4.10 Particle size distribution of AC and MAC

4.1.8 Zeta potential analysis

Zeta potential analysis is a useful technique in demonstrating the role of electrostatic repulsion between contaminant and adsorbent. In this regard, the zeta potential of AC and MAC were measured at the pH range of 2 to 10, and the obtained results are presented in Figure 4.11. The presented results show that the surface charges of the adsorbents were significantly changed by varying the pH of solution. This is attributed to functional groups present on the surface of adsorbents. Surface functional groups often contain oxygen or nitrogen that can be protonated or deprotonated by changing the pH of solution. As can be seen, the point of zero charge (PZC) of AC and MAC were approximately 3.8 and 5.2, respectively. The obtained data indicate that the PZC of MAC is higher than that of AC. This shift can be attributed to the change of surface functional groups during the magnetization procedure. Iron oxide nanoparticles are positively charged, and their surface functional groups are hydroxyl groups, so their deposition can positively charge the surface of AC [92]. Although the prepared adsorbents have different PZCs, both obtained values are lower than 7. This means that both adsorbents would have a negative external surface charge in deionized water (pH =7).

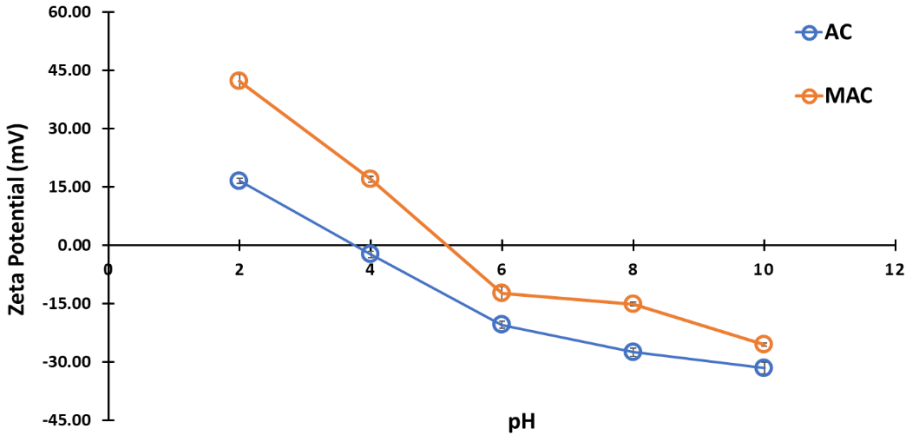

Figure 4.11 Zeta potential of AC and MAC at varying pH. Error bars represent the standard deviation of duplicate measurement

Adsorption experiment

In this section, the performances of the prepared adsorbents in removal of tetracycline and lincomycin are studied. Table 4.5 presents an overview of adsorption experiments performed during this research study along with the applied experimental conditions. According to the applied experimental approach, this research study can be categorized into four sets of adsorption experiments including:

1. Adsorptive removal of various levels of TC in water
2. Adsorptive removal of various levels of LM in water
3. Adsorptive removal of TC and LM from their mixture in water
4. Adsorptive removal of TC from liquid manure supernatant

Table 4.5 Summary of the adsorption experiments performed along with the applied experimental conditions

No.	Antibiotic	Media	T (°C)	C[i] (mg L^{-1})	Adsorbent (mg L^{-1})	pH[iii]	Time (day)	Replication
1	TC	Water	5-35	20-300	50 [ii], 100	5.3-6.2	10	20 and 300 mg L^{-1}
2	LM	Water	22	20-300	100	6.0-6.4	10	20 and 300 mg L^{-1}
3	TC and LM	Water	22	20-300	100	5.9-6.3	15	20 and 300 mg L^{-1}
4	TC	Manure	22	60	1500, 2500, 4000	8.0-8.2	8	All adsorption experiments

i Antibiotics concentration

ii 100 mg L^{-1} adsorbent was added to each solution, except the 20-ppm tetracycline solution that 50 mg L^{-1} adsorbent was added.

iii Presented values indicate the natural pH of the solution during the adsorption experiments.

4.2 Adsorption experiment in water

The adsorption experiments in water were studied in four stages: first, the equilibrium time was determined; second, the adsorptive removal of tetracycline from water were investigated at different temperatures using both AC and MAC; third, the same adsorption experiments were replicated for lincomycin at room temperature; fourth, the performances of AC and MAC in treatment of waters contaminated by the mixture of tetracycline and lincomycin were studied.

4.2.1 Single-solute adsorption of antibiotics from water

4.2.1.1 Determination of equilibrium time

In order to study the adsorption process, the equilibrium time should be determined first. The equilibrium time for lincomycin and tetracycline adsorption were determined based on the procedure described in section 3.2.4.1. To determine the equilibrium time for individual tetracycline and lincomycin adsorption, a set of adsorption experiments for each antibiotic were carried out. In these experiments, the concentrations of two solutions (100 and

200 mg L^{-1}) were monitored for 17 days. The results indicate that the concentration of tetracycline (Figure 4.12, panels a, c) and lincomycin (Figure 4.12, panels b, d) solutions containing either AC or MAC adsorbent became nearly constant after 10 days. Hence, an equilibrium time of 10 days were used in the adsorption experiments.

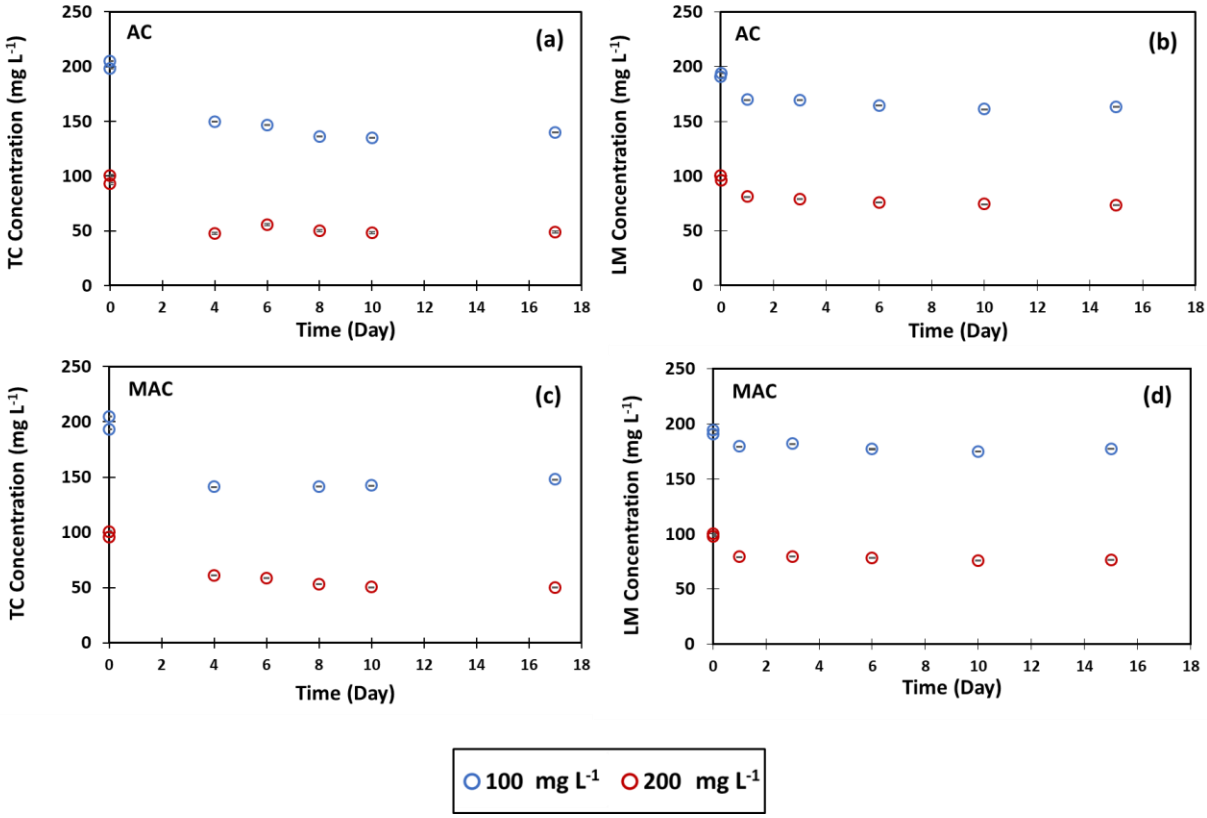

Figure 4.12 Concentration of tetracycline (a, c) and lincomycin (b, d) during the adsorption experiment with AC and MAC at room temperature (22 °C). Error bars represent the standard deviation of antibiotic concentration duplicate measurements.

4.2.1.2 Tetracycline adsorption

The adsorptive removal of tetracycline from water using AC and MAC was studied at four different temperatures (5, 15, 22 and 35 °C). The pH of adsorption medium varied from 5.3 to 6.2 during the adsorption experiments. The obtained four sets of adsorption data were fitted to Langmuir model in two different ways: first, each set of adsorption data was fitted separately to the Langmuir model; second, all sets of adsorption data were non-isothermally fitted to the temperature-dependent form of Langmuir model. Since non-isothermal model can provide direct estimation of the enthalpy change, the second way was used, and the obtained results are presented in Figure 4.13 and Table 4.6. The enthalpy change was also

calculated from the first approach and the results are presented in Appendix B. However, this method requires further data fitting which was unavoidably accompanied by higher calculation errors. In addition to Langmuir model, obtained adsorption data were fitted to Freundlich model and the obtained results are presented in Appendix C. Because Freundlich model cannot fit four sets of tetracycline adsorption data simultaneously, each set of adsorption data was fitted separately to the Freundlich model. It is obvious that this method is not able to express the temperature relationship between the different sets.

The insets in Figure 4.13 show that the values of equilibrium concentrations at some points are very low but they were not zero so that they can be used for adsorption calculations. Presented adsorption data show that although the adsorption capacities of both AC and MAC continually increased by increasing the tetracycline concentration at 35 °C, this trend was not as pronounced when the temperature decreased from 35 to 5°C. Hence, at 5 °C, adsorption capacities of AC and MAC slightly increased by increasing the tetracycline concentration to 100 mg L^{-1} and then became almost constant.

The adsorption data presented in Figure 4.13 reveals that adsorption capacity of adsorbents toward tetracycline increased by increasing the temperature. The maximum adsorption capacities of AC and MAC toward tetracycline are determined at reference temperatures (273 K) using temperature-dependent form of Langmuir model and the results are presented at Table 4.6. Based on the obtained parameters, the maximum adsorption capacities of AC at 5, 15, 22 and 35 °C were calculated as 323, 541, 777 and 1520 mg g^{-1}, respectively. Also, the maximum adsorption capacities of MAC at the mentioned temperatures were 324, 503, 685 and 1215 mg g^{-1}, respectively. The results indicate that the adsorption capacities increased by increasing the temperature, suggesting that higher temperature is more favourable for the adsorption process on AC and MAC. By considering the Le Chatelier's principle, this trend indicates the endothermic nature of this adsorption process. These observations regarding the endothermic nature of tetracycline adsorption are in agreement with the obtained positive signs of enthalpy changes for both AC and MAC. Also, the estimated values of enthalpy changes are compatible with those reported by other studies. Sayğılıa and Güzelb [93] studied the adsorption of tetracycline from aqueous solution on activated carbon prepared from tomato industrial processing waste. They reported that the enthalpy change for the tetracycline adsorption is 11.4 KJ mol^{-1}. Shao et al. [80] also investigated the effectiveness of $MnFe_2O_4$/activated carbon on tetracycline removal. Based on their calculation, the enthalpy change for the adsorption process was around 38 KJ mol^{-1}.

The data obtained also indicated that the adsorption capacity of AC has been decreased after magnetization. Part of this decrease can be attributed to the loss of surface area, which happened due to the deposition of iron oxide nanoparticles (γ-Fe_2O_3). Although the adsorption capacity of MAC is slightly lower than AC, it still has a high adsorption capacity toward tetracycline.

Moreover, three pKa values are reported for tetracycline: 3.31, 7.68 and 9.69 [94]. As a result, tetracycline has a positive charge at pH < 3.3, neutral charge at 3.31 < pH < 7.68, and a negative charge at pH > 7.68 [95]. Since the pH of adsorption medium varied from 5.3 to 6.2, tetracycline has neutral charge in this set of experiments. Also, it is clear that both adsorbents have a negative external surface charge in this pH range ($pH < pH_{pzc}$). This implies that electrostatic interaction has not played an effective role in this adsorption process. Based on the literature, it can be concluded that π–π interactions and hydrogen bonding are possibly two critical interactions governing this adoption process [23].

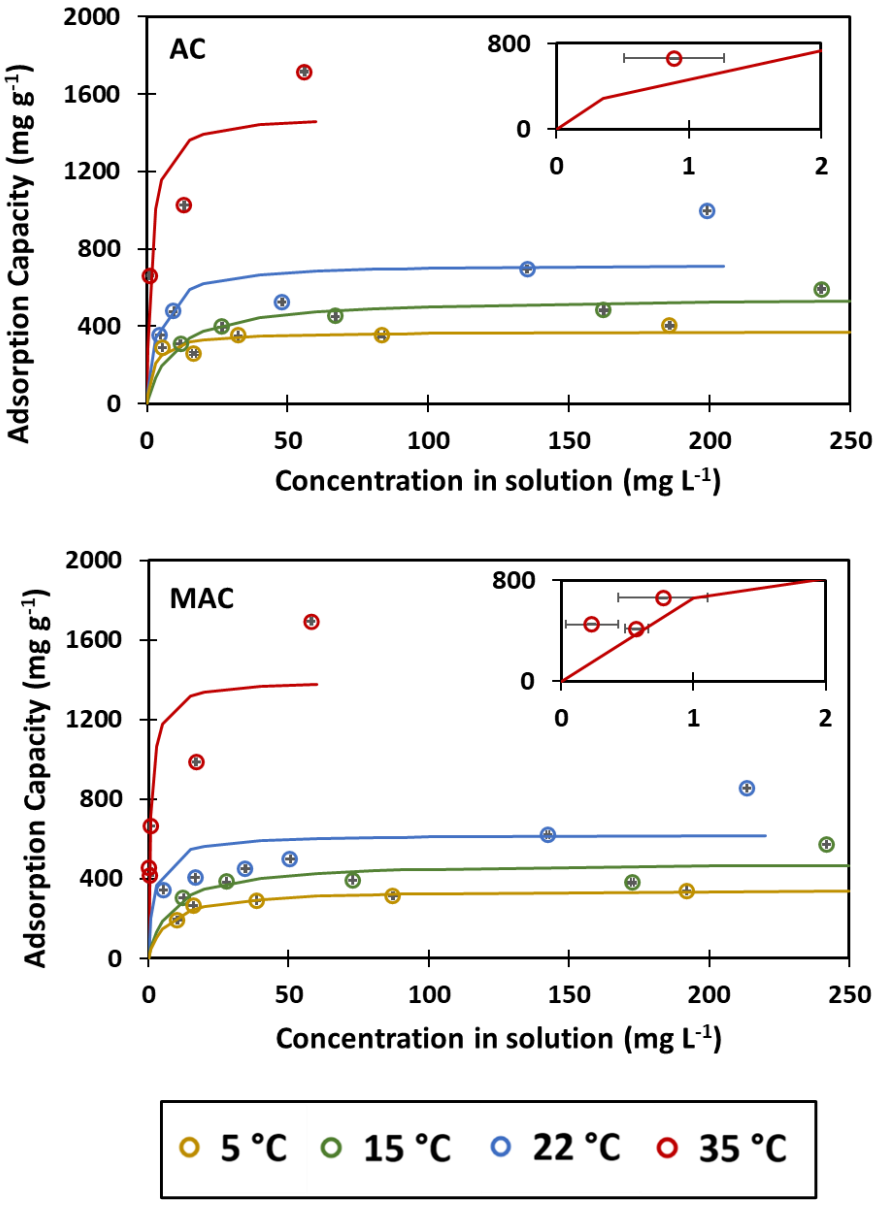

Figure 4.13 Adsorption of tetracycline on AC and MAC at 5, 15, 22 and 35 °C (pH: 5.3 - 6.2). Symbols represent the experimental results and lines represent the prediction by temperature-dependent Langmuir expressions. Error bars represent the standard deviation of antibiotic concentration duplicate measurements.

Table 4.6 Parameters of temperature-dependent Langmuir isotherm for tetracycline adsorption on AC and MAC (T: 5 - 35 °C, pH: 5.3 - 6.2)

Ads.	K^o_L (L mg^{-1}) × 10^5	δ (K^{-1})	q^o_{max} (mg g^{-1})	ΔH (KJ mol^{-1})	R^2	MAPE (%)
AC	2.3	0.05	249	24.5	0.88	23
MAC	2.3	0.04	260	26.6	0.91	22

Herein, the tetracycline adsorption data are compared with those reported in the literature to gain a broader context of the contribution of the data obtained from this study. In this regard, the maximum adsorption capacities of various ACs and MACs reported by other researchers either at different temperatures or various ranges of tetracycline concentrations are presented in Table 4.7. The presented data are sorted according to the temperature.

Interestingly, the presented results in Table 4.7 show that the adsorption capacities obtained in this work are compatible with those reported in the literature. For example, Zhang et al. [22] studied the removal of tetracycline from water by petroleum coke-derived activated carbon with a surface area of 2900 $m^2 g^{-1}$. Based on their results, the maximum adsorption capacity for tetracycline at 30 °C was 897.6 mg g^{-1} and increased to around 1121.5 mg g^{-1} by increasing the temperature to 50 °C. Their findings also confirm the endothermic nature of tetracycline adsorption by AC. In addition, Shao et al. [80] developed a magnetic activated carbon containing 40% magnetic phase ($MnFe_2O_4$/activated carbon) with a surface area of 512 $m^2 g^{-1}$, and investigated its performance in adsorptive removal of tetracycline from water. Their findings suggest that the maximum adsorption capacity for tetracycline at 25 °C was 262 mg g^{-1}.

A comparison between the obtained maximum adsorption capacities of AC and MAC toward tetracycline with those from other studies show the superior performance of the prepared adsorbent. The developed MAC not only shows higher performance compared to many other magnetized ACs but also its performance was superior to those obtained with AC as listed in Table 4.7. This can be attributed to relatively large surface area and high micro- and mesopore volumes of AC as well as using a proper synthesis procedure in magnetization of AC.

Table 4.7 also shows that other similar studies on the adsorption of tetracycline from water were carried out at room temperature or higher temperatures. Literature search yielded

no past study that was carried out on adsorptive removal of tetracycline from water using ACs or MACs at temperatures below 20 °C. For this reason, the obtained tetracycline adsorption data at 5 and 15 °C are very valuable, especially for cold regions with a relatively lower average temperature. These data can be considered as complementary to the currently available data in the literature.

Table 4.7 Comparison of tetracycline maximum adsorption capacities at different temperature, range of concentration by different ACs and MACs

Adsorbent	**T (°C)**	**C_0 (mg L^{-1})**	**q_e (mg g^{-1})**	**q_{max} (mg g^{-1})**	**Reference**
ACs					
Commercial AC	5	20-300	259-403	323	Present work
Commercial AC	15	20-300	309-592	547	Present work
Commercial AC	22	20-300	352-998	777	Present work
Iris tectorum derived AC	22	0.73–1.66	-	625.02	[96]
Plant sludge derived AC	25	100-1000	270-470	471	[23]
Petroleum coke derived AC	30	60-200	600-920	897.6	[22]
Commercial AC	35	20-300	429-1795	1493	Present work
Tomato derived AC	35	200-800	275-450	500	[93]
Petroleum coke derived AC	40	60-200	600-1000	961.5	[22]
Petroleum coke derived AC	50	60-200	600-1160	1121.5	[22]
Magnetic ACs					
γ-Fe_2O_3 /AC	5	20-300	193-340	324	Present work
γ-Fe2O3 /AC	15	20-300	305-572	503	Present work
γ-Fe2O3 /AC	22	20-300	346-854	685	Present work
$MnFe_2O_4$/AC	25	44-889	100-360	-	[80]
Ni/porous carbon	25	40-280	40-130	132.67	[97]
γ-Fe2O3 /AC	30	10-50	5- 30	25.44	[60]
γ-Fe2O3 /AC	35	20-300	418-1694	1215	Present work
Ni/porous carbon	45	40-280	90-400	397.25	[97]

In addition, the maximum adsorption capacity of prepared MAC was compared with those reported for various types of adsorbents to gain a more comprehensive view about the performance of the developed MAC. Table 4.8 presents the maximum adsorption capacity of tetracycline onto various types of adsorbents such as graphene oxide, chitosan, clay and silica, to name a few, and the presented data are sorted according to the adsorption capacity.

Table 4.8 shows that the developed MAC has a relatively high adsorption capacity toward tetracycline. Based on the presented data, only one type of adsorbent showed higher adsorption capacities toward tetracycline, which was Zeolitic Imidazolate Framework (ZIF-8). Therefore, it can be concluded that the performance of developed MAC in adsorptive removal of tetracycline is superior not only to many developed ACs and MACs but also to various types of adsorbents reported in the literature.

Table 4.8 Comparison of maximum adsorption capacities of various adsorbents toward tetracycline reported in literatures

Adsorbent	**q_{max} (mg g^{-1})**	**Reference**
Zeolitic Imidazolate Framework (ZIF-8)	3758.35	[98]
Petroleum coke derived AC	1121.5	[22]
Magnetic resin (Q100)	429.7	[99]
Graphene oxide	313	[20]
Multi-walled carbon nanotubes	309	[100]
La-impregnated MCM-41materials	303.3	[101]
Alkali biochar	58.82	[18]
Chitosan	41.35	[102]
Non-swelling clay mineral illite	32	[103]
Mesoporous BiOI microspheres	28.35	[104]
The Red soil (RS, UdicFerrosols)	12	[105]
Silica oxide	5.43	[106]
Aerobic granular sludge	4.61	[107]
Magnetic AC	1215	Present work

4.2.1.3 Lincomycin adsorption

Adsorption of lincomycin in water was studied at room temperature and the results are presented in Figure 4.14. During the adsorption experiments, the pH of adsorption medium varied from 6.0 to 6.4. The presented data indicate that the adsorption capacity of the adsorbents was slightly increased by increasing the lincomycin concentration and then became almost constant. Langmuir and Freundlich isotherm models were used to fit the lincomycin adsorption data at room temperature. According to the results, Langmuir model could predict the behaviour of lincomycin adsorption on both AC and MAC adsorbents more accurately (higher R^2) than Freundlich isotherm model. This reveals the monolayer nature of lincomycin adsorption on the carbon materials. The obtained parameters of Langmuir model are presented in Table 4.9, and those for Freundlich isotherm model are presented in Appendix C.

Similar to the data obtained for tetracycline adsorption, the presented results in Table 4.9 indicate that the adsorption capacity of AC toward lincomycin was slightly decreased after magnetization. This decrease can be mainly attributed to the loss of surface area, which happened due to the deposition of iron oxide nanoparticles (γ-Fe_2O_3). Although the adsorption capacity of MAC is slightly lower than AC, it still has a high adsorption capacity toward lincomycin.

In addition, the pKa value of lincomycin is 7.6, and as a result, lincomycin would have a positive charge at $pH < 7.6$, and negative charge at $pH > 7.6$ [108]. Therefore, as the pH of adsorption medium varied from 6.0 to 6.4, lincomycin has positive charge in this set of experiments. On the other hand, the result of zeta potential analysis indicated that both adsorbents have negative external surface charge at this pH range ($pH < pH_{pzc}$). This implies that electrostatic interactions may be involved in the adsorption process.

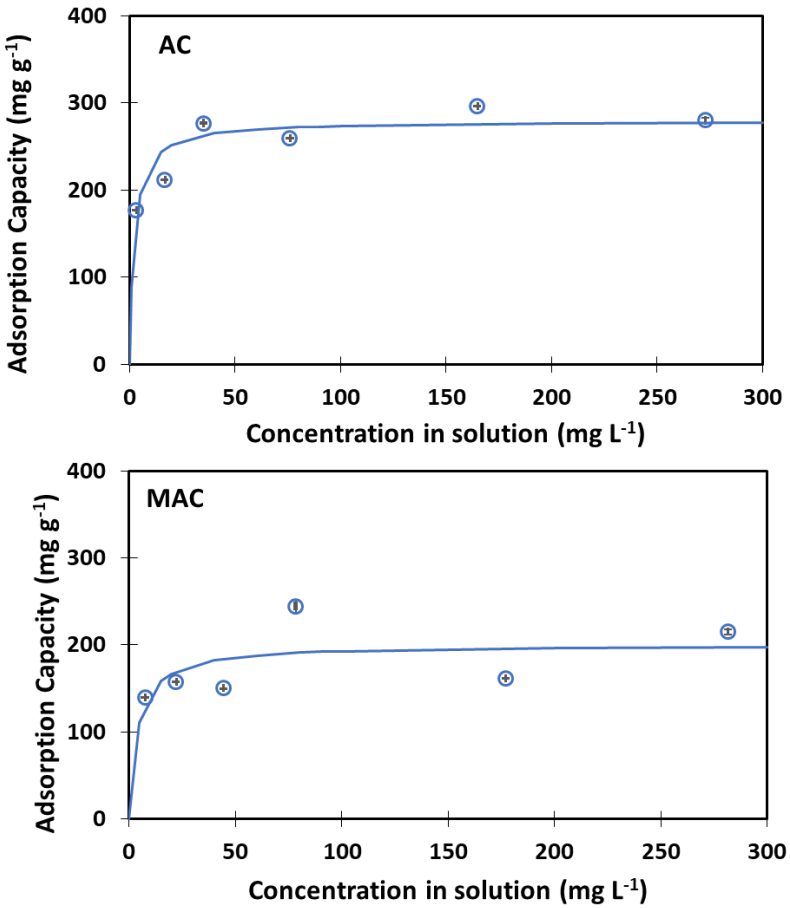

Figure 4.14 Adsorption of lincomycin on AC and MAC at room temperature (T= 22 °C, pH: 6.0 - 6.4). Symbols represent the experimental results and lines represent the prediction by Langmuir expression. Error bars represent the standard deviation of antibiotic concentration duplicate measurements.

Table 4.9 Parameters of Langmuir isotherm for lincomycin adsorption on AC and MAC (T= 22 °C, pH: 6.0 - 6.4)

Ads.	q_{max} (mg g^{-1})	K_L (L mg^{-1})	R^2	MAPE (%)
AC	280	0.46	0.999	6
MAC	201	0.25	0.957	13

To put the finding of present work in context of existing literature, the maximum adsorption capacities of lincomycin by AC and MAC are compared with those reported by others for various carbon-based adsorbents including AC, single-walled carbon nanotubes,

multi-walled carbon nanotubes and biochar. The presented data are sorted according to the adsorption capacity and presented in Table 4.10.

Table 4.10 shows that a few studies have been conducted on adsorptive removal of lincomycin. So far, only one other study investigated the adsorptive removal of lincomycin using AC has been found. Kim et al. [25] used coconut-based powder AC with a particle size range from 100 to 250 µm to remove lincomycin from water. They reported that the adsorption capacity of AC for lincomycin was approximately 115 mg g^{-1} when the equilibrium concentration was around 4.8 mg L^{-1}[25]. Interestingly, their result is close to the findings of this study where adsorption capacity of AC for lincomycin was around 177 mg g^{-1} at an equilibrium concentration of 3.1 mg L^{-1}.

Furthermore, no study has been found regarding adsorption of lincomycin onto any type of magnetic adsorbent. In other words, to the best of our knowledge, the developed MAC is the first magnetic adsorbent that has been used for removal of lincomycin so far. According to Table 4.10, not only the ability of magnetic recovery gives MAC a considerable advantage over other developed adsorbents, but its performance in removal of lincomycin is superior to the adsorbents developed by other research studies.

Table 4.10 Comparison of maximum adsorption capacities of various adsorbents toward lincomycin reported in literature

Adsorbent	**q_{max} (mg g^{-1})**	**Reference**
Single-walled carbon nanotubes	148	[25]
Coconut-based AC	132	[25]
Multi-walled carbon nanotubes	20	[25]
Manure-derived biochar	0.7	[109]
Commercial AC	280	Present work
Magnetic AC	201	Present work

4.2.1.4 Comparison of lincomycin and tetracycline adsorption

A simple comparison between the adsorption data of lincomycin and tetracycline reveals that the adsorption capacity of AC toward tetracycline (mg g^{-1}) is much higher than that of lincomycin at room temperature. This also applies to molar units since the molecular

weights of tetracycline and lincomycin are close to each other (MW_{TC}: 444.435 g mol^{-1} and MW_{LM}: 406.538 g mol^{-1}). In other words, a larger number of tetracycline molecules are adsorbed into the adsorbent compared to that of lincomycin molecules.

The observed differences in the adsorption capacities of prepared adsorbents toward tetracycline and lincomycin could be attributed to the different molecular structures of these two antibiotics that affect their mechanisms of adsorption by AC. It was found that the most important molecular parameter affecting the adsorption of antibiotics into AC is the number of aromatic rings [25, 26]. Although both antibiotics are able to attach onto activated carbon by the formation of hydrogen bonds, tetracycline molecule has four aromatic rings that enable this antibiotic to attach onto activated carbon through π-π interaction as well. In fact, π–π interaction occurs between π electrons of the activated carbon and π electrons of the tetracycline aromatic ring [25, 26]. This implies that the higher adsorption capacity of tetracycline onto AC in comparison to that of lincomycin can be attributed to the higher affinity of tetracycline to AC.

The obtained adsorption data reveal that the adsorption capacity of MAC toward both antibiotics are lower than that of AC. However, the adsorption data suggests that magnetization of AC affects the adsorption of lincomycin more than that of tetracycline. As a matter of fact, the maximum adsorption capacity of AC toward tetracycline and lincomycin at room temperature is decreased after magnetization by 13.85 and 28.2%, respectively.

Since adsorption is a surface-dependent phenomenon, part of these observations is attributed to the change of AC surface area after magnetization. However, surface area is not the only surface physicochemical parameter that can be affected through the magnetization process. As discussed in section 4.1.8, magnetization partially changed the surface chemistry of activated carbon as well. To verify how magnetization affects the adsorption capacity of AC toward tetracycline and lincomycin, the maximum adsorption capacities of AC and MAC per unit area of adsorbents are calculated and presented in Figure 4.15.

The presented results indicate that the maximum adsorption capacities per unit area of AC for lincomycin remains unchanged after the magnetization. In other words, the decrease in adsorption capacity of AC toward lincomycin is proportional to the BET surface area lost after the magnetization. Therefore, it can be interpreted that the observed change in adsorption capacity of AC toward lincomycin mostly happened due to the loss of surface area.

On the other hand, the presented data show that the maximum adsorption capacities per unit area of AC for tetracycline was increased after the magnetization. This can be

attributed to change in surface chemistry of AC, which happened during the magnetization process. Because the surface functional groups of iron oxides are hydroxyl groups, magnetization can increase the density of oxygen-containing functional groups on the surface of AC [92]. Consequently, the deposition of iron oxide nanoparticles can increase the strength of π-π interaction between activated carbon plates and tetracycline aromatic rings.

Finally, it can be interpreted that the magnetization process can affect the adsorption capacity of AC toward tetracycline and lincomycin mostly through decreasing the surface area and/or changing the surface chemistry. It was found that the applied magnetization procedure changed the adsorption capacity of AC toward lincomycin proportional to the loss of surface area. On the other hand, it was found that the adsorption capacity of AC toward tetracycline did not change proportionally to the loss of surface area, suggesting that change in the surface chemistry of AC may affect this adsorption process, besides the loss of surface area.

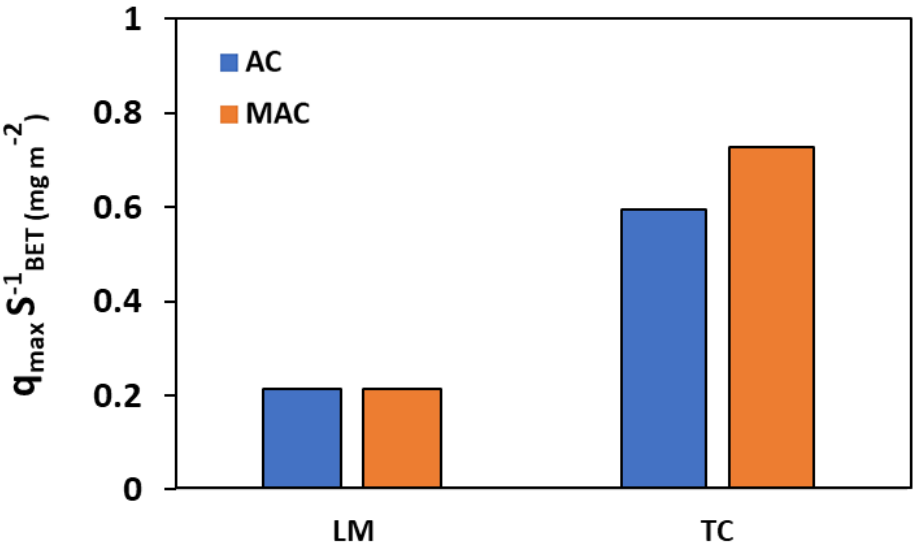

Figure 4.15 Maximum adsorption capacities of AC and MAC per unit area of adsorbents

4.2.2 Binary-solute adsorption of antibiotics from water

4.2.2.1 Determination of equilibrium time

To determine the equilibrium time for the adsorption of tetracycline and lincomycin mixture in water, a set of adsorption experiments with conditions explained in section 3.2.4.1 was carried out, and the results are presented in Figure 4.16.

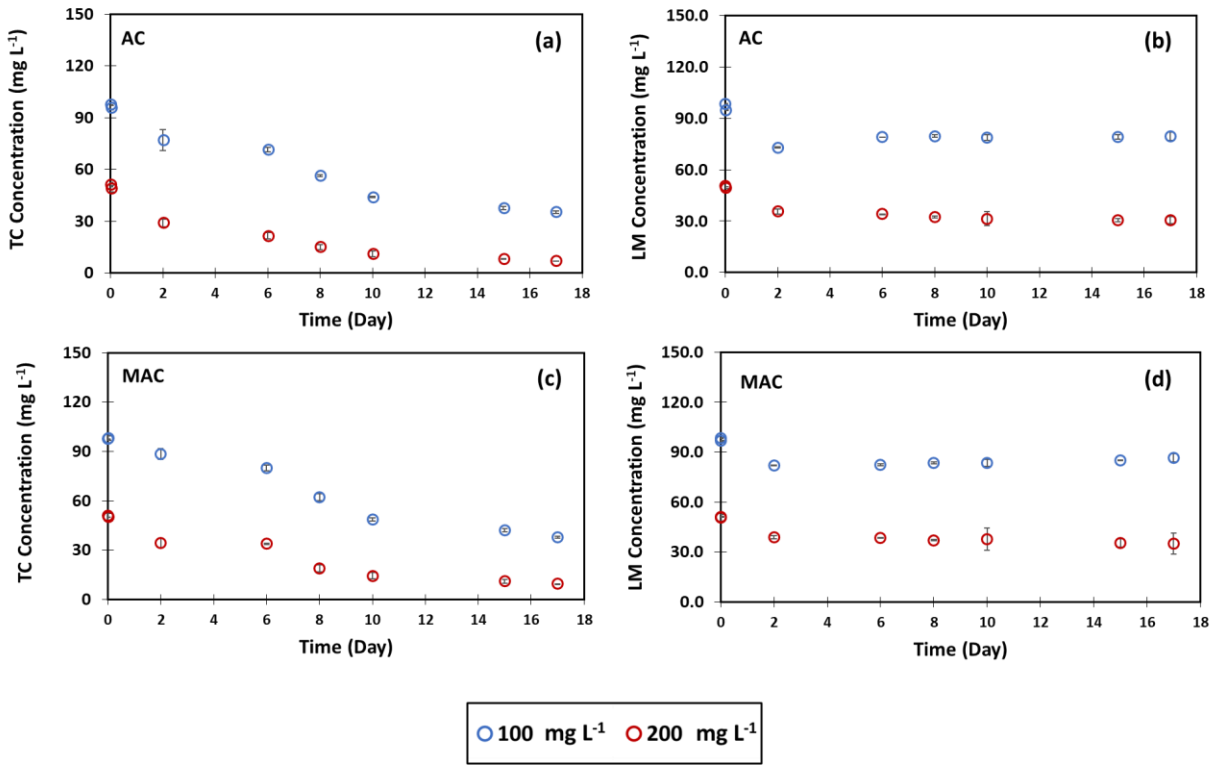

Figure 4.16 Concentration of tetracycline (a, c) and lincomycin (b, d) in mixture during the adsorption experiment at room temperature (22 °C). Error bars represent the standard deviation of antibiotic concentration duplicate measurements.

In these experiments, the concentrations of tetracycline and lincomycin in two mixture solutions (40 and 100 mg L^{-1}) were monitored for 17 days. The time required for both tetracycline and lincomycin concentrations to reach a constant value was considered as the equilibrium time. Although the concentration of lincomycin in the mixture (Figure 4.16, panels c, d) reached an almost constant value after 6 days, tetracycline concentration was still decreasing (Figure 4.16, panels a, b). The results indicated that the concentration of both tetracycline and lincomycin in mixture solutions containing either AC or MAC adsorbent became nearly constant after 15 days. Therefore, 15 days was assumed as the equilibrium time for the adsorption of tetracycline and lincomycin mixture.

4.2.2.2 Tetracycline and lincomycin in mixture

Herein, the adsorption of tetracycline and lincomycin onto both AC and MAC from their mixture were studied. The main goal of this study was to investigate how the adsorption capacity of prepared adsorbents would change in the presence of more than one antibiotic.

This study can take us a step closer to the understanding of the adsorption process in more complex, multi-component medium.

The mixture adsorption experiments were carried out at room temperature (22 °C). According to the adsorption data shown in Figure 4.17, by increasing the antibiotics initial concentration, the adsorption capacity of tetracycline in the mixture was increased, while that of lincomycin almost reached a constant value. The mixtures consisted of equal concentrations of tetracycline and lincomycin, so the antibiotics had equal chances for being adsorbed. However, the results indicate that the adsorbents showed higher adsorption capacity for tetracycline than lincomycin in the mixture. This may indicate that a higher force of attraction exists between AC and tetracycline compared to that of AC and lincomycin. Also, the results showed that increasing the antibiotics initial concentration did not affect the adsorption capacity of lincomycin at higher concentrations but increased the adsorption capacity of tetracycline in mixture. It can be concluded that the ratio of tetracycline adsorption capacity to lincomycin adsorption capacity (q_{TC}/q_{LM}) is more than 1.0, and its value increased by increasing the initial concentrations of antibiotics. In other words, the higher the initial concentration of mixture solutions, the more preferably tetracycline is adsorbed.

Langmuir and Freundlich isotherms were used to model the mixture adsorption data. Langmuir model either in a non-extended or extended format predicted mixture adsorption data well. Freundlich model was not able to model the obtained data well based on the obtained R^2 values, especially the case of lincomycin adsorption. In fact, Freundlich model could not precisely predict the adsorption data of lincomycin either as an individual or in the mixture indicating the monolayer nature of lincomycin adsorption onto activated carbon. The obtained results from Freundlich model were presented in Appendix C.

First, adsorption data regarding each antibiotic in mixture were fitted to Langmuir model separately, and the obtained isotherms are shown in Figure 4.17 and Table 4.11. In this model, each antibiotic was fitted to the Langmuir model without considering the presence of the other antibiotic in the adsorption media. A simple comparison between the obtained isotherms for AC and MAC reveals that the magnetization of AC decreased its adsorption capacities for both tetracycline and lincomycin in the mixture, and similar to the individual adsorption, the decrease in lincomycin adsorption was much higher than that of tetracycline.

The pH of adsorption medium was in the range of 5.9 - 6.3 during the adsorption experiments. It is important to note that tetracycline is electrically natural and lincomycin has a positive charge at this pH range based on their pKa values. Also, the results of zeta

potential analysis indicate that both adsorbents have negative external surface charge at this pH range (pH > pH_{pzc}). This implies that electrostatic interactions can be involved in the adsorption of lincomycin but not for tetracycline.

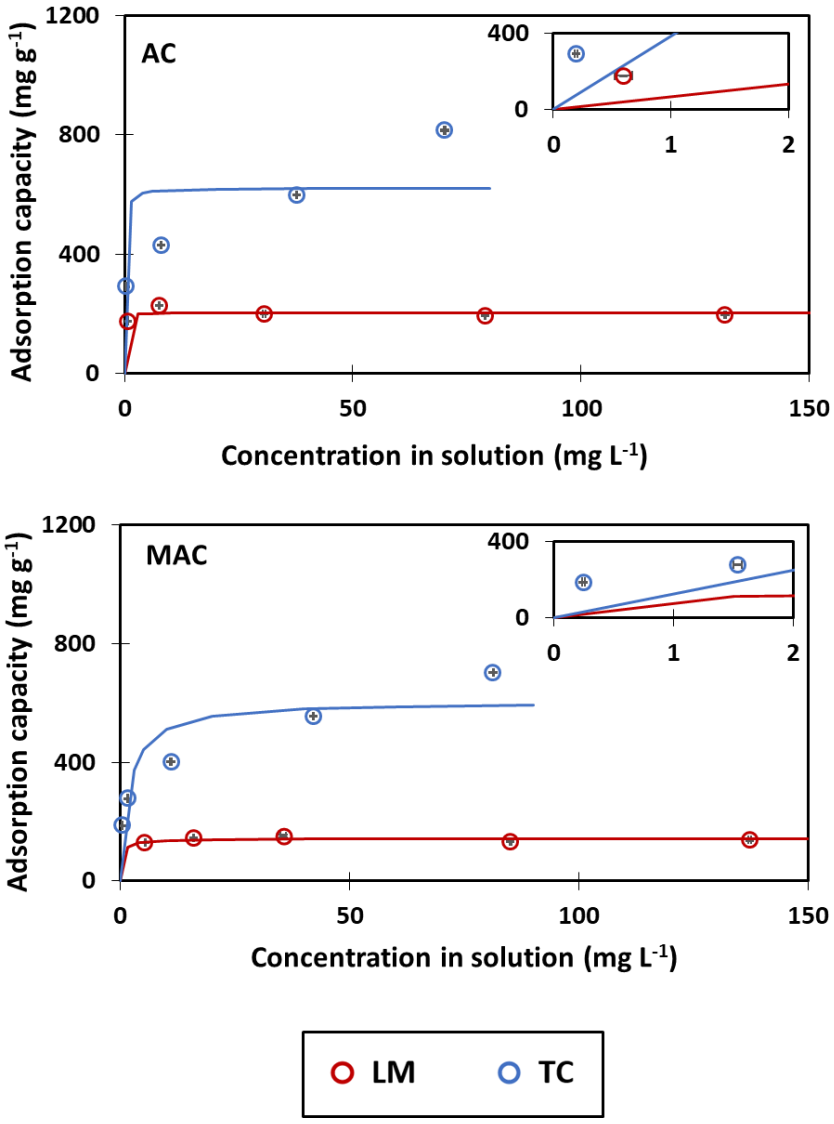

Figure 4.17 Adsorption of tetracycline and lincomycin on AC and MAC in mixture at room temperature (T= 22 °C, pH: 5.9 - 6.3). Symbols represent the experimental results and lines represent the prediction by Langmuir expression. Error bars are calculated based on the standard deviation between two HPLC injections.

Table 4.11 Parameters of Langmuir isotherm for tetracycline and lincomycin adsorption in mixture on AC and MAC (T= 22 °C, pH: 5.9 - 6.3)

Ads.	Antibiotic	q_{max} (mg g^{-1})	K_L (L mg^{-1})	R^2	MAPE (%)
AC	TC	622	8.22	0.956	20
	LM	204	11.57	1.000	4
MAC	TC	606	0.54	0.979	19
	LM	142	2.49	0.998	4

Figure 4.18 and Table 4.12 present the results of the overall adsorption of tetracycline and lincomycin in the mixture at room temperature. Herein, the overall adsorption capacities are obtained by summation of tetracycline and lincomycin adsorption capacities, and overall equilibrium concentrations are obtained by the summation of the tetracycline and lincomycin equilibrium concentrations in the mixture. A close look at Figure 4.18 reveals that the adsorption capacities of the adsorbents increased by increasing the antibiotics concentrations. Table 4.12 shows that the Langmuir isotherm model could predict the overall adsorption data of the antibiotics in the mixture with high accuracy (R^2 value). Also, the results indicate that the overall adsorption capacity of MAC in the mixture was slightly lower than that of AC, but its value is still very high. Most importantly, the results indicate that the overall adsorption capacities in the mixture are higher than those obtained for the individual antibiotics.

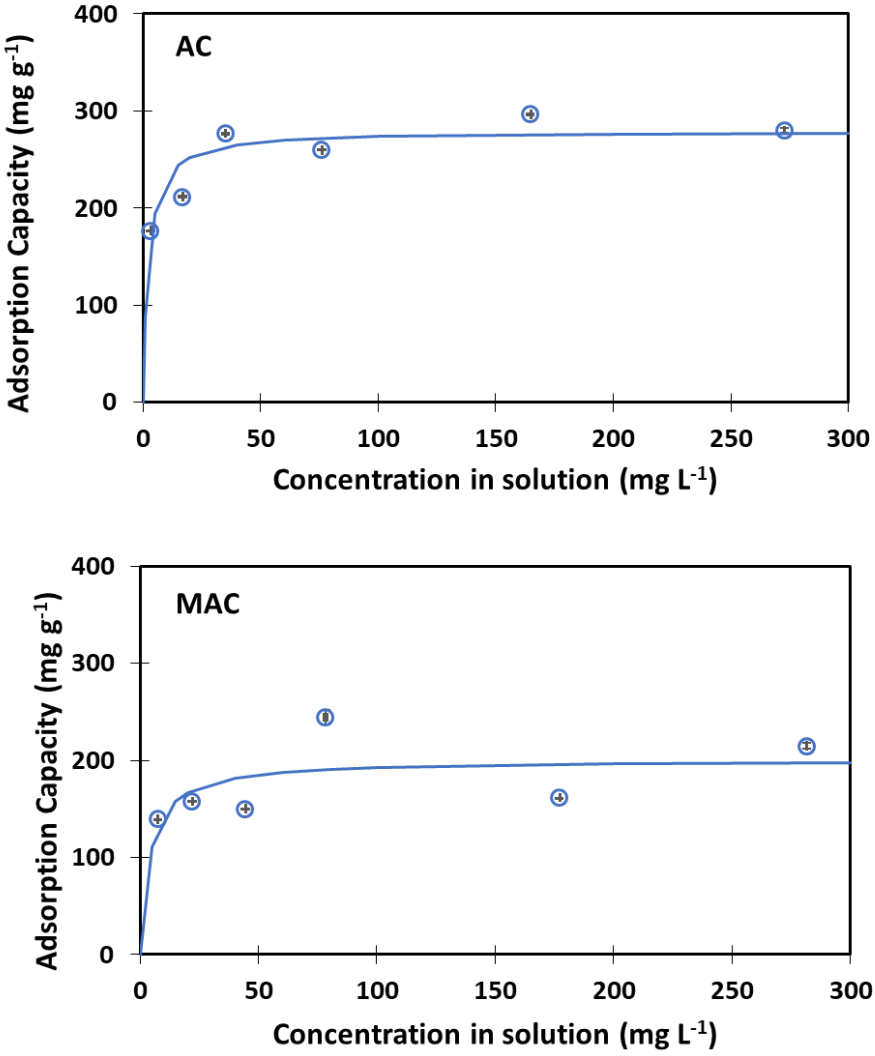

Figure 4.18 Overall adsorption of tetracycline and lincomycin on AC and MAC in the mixture at room temperature (T= 22 °C, pH: 5.9 - 6.3). Symbols represent the experimental results and lines represent the prediction by Langmuir expression. Error bars are calculated based on the standard deviation between two HPLC injections.

Table 4.12 Parameters of Langmuir isotherm for overall adsorption of tetracycline and lincomycin in mixture on AC and MAC (T= 22 °C, pH: 5.9 - 6.3)

Ads.	q_{max} (mg g^{-1})	K_L (L mg^{-1})	R^2	MAPE (%)
AC	911	0.13	0.970	23
MAC	806	0.07	0.981	10

In the preceding section the mixture adsorption data were fitted to the Langmuir model with a single solute (i.e. each antibiotic was treated as an individual) and the obtained isotherms were presented. In order to study the adsorption of mixture antibiotics more realistically, the obtained adsorption data were also fitted to multi-solute models such as Langmuir equations developed for multi-components media with different numbers of adjustable parameters. Among the used equations, the extended form of the Langmuir equation for binary mixtures proposed by Jain and Snoeyink [29] predicted the data with the highest R^2 value and the lowest number of adjustable parameters. This model assumes that both components are adsorbed on the same fraction of adsorption sites.

The results obtained from this model are presented in Figure 4.19 and Table 4.13. This model shows that the adsorption capacity of tetracycline in the mixture is increased by increasing the antibiotics initial concentration, while that of lincomycin slightly decreased. The obtained values for the maximum adsorption capacities are close to those acquired from the single solute model presented in Table 4.11. Also, the obtained K_L values are between those acquired from overall adsorptions in mixture and individual adsorptions in mixture (Table 4.11 and Table 4.12). The important point is that although the obtained R^2 values are in the same order as those obtained from the first mixture model (Table 4.11), it can claimed that this model is providing more accurate prediction because it considers the concentration of both antibiotics in the mixture and models them simultaneously.

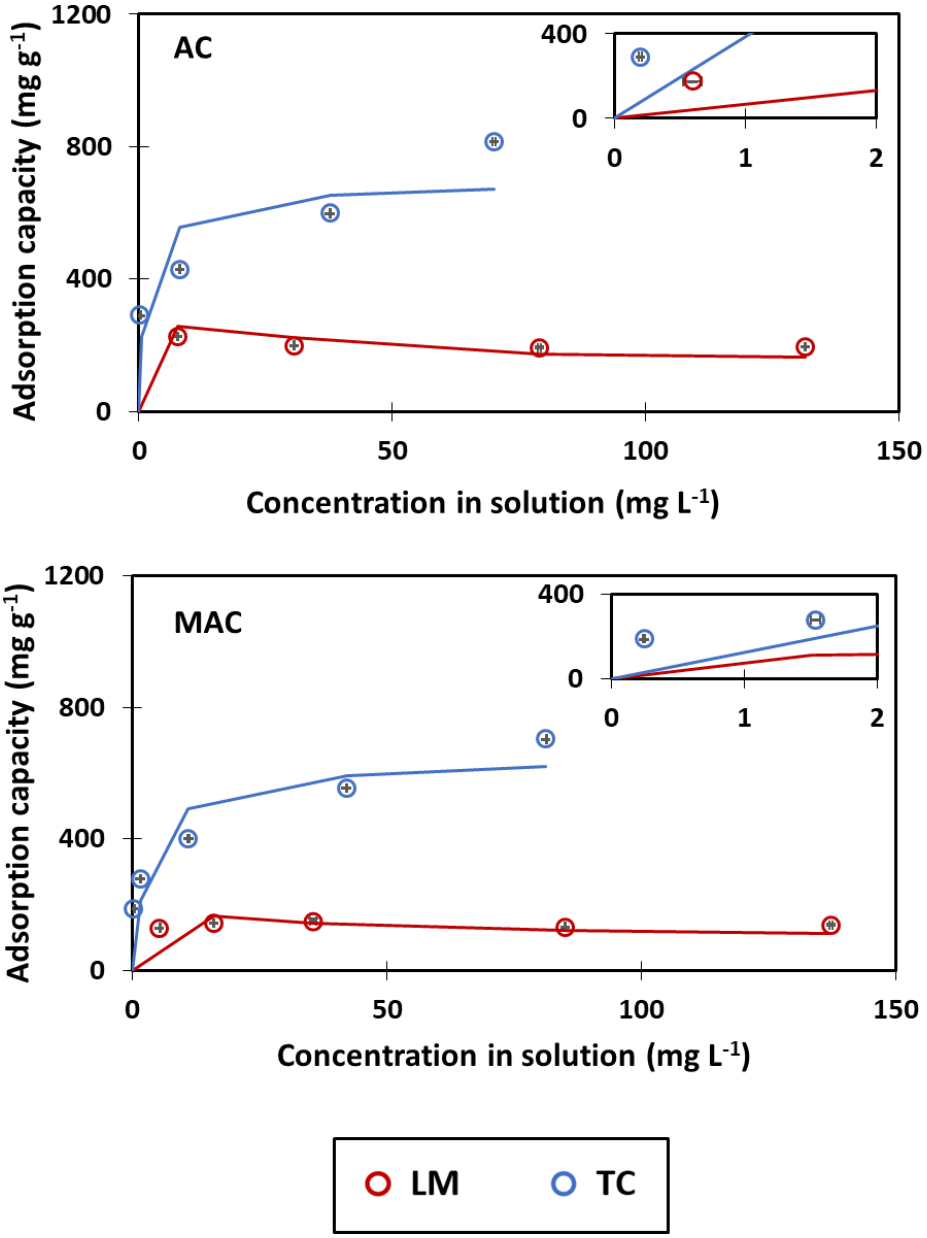

Figure 4.19 Adsorption of tetracycline and lincomycin on AC and MAC in mixture at room temperature (T= 22 °C, pH: 5.9 - 6.3). Symbols represent the experimental results and lines represent the prediction by extended Langmuir expression for binary mixtures. Error bars are calculated based on the standard deviation between two HPLC injections.

Table 4.13 Parameters of extended Langmuir isotherm for adsorption of tetracycline and lincomycin in mixture by AC and MAC (T= 22 °C, pH: 5.9 - 6.3)

Ads.	$K_{L,TC}$ (L mg^{-1})	$K_{L,LM}$ (L mg^{-1})	$q_{max,TC}$ (mg g^{-1})	$q_{max,LM}$ (mg g^{-1})	R^2	MAPE (%)
AC	2.1	2.1	737	275	0.983	8
MAC	0.7	0.9	659	182	0.972	8

4.2.2.3 Comparison of single and binary adsorption processes

The results of the single-solute adsorption process indicated that the prepared adsorbents show higher adsorption capacities for tetracycline than lincomycin. Therefore, it was expected that this would be the case in mixture adsorption experiments as well. The results of binary-solute adsorption experiments indicate that in equal mixtures of tetracycline and lincomycin, tetracycline was preferably adsorbed.

A comparison between the obtained adsorption data for single and binary adsorption processes reveals that the adsorption capacities of AC and MAC for both tetracycline and lincomycin are lower when they are in the mixture. To take a closer look, the ratio of the antibiotics' adsorption capacity onto AC in the mixture to the those of individuals are calculated in different antibiotics initial concentrations and presented in Figure 4.20.

The presented data show that the adsorption capacity of AC for lincomycin in the mixture was around 0.75 of those obtained in individual adsorption experiments. In other words, the adsorption capacity of AC for lincomycin is decreased by around 25 percent because of the presence of tetracycline in water. According to the Figure 4.20, this decrease in adsorption capacity of AC for lincomycin did not change significantly with mixture initial concentration. As a matter of fact, $q_{Mixture,LM}/q_{Single,\ LM}$ was decreased from 0.78 to 0.71 by increasing the mixture initial concentration from 80 to 300 mg L^{-1}.

On the other hand, the presented data points indicate that although the adsorption capacity of AC for tetracycline in mixtures was mostly lower than those of individuals, the value of $q_{Mixture,TC}/q_{Single,\ TC}$ is a function of the mixture initial concentration. According to Figure 4.20, the adsorption capacity of AC for tetracycline in mixture was 0.60 of that obtained in individual adsorption experiment at 80 mg L^{-1} and this value increased to around 1.0 by increasing the initial concentration to 300 mg L^{-1}.

As expected, the presence of each of these two antibiotics in mixture decreased the adsorption capacity of adsorbent toward the other one. This can be explained by the fact that the number of active sites is constant for each adsorbent. As a result, when both tetracycline and lincomycin are present in adsorption media, there is competition between them to occupy adsorption sites. Also, the results indicate that this decrease was much higher for lincomycin than tetracycline. As discussed in detail at the single-solute adsorption section, this could be also explained by the difference between the mechanisms that tetracycline and lincomycin adsorb onto activated carbon attributed to their different molecular structures.

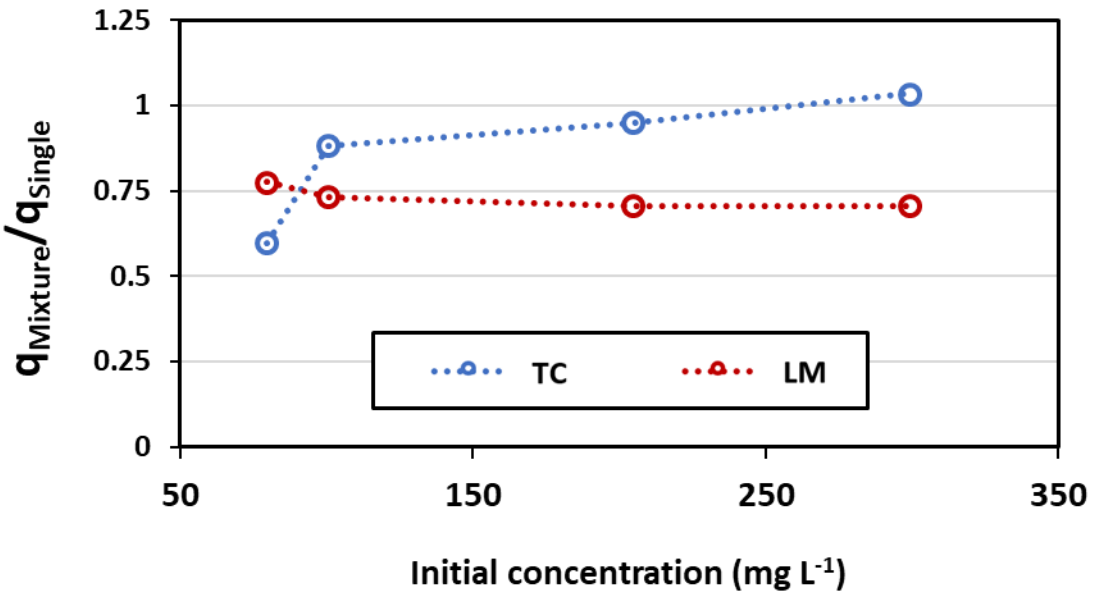

Figure 4.20 The ratio of the antibiotics' adsorption capacity by AC in mixture to the those of single solutes as a function of antibiotics' initial concentration

So far, the results regarding the adsorption of each of the antibiotics in the mixture were discussed and compared with a corresponding case in which each antibiotic was present in water separately. Here, the overall adsorption capacity of the adsorbents for the antibiotics in single and binary adsorption processes are compared. Figure 4.21 shows the overall adsorption capacities of AC and MAC for tetracycline and lincomycin as individuals and in the mixture at room temperature. Most notably, the results indicate that the overall adsorption capacities of adsorbents for the antibiotics in the mixture are higher than those obtained for the single-solute adsorptions. For example, the adsorption capacities of MAC at 200 mg L^{-1} solutions of lincomycin, tetracycline, and half-half mixture of tetracycline and lincomycin were 162, 622 and 688 mg g^{-1}, respectively. It can be concluded that, in the binary

adsorption, although adsorption capacity of the adsorbents for each antibiotic was lower compared to their individuals, the overall adsorption capacity was higher.

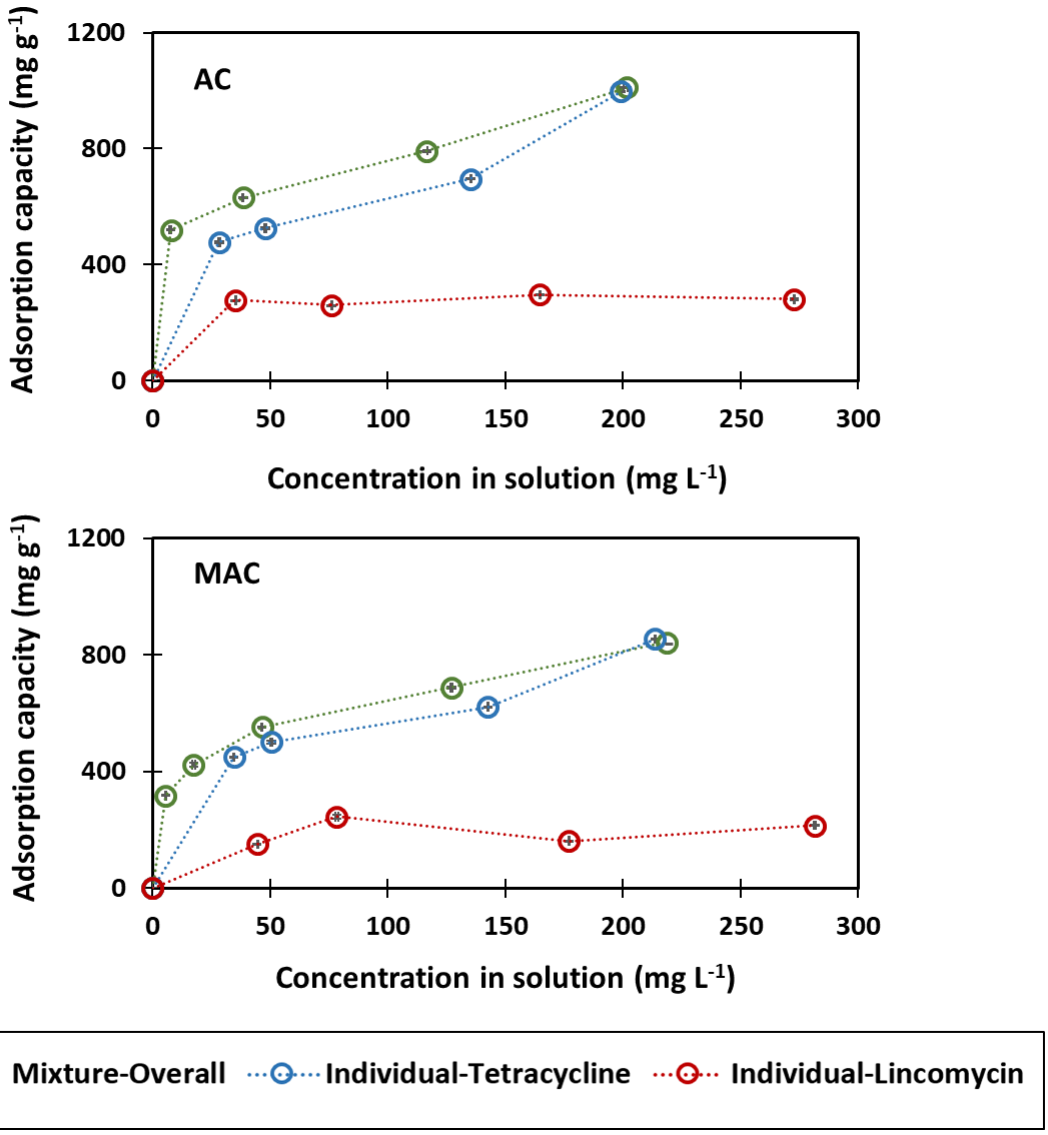

Figure 4.21 Overall adsorption capacities of AC and MAC for tetracycline and lincomycin as individuals and in the mixture at room temperature (22 °C). Symbols represent the experimental results. Error bars are calculated based on the standard deviation between two HPLC injections.

Here, the results of some research studies on the adsorptive removal of mixture of antibiotics from water are investigated to gain a broader view of the contribution of the obtained data to the literature. It is noteworthy that only a few research studies have been carried out in this area so far. Among these studies, some are focused on multi-component

adsorption of antibiotics coming from the same family. Boshir Ahmed et al. [110] studied single and multi-component adsorption of sulfonamide antibiotics including sulfamethazine, sulfamethoxazole and sulfathiazole onto a functionalized biochar from water. Their results show that the adsorption capacity of each antibiotic in the mixture was around three times lower than the single solute adsorption.

On the other hand, some other studies including this study focused on the multi-component adsorption of antibiotics coming from different families. For example, Longcheng Xu et al. [111] developed magnetic γ-Fe_2O_3 /mesoporous silica spheres and investigated their performance in single and binary adsorption of tetracycline (TC) and sulfamethazine (SMZ) from water. They carried out the binary adsorption experiments for TC at different initial concentrations range from 0.005 to 0.05 mmol L^{-1}, in the presence of 0.11 mmol L^{-1} SMZ and adsorption experiments for SMZ at the concentration range of 0.02 to 0.08 mmol L^{-1} in the presence of 0.08 mmol L^{-1} TC. Their results suggest that the simultaneous presence of both antibiotics decreased the adsorption through competition for binding sites of the adsorbent. According to their results, the value of $q_{Mixture}$ /q_{Single} for TC and SMZ was 0.8285 and 0.5325, respectively. Since the values of $q_{Mixture}$ /q_{Single} for TC were higher than those of SMZ, they conclude that the SMZ adsorption onto the adsorbent was more affected by the simultaneous presence of antibiotics than that for TC.

To the best of our knowledge, no study has been carried out regarding the simultaneous adsorption of tetracycline and lincomycin from water in the literature. Therefore, there is no solid data point to compare the obtained adsorption data with. However, the overall outcomes of the mixture experiments are quite compatible with the results of other studies in this area.

4.3 Adsorption experiment in liquid manure supernatant

The adsorption experiments in manure supernatant were carried out in two steps: first; the stability of tetracycline in liquid manure supernatant was studied and second, the performance of the prepared adsorbents for direct removal of tetracycline from liquid manure supernatant was investigated at a single concentration.

4.3.1 Tetracycline stability in liquid manure supernatant

According to the literature, the concentration of tetracycline in liquid manure does not remain constant over time and it can change based on the types of manure and environmental conditions. Kühne et.al. [112] studied the stability of tetracycline in liquid manure at ambient temperature and natural light conditions. Their findings suggest that the concentration of tetracycline in unventilated and ventilated pig slurry was decreased by around 69 and 50% after eight days, respectively [112]. In this study, the effect of natural light was minimized by using amber colour flasks but it is still needed to be assured that the concentration of tetracycline remains constant at the applied experimental conditions. This would assure that the variation of tetracycline concentration in liquid manure supernatant can only be attributed to the performance of adsorbent. A set of experiments was carried out to check the stability of tetracycline at high and low levels of concentrations (50 and 160 mg L^{-1}) based on the procedure explained in 3.2.4.2. Figure 4.22 depicts the obtained profiles of tetracycline concentration in liquid manure supernatant over 30 days (from fourth to the thirty-fourth day). Based on the acquired results, the concentration of tetracycline in liquid manure supernatant was almost constant for the first eight days of experiments and then gradually keep decreasing until the thirtieth day, reaching almost a constant value. The results reveal that the concentration of tetracycline in 160 mg L^{-1} manure solution decreased more significantly than that of 50 mg L^{-1}. Also, the concentration of tetracycline at 50 mg L^{-1} manure solution had smaller margin of errors, especially at the first ten days of experiment. Based on the obtained result, it was decided to carry out the adsorption experiments at a lower level of tetracycline concentration in manure supernatant (around 50 mg L^{-1}) rather than higher concentrations.

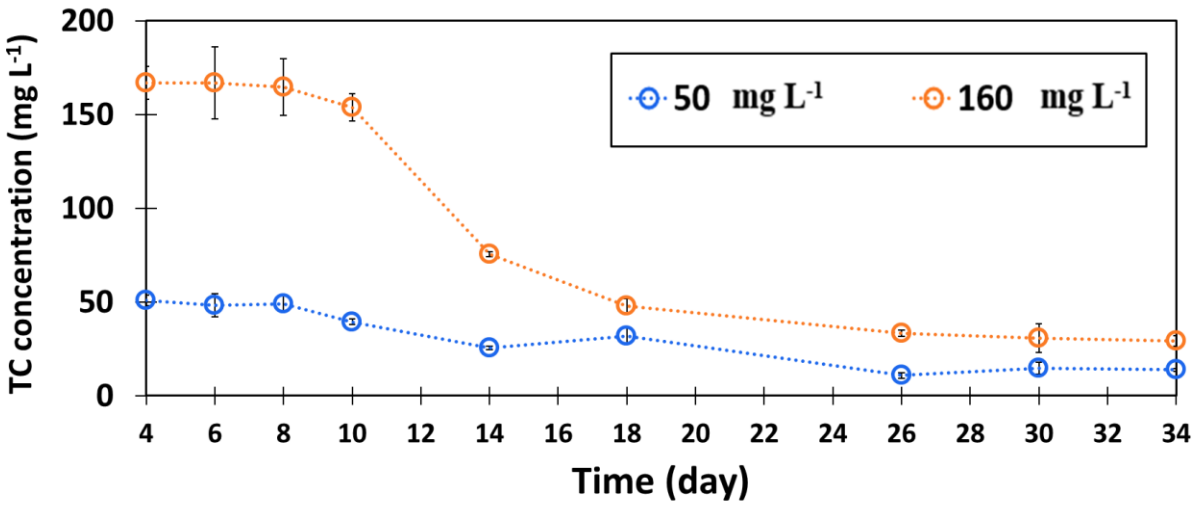

Figure 4.22 Profiles of tetracycline concentration in liquid manure supernatant as a function of time (symbols) for two initial concentrations. Error bars are calculated based on the standard deviation between duplicate samples.

4.3.2 Adsorption of tetracycline from liquid manure supernatant

The adsorption of tetracycline from liquid manure supernatant was studied at 60 mg L^{-1} manure solution using three different dosages of adsorbents and the profiles of tetracycline concentration as a function of time are presented in Figure 4.23. The concentration of tetracycline in liquid manure supernatant was also monitored in the absence of adsorbent (blue curve). This profile indicates that the concentration of tetracycline in liquid manure supernatant was almost constant during the adsorption experiment. The presented results indicate that prepared adsorbents can effectively remove tetracycline from liquid manure supernatant. The green and yellow concentration profiles, for example, indicate that the value of tetracycline concentration became almost zero in four to eight days after the addition of adsorbent.

The equilibrium concentration of tetracycline when 1500 mg L^{-1} adsorbent was added (orange profile) was used to determine the adsorption capacities of AC and MAC in liquid manure supernatant. The calculated adsorption capacities, as well as the amount of adsorbent and the ranges of pH during adsorption test are presented in Table 4.14. All the information is also presented for the adsorption of tetracycline (60 mg L^{-1}) from water to provide a basis for comparison between tetracycline adsorption from water and liquid manure supernatant. The presented data reveal that the amount of adsorbent used for tetracycline adsorption from liquid manure supernatant was 15 times higher than that of adsorption from water solution. It

also indicates that the adsorption capacity of the adsorbents toward tetracycline is much lower when the adsorption experiments were carried out in manure supernatant. This can be explained by the fact that when the adsorbent is added to a manure solution, manure particles can cover the adsorbent surface, and make the surface active sites inaccessible for tetracycline. Consequently, the adsorption capacity of the adsorbents toward tetracycline becomes lower and a higher dosage of adsorbent would be required to remove the same concentration of tetracycline. Moreover, the pH of adsorption media is the other important parameter that possibly caused the difference in the amount of adsorption capacity between water and manure supernatant media. According to the literature, the adsorption of tetracycline into activated carbon from water remains constant in the pH range of 4-7 and then keeps decreasing as the pH of adsorption media increases [25, 35]. This observation can be explained by the fact that increasing the pH of solution enhances the amount of ionization of oxygenated groups onto activated carbon. Consequently, the negative surface charge density of adsorbent increases resulting in the reduction of adsorption capacity.

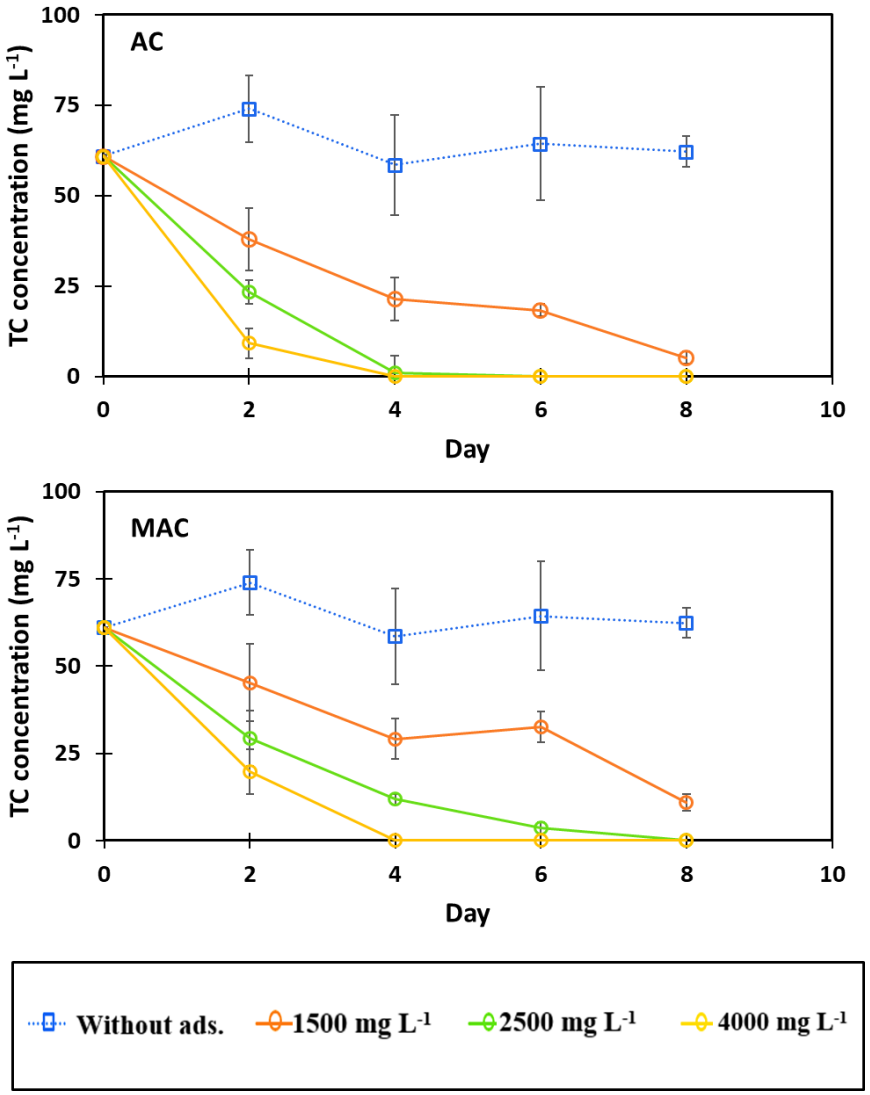

Figure 4.23 Profile of tetracycline concentration in liquid manure supernatant with different dosages of adsorbents at room temperature (T= 22 °C, pH: 8.0 - 8.2). Error bars are calculated based on the standard deviation between duplicate samples.

Table 4.14 Adsorption data regarding the removal of tetracycline (60 mg L^{-1}) from water and liquid manure supernatant using AC and MAC (T= 22 °C)

Ads.	Water			Manure supernatant		
	pH	adsorbent (mg L^{-1})	q (mg g^{-1})	pH	adsorbent (mg L^{-1})	q (mg g^{-1})
AC	5.3-6.2	100	477	8.0-8.2	1500	38
MAC	5.3-6.2	100	450	8.0-8.2	1500	34

No study has been carried out regarding the direct removal of antibiotics from liquid manure. According to the literature, the only related study was carried out by Fukahori et al. [113] in 2013. They studied the adsorption of sulfonamide antibiotics on zeolite HSZ-385 from distilled water and stored porcine urine. The pH of porcine urine was around 9 and it was used as an adsorption medium without any pH adjustment. Their findings suggest that the adsorption capacity for sulphonamide antibiotics in the porcine urine were lower than those obtained from distilled water (pH 9). For example, the adsorption capacity of HSZ-385 for sulfadimethoxinev declined by around 30% when the adsorption experiment was carried out in porcine urine. They explained that this decrease was attributed to the presence of organic matter within urine matrix, which competitively adsorbed onto the adsorbent.

5 SUMMARY, CONCLUSIONS AND RECOMMENDATIONS

The following chapter summarizes the conclusions from this research study and provides recommendations for future work.

5.1 Conclusions

- A commercial activated carbon was successfully magnetized through an ultrasonic-assisted co-precipitation method. The prepared adsorbent possesses high saturation magnetization (13 emu g^{-1}) with superparamagnetic properties.
- The developed magnetic activated carbon could effectively remove tetracycline and lincomycin in aqueous solution either individually or when both antibiotics are present in a mixture. The adsorption capacities of activated carbon toward both antibiotics are slightly decreased after the magnetization. This decrease was much higher for lincomycin than tetracycline
- Initial concentration of the antibiotics in the single- or binary-solute adsorption process affects the adsorption uptake.
- The adsorption capacity of MAC toward tetracycline is highly temperature dependent. The higher temperatures are more favourable for the adsorption of tetracycline by MAC, indicating endothermic nature of this process.
- The adsorption capacity of MAC toward tetracycline (mg g^{-1}) was up to 4 times higher than that of lincomycin at room temperature depending on the initial concentration of antibiotics in solution. Also, tetracycline was preferably adsorbed when both antibiotics were present in a mixture
- The presence of each antibiotic in mixture decreased the adsorption capacity of adsorbent toward the other one. In the binary-solute adsorption, although the adsorption capacity of the adsorbents for each antibiotic was lower compared to their individual adsorption, the overall adsorption capacity was higher.
- Langmuir and Freundlich isotherms were used to model the adsorption data. Langmuir model either in a non-extended or extended format predicted mixture adsorption data well. On the other hand, Freundlich model was not able to model the obtained data well based on the obtained R^2 values.

- The obtained adsorption data indicated that the direct and effective removal of tetracycline from liquid manure supernatant is possible, but it requires around 15 times larger amounts of adsorbent compared to adsorption in water.

5.2 Recommendations for future works

As part of this research study, a few new ideas were identified that would be interesting to pursue further. In this regard, it is recommended to:

- Investigate the desorption of antibiotics and regeneration of the developed magnetic activated carbon. For this aim, the performance of the magnetic adsorbent can be studied in sequential cycles of adsorption-desorption. This study would show how the performance as well as magnetic property of the adsorbent would change over time.
- Study the kinetics of tetracycline and lincomycin adsorption as an individual and in a mixture. These kinetic studies would be helpful to compare the rate and dynamics of adsorption in single- and binary-solute adsorption processes.
- Investigate the effect of antibiotic concentration and pH on the adsorptive removal of tetracycline from liquid manure. If a significant change is observed, pH adjustment of manure could be considered as a pre-treatment step to enhance the adsorption efficiency.
- Investigate how the magnetic property of adsorbents would change in manure media. This can include checking the possibility of leach and loss of magnetic components from the sorbent. This investigation can open doors for development of sustainable adsorbent with longer lifetime for direct removal of antibiotics from manure.

REFERENCES

[1] Public Health Agency of Canada, Canadian resistance report, 2017.

[2] S. Mithani, T.T. Tam, Canadian antimicrobial resistance surveillance system 2017 report - Executive summary - Canada.ca. , 2018.

[3] V. Homem, L. Santos, Degradation and removal methods of antibiotics from aqueous matrices e A review, J. Environ. Manage. 92 (2011) 2304–2347. doi:10.1016/j.jenvman.2011.05.023.

[4] M. Baghdadi, E. Ghaffari, B. Aminzadeh, Removal of carbamazepine from municipal wastewater effluent using optimally synthesized magnetic activated carbon : Adsorption and sedimentation kinetic studies, Biochem. Pharmacol. 4 (2016) 3309–3321. doi:10.1016/j.jece.2016.06.034.

[5] B. Kakavandi, A.J. Jafari, R.R. Kalantary, S. Nasseri, A. Ameri, A. Esrafily, Synthesis and properties of Fe3O4 -activated carbon magnetic nanoparticles for removal of aniline from aqueous solution : equilibrium , kinetic and thermodynamic studies, Iranian J. Environ. Health Sci. Eng. 10 (2013) 2–10.

[6] Government of Canada, Responsible use of Medically Important Antimicrobials in Animals, Responsible Use Medically Important Antimicrob. Anim. (2018).

[7] B. Verma, J. V Headley, R.D. Robarts, B. Verma, J. V Headley, R.D. Robarts, Behaviour and fate of tetracycline in river and wetland waters on the Canadian Northern Great Plains, J. Environ. Sci. Heal. 4529 (2015). doi:10.1080/10934520601011163.

[8] I. Chopra, M. Roberts, Tetracycline Antibiotics : Mode of Action , Applications , Molecular Biology , and Epidemiology of Bacterial Resistance Tetracycline Antibiotics : Mode of Action , Applications , Molecular Biology , and Epidemiology of Bacterial Resistance, Microbiol Mol Biol Rev. 65 (2001) 232–260. doi:10.1128/MMBR.65.2.232.

[9] V. Ha, T. Thi, B. Lee, Great improvement on tetracycline removal using ZnO rod-activated carbon fiber composite prepared with a facile microwave method, J. Hazard. Mater. 324 (2016) 329–339. doi:10.1016/j.jhazmat.2016.10.066.

[10] R.D.P. Drogui, Tetracycline antibiotics in the environment : a review, Environ. Chem. Lett. 11 (2013) 209–227. doi:10.1007/s10311-013-0404-8.

[11] M. Rajeswaran, T. Srikrishnan, Crystal and molecular structure and absolute configuration of lincomycin hydrochloride monohydrate, Carbohydr. Res. 339 (2004) 2111–2115. doi:10.1016/j.carres.2004.05.032.

[12] R.R. Herr, G. Slomp, Lincomycin. 11. Characterization and Gross Structure, J Am Chem Soc. I (1967) 2444–2447.

[13] T. Deblonde, C. Cossu-leguille, P. Hartemann, Emerging pollutants in wastewater: A review of the literature, Int. J. Hyg. Environ. Health. 214 (2015) 442–448.

doi:10.1016/j.ijheh.2011.08.002.

[14] X. Miao, F. Bishay, Occurrence of Antimicrobials in the Final Effluents of Wastewater Treatment Plants in Canada, Environ. Sci. Technol. 38 (2004) 3533–3541. doi:10.1021/es030653q.

[15] J. Rivera-utrilla, M. Sánchez-polo, M.Á. Ferro-garcía, G. Prados-joya, Pharmaceuticals as emerging contaminants and their removal from water . A review, Chemosphere. 93 (2013) 1268–1287. doi:10.1016/j.chemosphere.2013.07.059.

[16] M.B. Ahmed, J.L. Zhou, H.H. Ngo, W. Guo, Science of the Total Environment Adsorptive removal of antibiotics from water and wastewater : Progress and challenges, Sci. Total Environ. 532 (2015) 112–126. doi:10.1016/j.scitotenv.2015.05.130.

[17] X. Tan, Y. Liu, G. Zeng, X. Wang, X. Hu, Y. Gu, Chemosphere Application of biochar for the removal of pollutants from aqueous solutions, Chemosphere. 125 (2015) 70–85. doi:10.1016/j.chemosphere.2014.12.058.

[18] P. Liu, W. Liu, H. Jiang, J. Chen, W. Li, H. Yu, Modification of bio-char derived from fast pyrolysis of biomass and its application in removal of tetracycline from aqueous solution, Bioresour. Technol. 121 (2012) 235–240. doi:10.1016/j.biortech.2012.06.085.

[19] Y. Zou, H. Huang, M. Chu, J. Lin, D. Yin, Y. Li, Adsorption Research of Tetracycline from Water by HCl-modified Zeolite, Adv. Mater. Res. 574 (2012) 43–47. doi:10.4028/www.scientific.net/AMR.573-574.43.

[20] Y. Gao, Y. Li, L. Zhang, H. Huang, J. Hu, S. Mazhar, X. Su, Adsorption and removal of tetracycline antibiotics from aqueous solution by graphene oxide, J. Colloid Interface Sci. 368 (2012) 540–546. doi:10.1016/j.jcis.2011.11.015.

[21] I.W.A. Publishing, W. Science, Adsorption removal of tetracycline from aqueous solution by anaerobic granular sludge: equilibrium and kinetic studies, Water Sci Technol. 67 (2013) 1490–1496. doi:10.2166/wst.2013.016.

[22] D. Zhang, J. Yin, J. Zhao, H. Zhu, C. Wang, Adsorption and removal of tetracycline from water by petroleum coke-derived highly porous activated carbon, Biochem. Pharmacol. 3 (2015) 1504–1512. doi:10.1016/j.jece.2015.05.014.

[23] J. Rivera-utrilla, C. V Gómez-pacheco, M. Sánchez-polo, J.J. López-peñalver, R. Ocampo-pérez, Tetracycline removal from water by adsorption / bioadsorption on activated carbons and sludge-derived adsorbents, J. Environ. Manage. 131 (2013) 16–24. doi:10.1016/j.jenvman.2013.09.024.

[24] R.W. Coughlin, Role of Surface Acidity in the Adsorption of Organic Pollutants on the Surface of Carbon, Environ. Sci. Technol. 2 (1968) 291–297.

[25] H. Kim, Y. Sik, V.K. Sharma, Adsorption of antibiotics and iopromide onto single-walled and multi-walled carbon nanotubes, Chem. Eng. J. 255 (2014) 23–27. doi:10.1016/j.cej.2014.06.035.

[26] C. Libra, A. Saupe, Fundamentals of Adsorption onto Activated Carbon in Water and Wastewater Treatment, 2011. doi:10.1002/9783527639441.ch2.

[27] E.S. Tarleton, R. J. Wakeman, Solid/Liquid Separation : Equipment Selection and Process Design, 2006. doi:10.1016/B978-1-85617-421-3.X5000-7.

[28] K.J.H. and G.T. John C. Crittenden, R. Rhodes Trussell, David W. Hand, MWH's Water Treatment: Principles and Design, 2012. doi:10.1002/9781118131473.

[29] E. Worch, Adsorption Technology in Water Treatment, 2012. doi:10.1515/9783110240238.

[30] O. Sahu, N. Singh, Significance of bioadsorption process on textile industry wastewater, Elsevier Ltd., 2018. doi:10.1016/b978-0-08-102491-1.00013-7.

[31] E. Investigation, Basic Principles of Adsorption, (1992) 36–47.

[32] A. Takdastan, A.H. Mahvi, E.C. Lima, M. Shirmardi, A.A. Babaei, G. Goudarzi, A. Neisi, M.H. Farsani, M. Vosoughi, Preparation, characterization, and application of activated carbon from low-cost material for the adsorption of tetracycline antibiotic from aqueous solutions, Water Sci. Technol. 74 (2016) 2349–2363. doi:10.2166/wst.2016.402.

[33] H.R. Pouretedal, N. Sadegh, Effective removal of Amoxicillin , Cephalexin , Tetracycline and Penicillin G from aqueous solutions using activated carbon nanoparticles prepared from vine wood, J. Water Process Eng. 1 (2014) 64–73. doi:10.1016/j.jwpe.2014.03.006.

[34] K. Raby, A. Avalos Ramirez, M. Heitz, Elimination of nitrogen present in swine manure using a high-efficiency biotrickling filter, Environ. Technol. (United Kingdom). 34 (2013) 813–824. doi:10.1080/09593330.2012.720615.

[35] D. Mehta, S. Mazumdar, S.K. Singh, Magnetic adsorbents for the treatment of water/wastewater— A review, J. Water Process Eng. 7 (2015) 244–265. doi:10.1016/j.jwpe.2015.07.001.

[36] P.C. Singer, K. Bilyk, Enhanced coagulation using a magnetic ion exchange resin, Water Res. 36 (2002) 4009–4022.

[37] Y. Ji, Y. Wang, J. Sun, T. Yan, J. Li, T. Zhao, X. Yin, Enhancement of biological treatment of wastewater by magnetic field, Bioresour. Technol. 101 (2010) 8535–8540. doi:10.1016/j.biortech.2010.05.094.

[38] S. Ni, J. Ni, N. Yang, J. Wang, Effect of magnetic nanoparticles on the performance of activated sludge treatment system, Bioresour. Technol. 143 (2013) 555–561. doi:10.1016/j.biortech.2013.06.041.

[39] K.M. Lompe, Magnetic Powdered Activated Carbon for Drinking Water Treatment, (2018).

[40] O. Philippova, A. Barabanova, V. Molchanov, A. Khokhlov, Magnetic polymer beads : Recent trends and developments in synthetic design and applications, Eur. Polym. J. 47 (2011) 542–559. doi:10.1016/j.eurpolymj.2010.11.006.

[41] D. Mohan, A. Sarswat, V.K. Singh, M. Alexandre-franco, C.U. Pittman, Development

of magnetic activated carbon from almond shells for trinitrophenol removal from water, Chem. Eng. J. 172 (2011) 1111–1125. doi:10.1016/j.cej.2011.06.054.

[42] I. Salehi, M. Shirani, A. Semnani, M. Hassani, S. Habibollahi, Comparative Study Between Response Surface Methodology and Artificial Neural Network for Adsorption of Crystal Violet on Magnetic Activated Carbon, Arab J Sci Eng. 41 (2016) 2611–2621. doi:10.1007/s13369-016-2109-3.

[43] S. Kulkarni, J. Kaware, Regeneration and Recovery in Adsorption- a Review, Innov. Sci. Eng. Technol. 1 (2014) 61–64.

[44] A.S. Teja, P.Y. Koh, Synthesis, properties, and applications of magnetic iron oxide nanoparticles, Prog. Cryst. Growth Charact. Mater. 55 (2009) 22–45. doi:10.1016/j.pcrysgrow.2008.08.003.

[45] K. Gotoh, Powder Technology Handbook (Third Edition), 2006. doi:10.1163/156855206777213384.

[46] R. Gerber, R.R. Birss, High gradient magnetic separation, Res. Stud. Press Div. John Wiley Sons, Ltd., 1983,. (1983) 209.

[47] D.L. Cummings, D.A. Himmelblau, J.A. Oberteuffer, G.J. Powers, Capture of small paramagnetic particles by magnetic forces from low speed fluid flows, AIChE J. 22 (1976) 569–575.

[48] L. Svarovsky, Solid-liquid separation, Elsevier, 2000.

[49] D. Fabris, V. Garg, K. Sapag, L.C.A. Oliveira, R.V.R.A. Rios, R.M. Lago, Activated carbon / iron oxide magnetic composites for the adsorption of contaminants in water, Carbon N. Y. 40 (2002) 2177–2183.

[50] G. Mckay, Solution to the homogeneous surface diffusion model for batch adsorption systems using orthogonal collocation, Chem. Eng. J. 81 (2001) 213–221.

[51] Y.S. Kang, S. Risbud, Synthesis and Characterization of Nanometer-Size Fe3O4 and γ-Fe2O3 Particles, Chem. Mater. 5 (1996) 2209–2211. doi:10.1021/cm960157j.

[52] H.S. Saroyan, D.A. Giannakoudakis, C.S. Sarafidis, N.K. Lazaridis, E.A. Deliyanni, Effective impregnation for the preparation of magnetic mesoporous carbon: application on dye adsorption, J. Chem. Technol. Biotechnol. 92 (2017) 1899–1911. doi:10.1002/j.

[53] A. Cazetta, O. Pezoti, K. C.Bedin, T. L.Silva, A. Junior, T. Asefa, V.C. Almeida, Magnetic Activated Carbon Derived from Biomass Waste by Concurrent Synthesis: E ffi cient Adsorbent for Toxic Dyes, ACS Sustain. Chem. Eng. 4 (2016) 1058–1068. doi:10.1021/acssuschemeng.5b01141.

[54] M. Huy, N. Hoa, T. Dung, T. Thu, S. Pham, V.K. Nguyen, Activated carbon / Fe3O4 nanoparticle composite : Fabrication , methyl orange removal and regeneration by hydrogen peroxide, Chemosphere. 85 (2011) 1269–1276. doi:10.1016/j.chemosphere.2011.07.023.

[55] J. Lee, S. Jin, Y. Hwang, J.G. Park, H.M. Park, T. Hyeon, Simple synthesis of

mesoporous carbon with magnetic nanoparticles embedded in carbon rods, Carbon N. Y. 43 (2005) 2536–2543. doi:10.1016/j.carbon.2005.05.005.

[56] M. Auffan, W. Achouak, J. Rose, M.A. Roncato, C. Chanéac, D.T. Waite, A. Masion, J.C. Woicik, M.R. Wiesner, J.Y. Bottero, Relation between the redox state of iron-based nanoparticles and their cytotoxicity toward Escherichia coli, Environ. Sci. Technol. 42 (2008) 6730–6735. doi:10.1021/es800086f.

[57] R.M. Cornell, U. Schwertmann, The Iron Oxides, Second Edition, (2003).

[58] M. Zahoor, M. Mahramanlioglu, Adsorption of Imidacloprid on Powdered Activated Carbon and Magnetic Activated Carbon, 25 (2011) 55–63.

[59] A.C. Martins, O. Pezoti, A.L. Cazetta, K.C. Bedin, D.A.S. Yamazaki, G.F.G. Bandoch, T. Asefa, J. V. Visentainer, V.C. Almeida, Removal of tetracycline by NaOH-activated carbon produced from macadamia nut shells: Kinetic and equilibrium studies, Chem. Eng. J. 260 (2015) 291–299. doi:10.1016/j.cej.2014.09.017.

[60] X. Zhu, Y. Liu, F. Qian, C. Zhou, S. Zhang, J. Chen, Preparation of magnetic porous carbon from waste hydrochar by simultaneous activation and magnetization for tetracycline removal, Bioresour. Technol. 154 (2014) 209–214. doi:10.1016/j.biortech.2013.12.019.

[61] N. Ayawei, A.N. Ebelegi, D. Wankasi, Modelling and Interpretation of Adsorption Isotherms, J. Chem. 2017 (2017) 1–11. doi:10.1155/2017/3039817.

[62] F.E. Soetaredjo, Clay Materials for Environmental Remediation, n.d.

[63] E. Rezaei, B. Schlageter, M. Nemati, B. Predicala, Evaluation of metal oxide nanoparticles for adsorption of gas phase ammonia, Biochem. Pharmacol. 5 (2017) 422–431. doi:10.1016/j.jece.2016.12.026.

[64] H.N. Tran, S.J. You, H.P. Chao, Thermodynamic parameters of cadmium adsorption onto orange peel calculated from various methods: A comparison study, J. Environ. Chem. Eng. 4 (2016) 2671–2682. doi:10.1016/j.jece.2016.05.009.

[65] Y. Liu, Is the Free Energy Change of Adsorption Correctly Calculated?, (2009) 1981–1985. doi:10.1021/je800661q.

[66] H.A. El-Araby, A.M.M.A. Ibrahim, A.H. Mangood, A.A.-H. Abdel-Rahman, Sesame Husk as Adsorbent for Copper(II) Ions Removal from Aqueous Solution, J. Geosci. Environ. Prot. 05 (2017) 109–152. doi:10.4236/gep.2017.57011.

[67] C.G. Hill, An introduction to chemical engineering kinetics & reactor design, 1977.

[68] H.N. Tran, S.J. You, A. Hosseini-Bandegharaei, H.P. Chao, Mistakes and inconsistencies regarding adsorption of contaminants from aqueous solutions: A critical review, Water Res. 120 (2017) 88–116. doi:10.1016/j.watres.2017.04.014.

[69] A.A. Khan, R.P. Singh, Adsorption thermodynamics of carbofuran on Sn (IV) arsenosilicate in H+, Na+ and Ca2+ forms, Colloids and Surfaces. 24 (1987) 33–42. doi:10.1016/0166-6622(87)80259-7.

[70] S.K. Milonjić, A consideration of the correct calculation of thermodynamic parameters of adsorption, J. Serbian Chem. Soc. 72 (2007) 1363–1367. doi:10.2298/JSC0712363M.

[71] A.M. Abdalla, S. Ghosh, I.K. Puri, Decorating carbon nanotubes with co-precipitated magnetite nanocrystals, Diam. Relat. Mater. 66 (2016) 90–97. doi:10.1016/j.diamond.2016.04.003.

[72] G.A. Dorofeev, A.N. Streletskii, I. V Povstugar, A. V Protasov, E.P. Elsukov, Determination of Nanoparticle Sizes by the X ray Diffraction Method, (2012). doi:10.1134/S1061933X12060051.

[73] Z. Yue, S.E. Bender, J. Wang, J. Economy, Removal of chromium Cr (VI) by low-cost chemically activated carbon materials from water, 166 (2009) 74–78. doi:10.1016/j.jhazmat.2008.10.125.

[74] M. WOJNICKI, Spectrophotometric Analysis of the Kinetic of Pd(II) Chloride Complex Ions Sorption Process from Diluted Aqua Solutions Using Commercially Available Activated Carbon, 62 (2017) 2405–2411. doi:10.1515/amm-2017-0354.

[75] T. Yamashita, P. Hayes, Analysis of XPS spectra of Fe 2 + and Fe 3 + ions in oxide materials, 254 (2008) 2441–2449. doi:10.1016/j.apsusc.2007.09.063.

[76] M. Iram, C. Guo, Y. Guan, A. Ishfaq, H. Liu, Adsorption and magnetic removal of neutral red dye from aqueous solution using Fe3O4 hollow nanospheres, J. Hazard. Mater. 181 (2010) 1039–1050. doi:10.1016/j.jhazmat.2010.05.119.

[77] U. De Provence, Adsorption by Powders and Porous Solids, n.d.

[78] Shao-Wen C, Ying-Jie Z, Ming-Yan M, Liang L, Ling Z, Hierarchically nanostructured magnetic hollow spheres of Fe3O4 and γ-Fe2O3: preparation and potential application in drug delivery, J. Phys. Chem. C. 112 (2008) 1851–1856. doi:10.1021/jp077468+.

[79] M. Hedayati, M. Esmaieli, Tetracycline adsorption by H3PO4 -activated carbon produced from apricot nut shells : A batch study, Process Saf. Environ. Prot. 102 (2016) 700–709. doi:10.1016/j.psep.2016.05.025.

[80] L. Shao, Z. Ren, G. Zhang, L. Chen, Facile synthesis, characterization of a MnFe 2O 4/activated carbon magnetic composite and its effectiveness in tetracycline removal, Mater. Chem. Phys. 135 (2012) 16–24. doi:10.1016/j.matchemphys.2012.03.035.

[81] J. Xu, P. Xin, Y. Gao, B. Hong, H. Jin, D. Jin, X. Peng, J. Li, J. Gong, H. Ge, X. Wang, Magnetic properties and methylene blue adsorptive performance of CoFe 2 O 4 / activated carbon nanocomposites, Mater. Chem. Phys. 147 (2014) 915–919. doi:10.1016/j.matchemphys.2014.06.037.

[82] E.K. Faulconer, N.V.H. Von Reitzenstein, D.W. Mazyck, Optimization of magnetic powdered activated carbon for aqueous Hg (II) removal and magnetic recovery, J. Hazard. Mater. 199–200 (2012) 9–14. doi:10.1016/j.jhazmat.2011.10.023.

[83] W.W. Tang, G.M. Zeng, J.L. Gong, Y. Liu, X.Y. Wang, Y.Y. Liu, Z.F. Liu, L. Chen, X.R. Zhang, D.Z. Tu, Simultaneous adsorption of atrazine and Cu (II) from wastewater by magnetic multi-walled carbon nanotube, Chem. Eng. J. 211–212 (2012) 470–478.

doi:10.1016/j.cej.2012.09.102.

[84] C. Saucier, P. Karthickeyan, V. Ranjithkumar, E.C. Lima, G.S. dos Reis, I.A.S. de Brum, Efficient removal of amoxicillin and paracetamol from aqueous solutions using magnetic activated carbon, Environ. Sci. Pollut. Res. 24 (2017) 5918–5932. doi:10.1007/s11356-016-8304-7.

[85] Y. Liu, X. Zhu, F. Qian, S. Zhang, J. Chen, Magnetic activated carbon prepared from rice straw-derived hydrochar for triclosan removal, RSC Adv. 4 (2014) 63620–63626. doi:10.1039/c4ra11815d.

[86] A.L. Cazetta, O. Pezoti, K.C. Bedin, T.L. Silva, A. Paesano Junior, T. Asefa, V.C. Almeida, Magnetic Activated Carbon Derived from Biomass Waste by Concurrent Synthesis: Efficient Adsorbent for Toxic Dyes, ACS Sustain. Chem. Eng. 4 (2016) 1058–1068. doi:10.1021/acssuschemeng.5b01141.

[87] S. Palanisamy, Y. Wang, Superparamagnetic iron oxide nanoparticulate system: synthesis, targeting, drug delivery and therapy in cancer, 48 (2019). doi:10.1039/c9dt00459a.

[88] A. Blanco, A.B. Fuertes, P. Gorria, M. Sevilla, Synthesis of magnetically separable adsorbents through the incorporation of protected nickel nanoparticles in an activated carbon, 44 (2006) 1954–1957. doi:10.1016/j.carbon.2006.02.013.

[89] W. Oh, S. Lua, Z. Dong, T. Lim, Performance of magnetic activated carbon composite as peroxymonosulfate activator and regenerable adsorbent via sulfate radical-mediated oxidation processes, J. Hazard. Mater. 284 (2015) 1–9. doi:10.1016/j.jhazmat.2014.10.042.

[90] M. Fayazi, M. Ghanei-motlagh, M. Ali, The adsorption of basic dye (Alizarin red S) from aqueous solution onto activated carbon / γ -Fe 2 O 3 nano-composite : Kinetic and equilibrium studies, Mater. Sci. Semicond. Process. 40 (2015) 35–43. doi:10.1016/j.mssp.2015.06.044.

[91] Z. Liu, F. Zhang, R. Sasai, Arsenate removal from water using Fe 3 O 4 -loaded activated carbon prepared from waste biomass, Chem. Eng. J. 160 (2010) 57–62. doi:10.1016/j.cej.2010.03.003.

[92] K. Maren, D. Menard, B. Barbeau, The influence of iron oxide nanoparticles upon the adsorption of organic matter on magnetic powdered activated carbon, Water Res. 123 (2017) 30–39. doi:10.1016/j.watres.2017.06.045.

[93] H. Sayğili, F. Güzel, Effective removal of tetracycline from aqueous solution using activated carbon prepared from tomato (Lycopersicon esculentum Mill.) industrial processing waste, Ecotoxicol. Environ. Saf. 131 (2016) 22–29. doi:10.1016/j.ecoenv.2016.05.001.

[94] X. Zhang, X. Lin, Y. He, X. Luo, Phenolic hydroxyl derived copper alginate microspheres as superior adsorbent for effective adsorption of tetracycline, 136 (2019) 445–459. doi:10.1016/j.ijbiomac.2019.05.165.

[95] W. Xiong, G. Zeng, Z. Yang, Y. Zhou, C. Zhang, M. Cheng, Y. Liu, L. Hu, J. Wan, C. Zhou, R. Xu, X. Li, Adsorption of tetracycline antibiotics from aqueous solutions on nanocomposite multi-walled carbon nanotube functionalized MIL-53(Fe) as new adsorbent, Sci. Total Environ. 627 (2018) 235–244. doi:10.1016/j.scitotenv.2018.01.249.

[96] G. Li, D. Zhang, M. Wang, J. Huang, L. Huang, Preparation of activated carbons from Iris tectorum employing ferric nitrate as dopant for removal of tetracycline from aqueous solutions, Ecotoxicol. Environ. Saf. 98 (2013) 273–282. doi:10.1016/j.ecoenv.2013.08.015.

[97] A. Xie, J. Cui, Y. Chen, J. Lang, C. Li, Y. Yan, J. Dai, Simultaneous activation and magnetization toward facile preparation of auricularia-based magnetic porous carbon for efficient removal of tetracycline, J. Alloys Compd. 784 (2019) 76–87. doi:10.1016/j.jallcom.2018.12.375.

[98] V.A. Online, Z. Xiong, C. Li, J. Zhang, Zeolitic imidazolate metal organic framework ZIF-8 with ultra-high adsorption capacity bound tetracycline in aqueous solution, (2015). doi:10.1039/C5RA15497A.

[99] Q. Zhou, Z. Li, C. Shuang, A. Li, M. Zhang, M. Wang, Efficient removal of tetracycline by reusable magnetic microspheres with a high surface area, Chem. Eng. J. 210 (2012) 350–356. doi:10.1016/j.cej.2012.08.081.

[100] L. Zhang, X. Song, X. Liu, L. Yang, F. Pan, J. Lv, Studies on the removal of tetracycline by multi-walled carbon nanotubes, Chem. Eng. J. 178 (2011) 26–33. doi:10.1016/j.cej.2011.09.127.

[101] P. Taylor, B.K. Vu, O. Snisarenko, H.S. Lee, E.W. Shin, Adsorption of tetracycline on La - impregnated MCM - 41 materials, (2010) 37–41. doi:10.1080/09593330903453210.

[102] J. Kang, H. Liu, Y. Zheng, J. Qu, J.P. Chen, Systematic study of synergistic and antagonistic effects on adsorption of tetracycline and copper onto a chitosan, J. Colloid Interface Sci. 344 (2010) 117–125. doi:10.1016/j.jcis.2009.11.049.

[103] P. Chang, Z. Li, J. Jean, W. Jiang, C. Wang, K. Lin, Adsorption of tetracycline on 2 : 1 layered non-swelling clay mineral illite, Appl. Clay Sci. 67–68 (2012) 158–163. doi:10.1016/j.clay.2011.11.004.

[104] W. Zhang, Q. Zhang, F. Dong, Visible-light photocatalytic removal of NO in air over BiOX (X = Cl, Br, I) single-crystal nanoplates prepared at room temperature, Ind. Eng. Chem. Res. 52 (2013) 6740–6746. doi:10.1021/ie400615f.

[105] Y. Wang, R. Sun, A. Xiao, S. Wang, D. Zhou, Phosphate affects the adsorption of tetracycline on two soils with different characteristics, Geoderma. 156 (2010) 237–242. doi:10.1016/j.geoderma.2010.02.022.

[106] M. Brigante, P.C. Schulz, Remotion of the antibiotic tetracycline by titania and titania – silica composed materials, J. Hazard. Mater. 192 (2011) 1597–1608.

doi:10.1016/j.jhazmat.2011.06.082.

[107] Adsorption removal of tetracycline from aqueous solution by anaerobic granular sludge: equilibrium and kinetic studies, (2006) 1–9.

[108] W. Luo, B. Yin, C.Y.W. Ang, L. Rushing, H.C.T. Jr, Determination of lincomycin residues in salmon tissues by gas chromatography with nitrogen-phosphorus detection, 687 (1996) 405–411.

[109] C. Liu, Y. Chuang, H. Li, B.J. Teppen, S.A. Boyd, J.M. Gonzalez, C.T. Johnston, Sorption of Lincomycin by Manure-Derived Biochars from Water, (2016) 519–527. doi:10.2134/jeq2015.06.0320.

[110] M.B. Ahmed, J.L. Zhou, H.H. Ngo, W. Guo, A.H. Johir, Single and competitive sorption properties and mechanism of functionalized biochar for removing sulfonamide antibiotics from water Sulfonamide structures Sulfonamide species General formula of sulfonamides, Chem. Eng. J. 311 (2017) 348–358. doi:10.1016/j.cej.2016.11.106.

[111] L. Xu, J. Dai, J. Pan, X. Li, P. Huo, Y. Yan, X. Zou, R. Zhang, Performance of rattle-type magnetic mesoporous silica spheres in the adsorption of single and binary antibiotics, Chem. Eng. J. 174 (2011) 221–230. doi:10.1016/j.cej.2011.09.003.

[112] M. Kühne, D. Ihnen, G. Möller, O. Agthe, Stability of Tetracycline in Water and Liquid Manure, J. Vet. Med. Ser. A Physiol. Pathol. Clin. Med. 47 (2000) 379–384. doi:10.1046/j.1439-0442.2000.00300.x.

[113] S. Fukahori, T. Fujiwara, N. Funamizu, K. Matsukawa, R. Ito, Adsorptive removal of sulfonamide antibiotics in livestock urine using the high-silica zeolite HSZ-385, Water Sci. Technol. 67 (2013) 319–325. doi:10.2166/wst.2012.513.

APPENDIX A

Calibration curves used for determination of TC and LM concentrations

The concentration of tetracycline and lincomycin in water was determined using HPLC based on the procedure explained in section 3.2.5. Figure A.1 depicts the developed calibration curves for determination of tetracycline and lincomycin concentrations in water. In addition, the calibration curves developed for determining the antibiotics concentration in the mixture solutions are presented in Figure A.2.

In addition, the concentration of tetracycline in liquid manure supernatant was determined based on the procedure explained in in section 3.2.5, and the developed calibration curve is presented in Figure A.3.

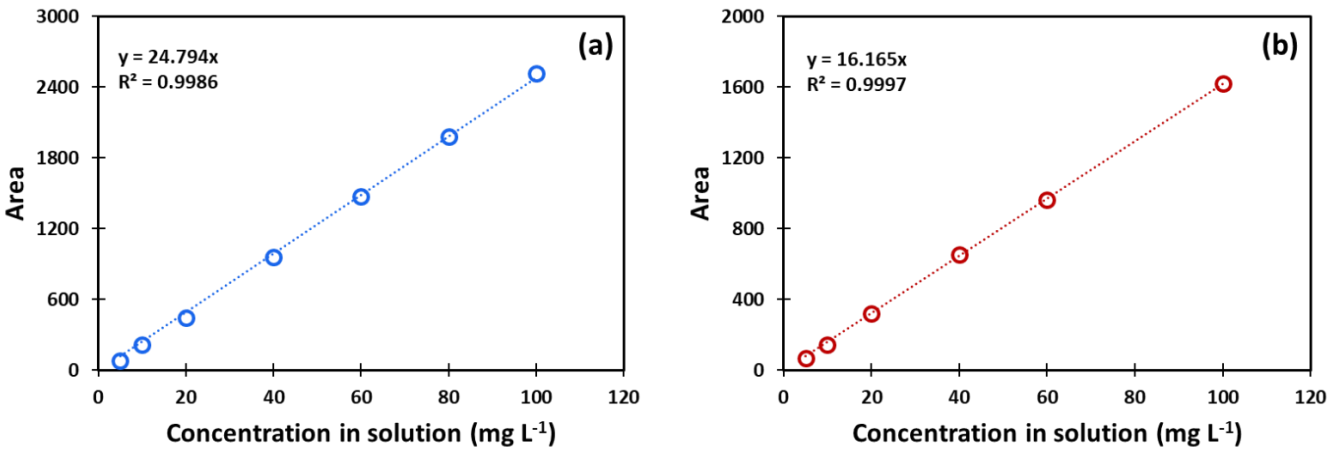

Figure A.1 Tetracycline (a) and lincomycin (b) calibration curves in deionized water

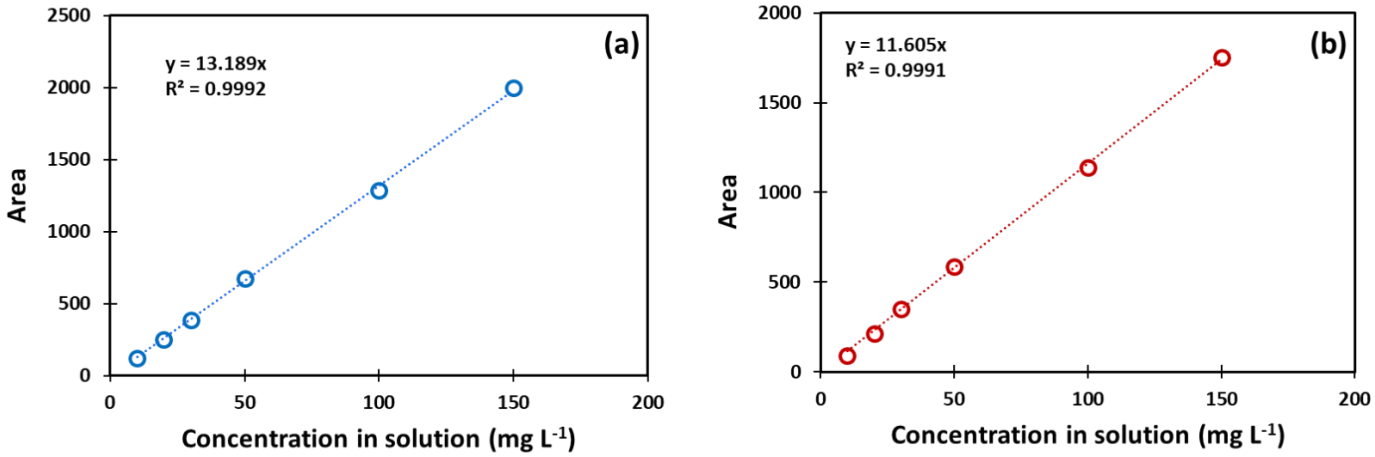

Figure A.2 Tetracycline (a) and lincomycin (b) calibration curves in the mixture solutions

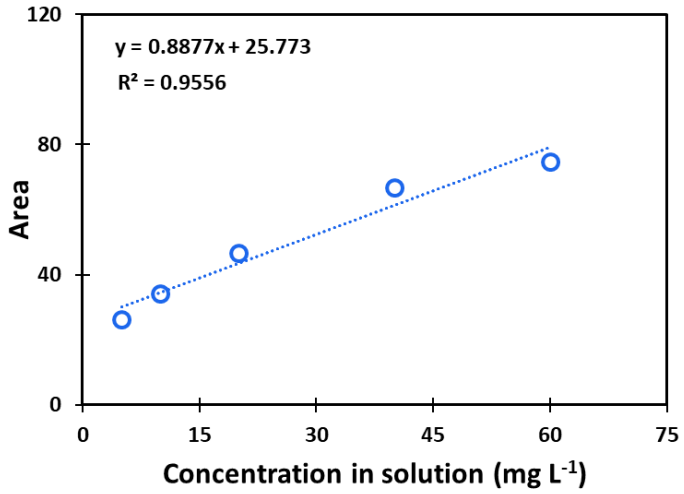

Figure A.3 Tetracycline calibration curve in the prepared liquid manure supernatant

APPENDIX B

Calculating enthalpy changes for the TC adsorption process

Each set of tetracycline adsorption data was fitted separately to the Langmuir isotherm model and the obtained results are presented in Figure B.1 and Table B.1. Also, the insets in Figure B.1 magnify the obtained adsorption data at very low range of tetracycline concentration (0-2 mg L^{-1}). Based on the acquired results, the enthalpy changes for the tetracycline adsorption process were calculated as explained in section 2.4.3. For this aim, Van't Hoff plots for tetracycline adsorption on AC and MAC are prepared and presented in Figure B.2. The obtained enthalpy changes are presented within Figure B.2.

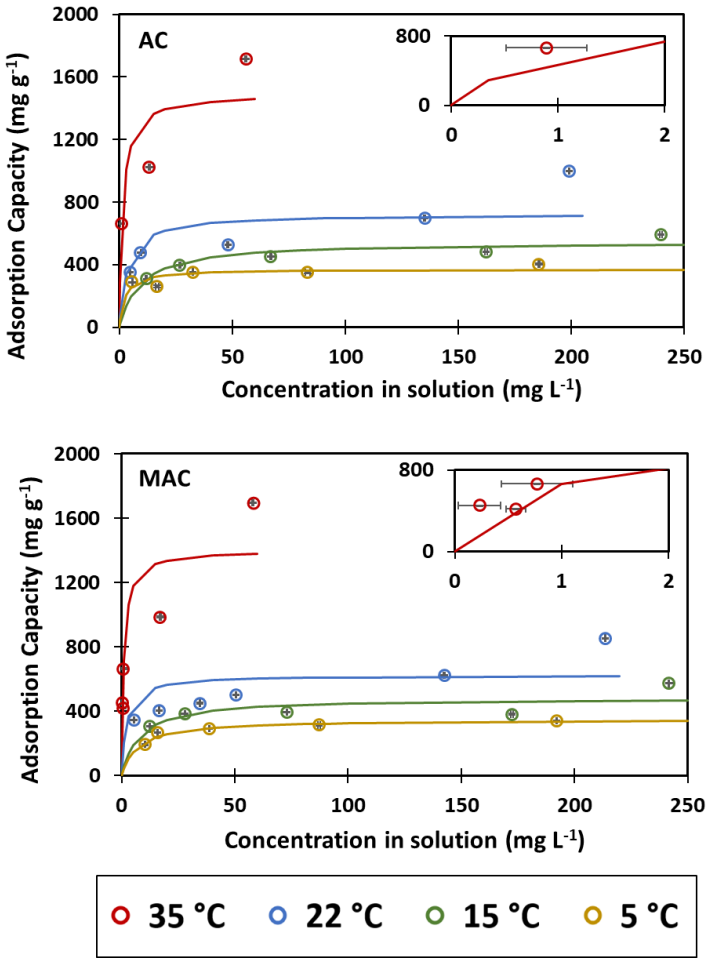

Figure B.1 Adsorption of tetracycline on AC and MAC at 5, 15, 22 and 35 °C (pH: 5.3 - 6.2). Symbols represent the experimental results and lines represent the prediction by Langmuir isotherm model. Error bars are calculated based on the standard deviation between two HPLC injections.

Table B.1 Parameters of Langmuir isotherm for tetracycline adsorption on AC and MAC (T: 5 - 35 °C, pH: 5.3 - 6.2)

Ads.	T (°C)	q_{max} (mg g^{-1})	K_L (L mg^{-1})	R^2	MAPE (%)
AC	5	371	0.42	0.996	8
	15	548	0.11	0.981	13
	22	722	0.30	0.987	22
	35	1493	0.69	0.974	20
MAC	5	347	0.15	0.999	4
	15	482	0.13	0.923	15
	22	622	0.48	0.894	20
	35	1400	1.05	0.958	23

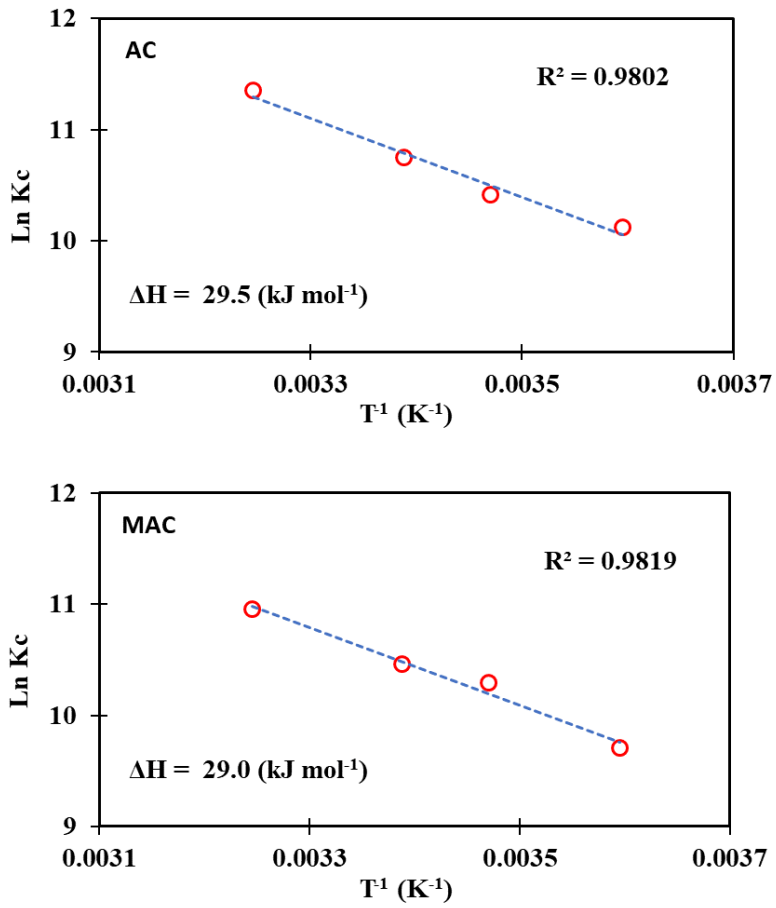

Figure B.2 Van't Hoff plots for the tetracycline adsorption onto AC and MAC at 5-35 °C and the corresponding enthalpy changes

APPENDIX C

Fitting TC and LM adsorption data to Freundlich model

Besides Langmuir isotherm, Freundlich isotherm was used to model the adsorption of tetracycline and lincomycin onto AC and MAC in water. The tetracycline adsorption data for AC and MAC at 5, 15, 22 and 35 °C were fitted to Freundlich model, and the obtained results are presented in Figure C.1 and Table C.2. Also, the insets in Figures C.1 and C.3 magnify the obtained adsorption data at very low range of tetracycline and lincomycin concentrations (0-2 mg L^{-1}). Freundlich isotherm was also used to model the adsorption of lincomycin on AC and MAC at room temperature, and the acquired results are presented in Figure C.2 and Table C.2. Freundlich isotherm was used to model the adsorption of tetracycline and lincomycin on AC and MAC in mixture at room temperature, and the acquired results are presented in Figure C.3 and Table C.3.

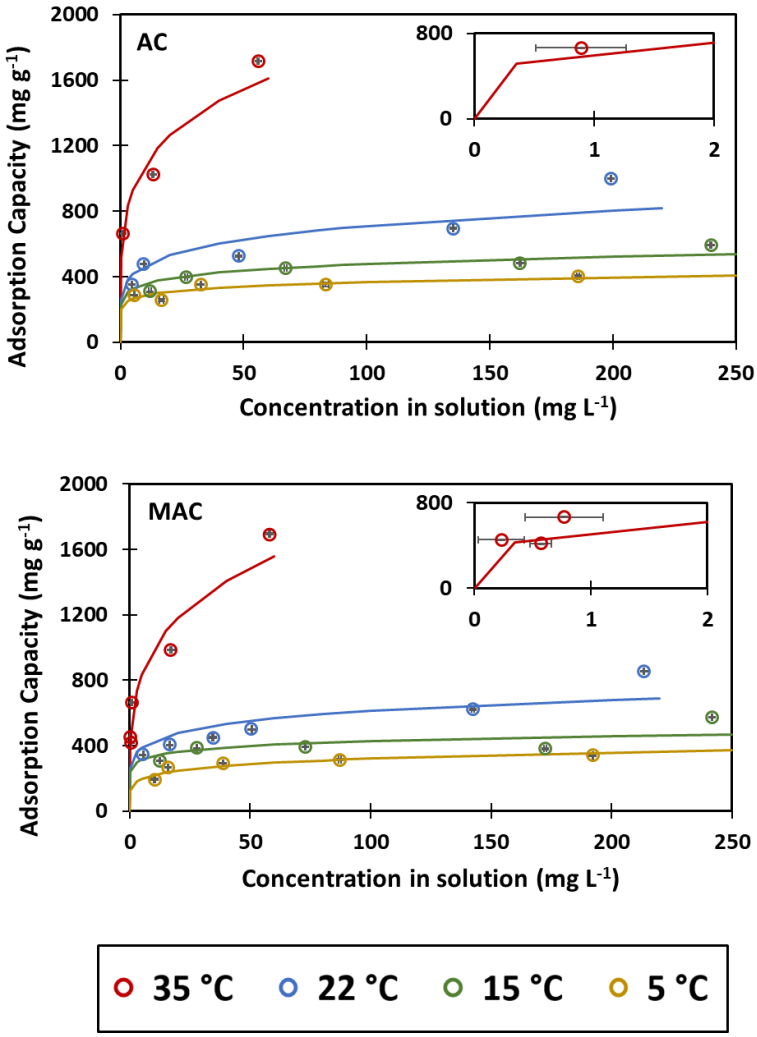

Figure C.1 Adsorption of tetracycline on AC and MAC at 5, 15, 22 and 35 °C (pH: 5.3 - 6.2). Symbols represent the experimental results and lines represent the prediction by Freundlich expressions. Error bars are calculated based on the standard deviation between two HPLC injections.

Table C.1 Parameters of Freundlich isotherm for tetracycline adsorption on AC and MAC (T: 5 - 35 °C, pH: 5.3 - 6.2)

Ads.	T (°C)	K_F (mg g^{-1})(L mg^{-1})$^{1/n}$	n	R^2	MAPE (%)
AC	5	224	9.3	0.698	6
	15	266	7.9	0.787	7
	22	313	5.6	0.819	14
	35	652	4.6	0.952	10
MAC	5	204	10.3	0.999	5
	15	267	9.8	0.566	9
	22	306	6.7	0.690	11
	35	595	3.9	0.932	13

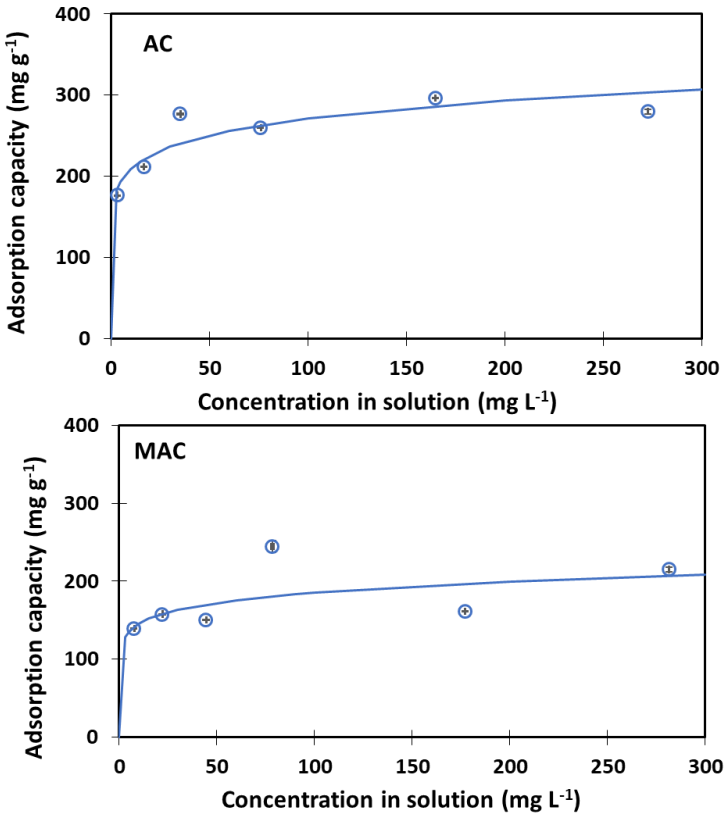

Figure C.2 Adsorption of lincomycin on AC and MAC at room temperature (T= 22 °C, pH: 6.0 - 6.4). Symbols represent the experimental results and lines represent the prediction by Freundlich expression. Error bars are calculated based on the standard deviation between two HPLC injections.

Table C.2 Parameters of Freundlich isotherm for lincomycin adsorption on AC and MAC (T= 22 °C, pH: 6.0 - 6.4).

Ads.	K_F (mg g^{-1})(L mg^{-1})$^{1/n}$	n	R^2	MAPE (%)
AC	161	8.9	0.847	5
MAC	115	9.6	0.400	10

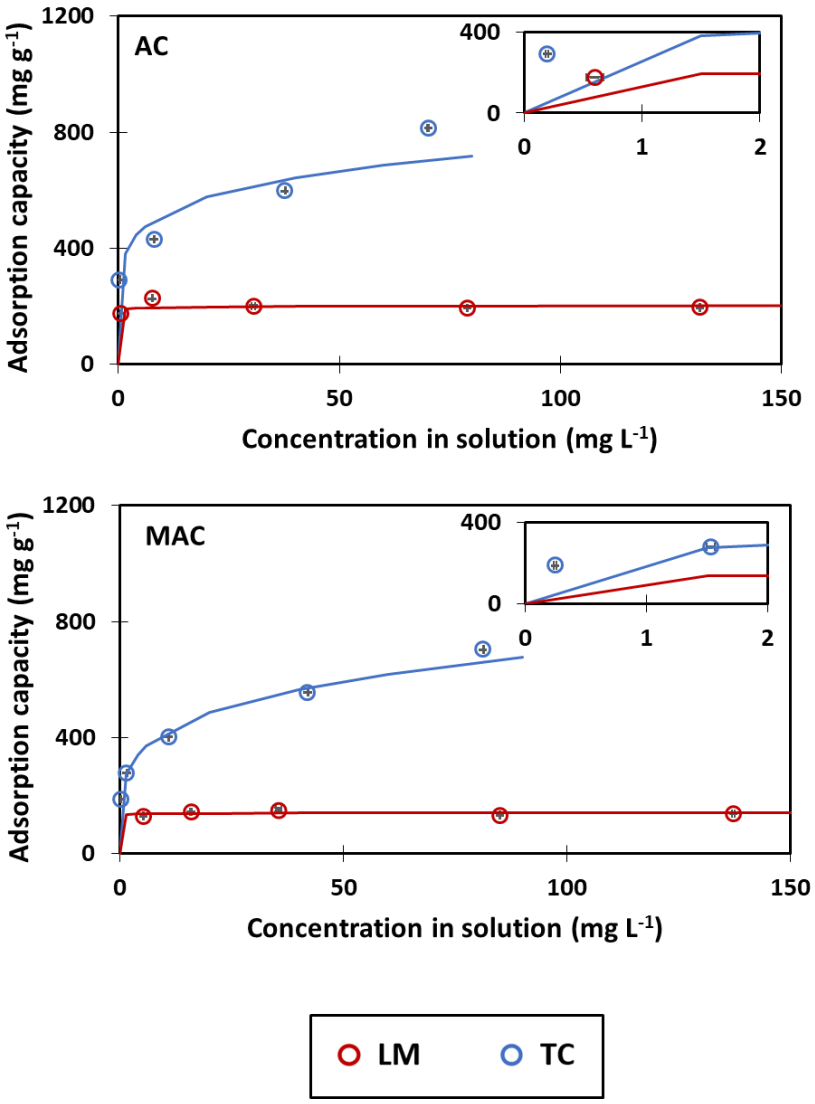

Figure C.3 Adsorption of tetracycline and lincomycin on AC and MAC in mixture at room temperature (T= 22 °C, pH: 5.9 - 6.3). Symbols represent the experimental results and lines represent the prediction by Freundlich expression. Error bars are calculated based on the standard deviation between two HPLC injections.

Table C.3 Parameters of Freundlich isotherm for tetracycline and lincomycin adsorption in mixture on AC and MAC (T= 22 °C, pH: 5.9 - 6.3)

Ads.	Antibiotic	K_F (mg g^{-1})(L mg^{-1})$^{1/n}$	n	R^2	MAPE (%)
AC	TC	357	6.3	0.913	7
	LM	191	83.3	0.081	4
MAC	TC	251	4.5	0.992	2
	LM	135	116.3	0.033	3